VARIABLE SPEED CHILLED WATER SYSTEM MODELING & OPTIMIZATION

A Thesis

Submitted to the Faculty

of

Purdue University

by

Neal L. Trautman

In Partial Fulfillment of the

Requirements for the Degree

of

Master of Science in Mechanical Engineering

August 2020

Purdue University

Indianapolis, Indiana

THE PURDUE UNIVERSITY GRADUATE SCHOOL
STATEMENT OF THESIS APPROVAL

Dr. Ali Razban

Department of Mechanical and Energy Engineering

Dr. Jie Chen

Department of Mechanical and Energy Engineering

Dr. Eric Adams

Department of Mechanical and Energy Engineering

Approved by:

Dr. Jie Chen

Head of Graduate Program

In dedication to all my friends and family who have supported me over the years.

ACKNOWLEDGMENTS

I would like to extend my sincere gratitude toward Jeff Christian and the Eiteljorg Museum of Indianapolis. I could not have done this without the Eiteljorg's willingness to help students with their research and without Jeff's assistance collecting data from the museum's chilled water system. I am eternally grateful for all the support that was provided.

I would also like to express my thanks toward my academic advisor Ali Razban. Without his consistent guidance and support I would not have been able to finish my work. It has been a pleasure to work alongside you for the past couple years.

Finally, I would like to express my thanks to all my friends and family who stood beside me through good times and bad. It is your support that kept me going when things were difficult. I am extremely lucky to have you all in my life.

TABLE OF CONTENTS

Page

LIST OF TABLES vii

LIST OF FIGURES viii

SYMBOLS xi

ABBREVIATIONS xiii

ABSTRACT xiv

1 INTRODUCTION 1

1.1 System Description 1

1.1.1 Absorption Chillers 2

1.1.2 Vapor Compression Chillers 4

1.1.3 Condenser Type 9

1.1.4 Variable Frequency Drives 13

2 LITERATURE REVIEW 19

2.1 Overview 19

2.2 Cooling Load Prediction 19

2.3 Cooling Tower Modeling 20

2.4 Chiller Modeling 21

2.5 Literary Gap 22

3 CASE STUDY 24

4 MODELING 30

4.1 Overview 30

4.2 Cooling Load Prediction 31

4.3 Pump Modeling 36

4.4 Cooling Tower Modeling 39

4.4.1 Physical Equations 43

Page

4.5 Chiller Modeling 52
4.6 Combined Model 65
4.7 Optimization 69
5 RESULTS & DISCUSSION 73
5.1 Control Strategies 83
5.2 Potential Improvements 85
5.3 Discussion 86
5.4 Conclusion 88
REFERENCES 89

LIST OF TABLES

Table Page

3.1 Overview of Data Collection 27

4.1 Overview of Modeling Inputs & Outputs 31

4.2 Cooling Load Prediction Model Inputs & Data Sources 33

4.3 Cooling Load Regression Coefficients 34

4.4 Pump Model Inputs & Data Sources 37

4.5 Cooling Tower Model Input Data Sources 43

4.6 Cooling Tower Constants 51

4.7 Chiller Model Input Data Sources 54

5.1 Control Strategy Scenarios 73

5.2 Control Scenarios Energy Savings Compared to Baseline 82

LIST OF FIGURES

Figure Page

1.1 Chiller Classifications 2
1.2 Absorption Refrigeration System Schematic [3] 3
1.3 Ideal Vapor Compression Cycle [5] 4
1.4 Centrifugal Compressor Diagram [6] 6
1.5 Reciprocating Compressor Diagram [7] 7
1.6 Scroll Compressor Diagram [9] 8
1.7 Screw Compressor Diagram [10] 9
1.8 Counter-flow Cooling Tower Diagram [11] 11
1.9 Evaporative Condenser Diagram [12] 12
1.10 Performance Comparison of Fixed vs. Variable Speed Chillers [13] 14
1.11 Variable Primary Flow Configuration [21] 16
1.12 Constant Primary Variable Secondary Configuration [21] 17
3.1 Sketchup Drawing of the Eiteljorg Museum 24
3.2 Eiteljorg's Carrier 19XRV 300 Ton Chiller 25
3.3 Eiteljorg's VT-301-0 BAC Cooling Towers 26
3.4 Eiteljorg Chilled Water Diagram & Data Collection Points 28
4.1 Discrete & Moving Average of Cooling Load 32
4.2 Measured & Predicted Building Cooling Load 35
4.3 Measured vs. Predicted Cooling Load 35
4.4 Measured vs. Predicted Cooling Load for Training & Validation Datasets . 36
4.5 Pump Power vs. Flow Rate 38
4.6 Cooling Tower Fan Line Amps vs. Fan Speed (%) 40
4.7 Cooling Tower Fan Power vs. Fan Speed(%) 40
4.8 Cooling Tower Speed vs. Wetbulb & Tower Outlet Temperature (Jul.) . . 41

Figure Page

4.9 Cooling Tower Speed vs. Wetbulb & Tower Outlet Temperature (Oct.) . . 42

4.10 Mass & Energy Balance on Incremental Tower Volume [44] 44

4.11 Saturation Air Enthalpy vs. Temperature 47

4.12 Log-Log Plot of Ntu vs. Mass flow Ratio of Water to Air 50

4.13 Measured vs. Predicted Tower Outlet Water Temperature 51

4.14 Measured & Predicted Tower Outlet Water Temperature 52

4.15 Measured vs. Predicted Chiller Efficiency (Modified Gordon Model) 55

4.16 Measured vs. Predicted Chiller Efficiency (Variable Flow Rate Gordon Model) 58

4.17 Measured vs. Predicted Chiller Efficiency (Combined Gordon Model) . . . 59

4.18 System Power vs. Fan Speed & Pump Power (Inlet Water Temperature) . 60

4.19 System Power vs. Fan Speed & Pump Power (Outlet Water Temperature) 61

4.20 System Power vs. Fan Speed & Pump Power (Average Water Temperature) 62

4.21 Chiller Efficiency vs. Cooling Load for Various Avg. Condenser Temp. . . 64

4.22 Chiller Efficiency vs. Avg. Condenser Temp. & Cooling Load 65

4.23 Flow Chart of Component Model Interactions 67

4.24 Actual & Modeled Chiller Power (7-11 to 7-19) 68

4.25 Acutal & Modeled Condenser Inlet & Outlet Water Temperature 69

4.26 Optimization Flow Chart 71

5.1 Scenario 1 & 2 System Power Consumption (7-11 to 7-19) 75

5.2 Scenario 1 & 2 System Power Consumption (9-1 to 9-9) 75

5.3 Scenario 1 & 2 System Power Consumption (10-21 to 10-29) 76

5.4 Scenario 2 & 3 System Power Consumption (7-11 to 7-19) 77

5.5 Scenario 2 & 3 System Power Consumption (9-1 to 9-9) 77

5.6 Scenario 2 & 3 System Power Consumption (10-21 to 10-29) 78

5.7 Scenario 3 & 4 System Power Consumption (7-11 to 7-19) 79

5.8 Scenario 3 & 4 System Power Consumption (9-1 to 9-9) 79

5.9 Scenario 3 & 4 System Power Consumption (10-21 to 10-29) 80

Figure Page

5.10 Scenario Energy Consumption (7-11 to 7-19) 81
5.11 Scenario Energy Consumption (9-1 to 9-9) 81
5.12 Scenario Energy Consumption (10-21 to 10-29) 82
5.13 Optimal Fan Speed vs. Wet-bulb Temperature 83
5.14 Optimal Approach vs. Wet-bulb Temperature 84

SYMBOLS

A_V	surface area of water droplets per unit volume cooling tower
C_{pm}	constant pressure specific heat of moist air
C_{pw}	constant pressure specific heat of liquid water
C_s	derivative of saturated air enthalpy with respect to temperature
h_a	enthalpy of moist air per unit mass dry air
h_C	convection heat transfer coefficient
h_D	mass transfer coefficient
h_f	enthalpy of liquid water
h_g	enthalpy of water vapor
h_s	enthalpy of saturated air
$\dot{m}_a$	mass flow rate of dry air
$\dot{m}_w$	mass flow rate of water
m^*	ratio of air to water effective capacitance rate
K	heat exchanger coefficient
L	rate of heat gain/loss from environment
Le	lewis number
P_c	chiller power
P_f	fan power
P_p	pump power
P_T	total power
$\dot{Q}$	rate of heat transfer
Q_L	cooling load
$Q_{L,2hr}$	cooling load 2 hours prior
R	heat exchanger thermal resistance

ΔS_{int}	internal rate of entropy generation
T_a	air temperature
T_w	water temperature
UA	overall heat transfer conductance
V	volume
$\dot{V}$	volumetric flow rate
V_T	total tower volume
ϵ_a	air-side heat transfer effectiveness
ρ	density
ω	specific humidity
Subscripts	
a	air stream conditions
avg	average
e	effective
$evap$	evaporator
$cond$	condenser
i	inlet
k	specific time step
max	maximum
o	outlet
s	saturated
w	water stream conditions

ABBREVIATIONS

ANN	Artificial neural network
ASHRAE	American Society of Heating, Refrigeration and Air-Conditioning Engineers
CFM	Cubic feet per minute
COP	Coefficient of performance(kW/Ton)
GPM	Gallons per minute
HVAC	Heating, Ventilation and Air Condition
NREL	National Renewable Energy Laboratory
NTU	Number of heat transfer units
RH	Relative humidity
RSME	Root-mean-square error
USCRN	U.S. Climate Reference Network
USRSRN	U.S Regional Climate Reference Network
VFD	Variable frequency drive

ABSTRACT

Trautman, Neal L., M.S.M.E., Purdue University, August 2020. Variable Speed Chilled Water System Modeling & Optimization. Major Professor: Ali Razban.

The emergence of increasingly affordable variable speed drive technology has changed the approach for how chilled water systems equipped with variable speed drives should be controlled. The purpose of this study was to estimate the potential energy savings that can be achieved through optimization of a single chiller system equipped with variable frequency drives on all pieces of equipment in the condenser water system. Data for a case study was collected from a local museum's chilled water system. The chilled water system was already equipped with variable frequency drives on the condenser water pump, cooling tower fan and the centrifugal chiller, but the building automation system did not possess appropriate control logic for controlling equipment speed to reduce the system's energy consumption. To accomplish the objective, physical component models of the centrifugal chiller, cooling tower and condenser water pump were established with the goal of incorporating the system's condenser water flow rate and cooling tower fan speeds as optimization variables. Furthermore, a simple cooling load prediction algorithm was developed using a multiple non-linear regression model in order to approximate the buildings cooling load subject to a range of environmental conditions. The inputs and outputs of the individual component models were linked to estimate how adjusting the cooling tower fan and condenser water pump speed would influence the system's overall performance. The overall system model was then optimized using a generalized reduced gradient optimization algorithm to determine the potential energy savings through speed control with VFDs and ascertain a simple control logic strategy for the building automation system to operate the system. After running the optimization algorithm it was

discovered that optimizing the cooling tower fan speed could save approximately 12-15% of the system's energy consumption. Alternatively, optimizing both the cooling tower fan speed and the condenser pump power demand offered almost no energy saving potential over optimizing the cooling tower fan alone. The control strategies investigated were to control the cooling tower fan speed directly based on the ambient wet-bulb temperature and indirectly control the fan to achieve an optimal tower approach based on the ambient wet-bulb temperature. Based on the results of the optimization process, the correlation between the optimal fan speed and the wet-bulb temperature was substandard while the correlation between optimal tower approach and the ambient wet-bulb temperature was superior.

1. INTRODUCTION

The U.S. Energy Information Administration estimated that in 2018, space cooling of commercial and residential buildings consumed 377 billion kWh of electricity, or approximately 9% of the total U.S. electricity consumption across all sectors [1]. In the United States, vapor compression and absorption chillers supply space cooling in approximately 2.9% of commercial buildings. However, since chillers frequently service large facilities with sizeable cooling demands, they provide cooling for around 20% of the total commercial building floor space [2]. Considering the impact chiller systems have on the energy consumption profile of large commercial and industrial facilities, measures to improve the efficiency of chiller cooling systems can save a significant amount of energy and money.

1.1 System Description

The goal of this section is to introduce chiller powered cooling systems and develop an understanding of the variation between different potential system designs. Chiller cooling systems can be classified by the method that heat is removed from the condenser and by the system's method of converting the internal refrigerant from one phase to another. As seen in Figure 1.1, there are two major types of chillers, absorption and vapor compression, which can be used to provide cooling loads for HVAC systems and industrial processes. These chillers can be further classified as air cooled, water cooled or evaporatively cooled based on the condenser's heat rejection method.

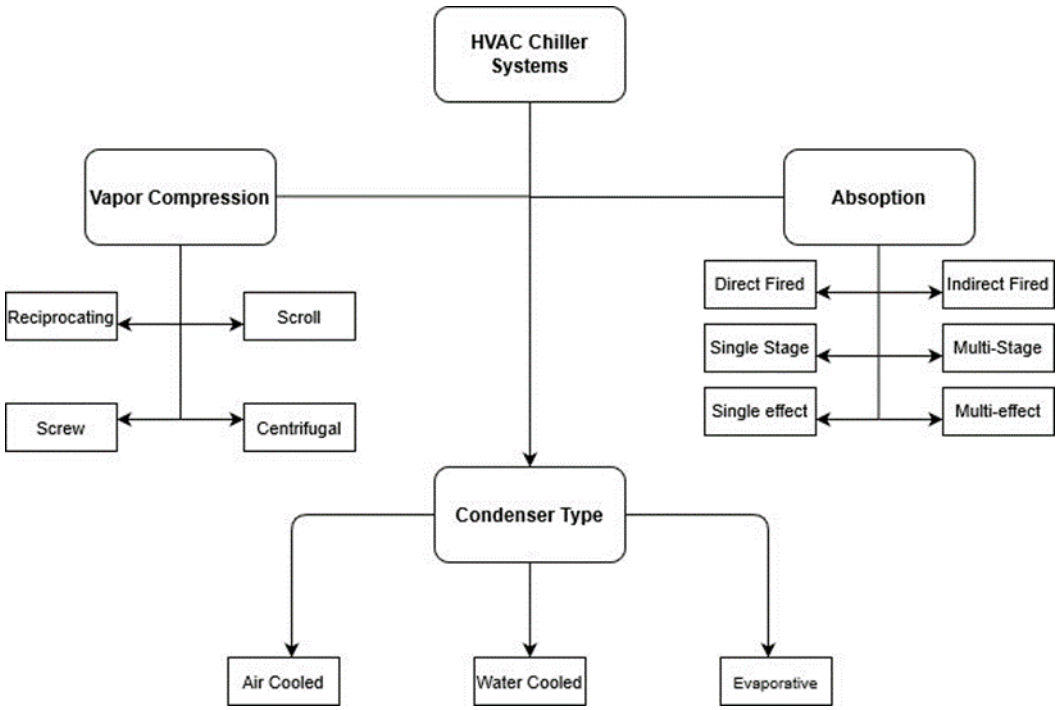

Fig. 1.1.: Chiller Classifications

1.1.1 Absorption Chillers

Figure 1.2 shows a diagram of a typically absorption chiller system. The system is comprised of an evaporator, condenser, absorber, generator, absorbant pump, and control valves that operate in conjunction to pull heat from the evaporator and discharge it through the condenser.

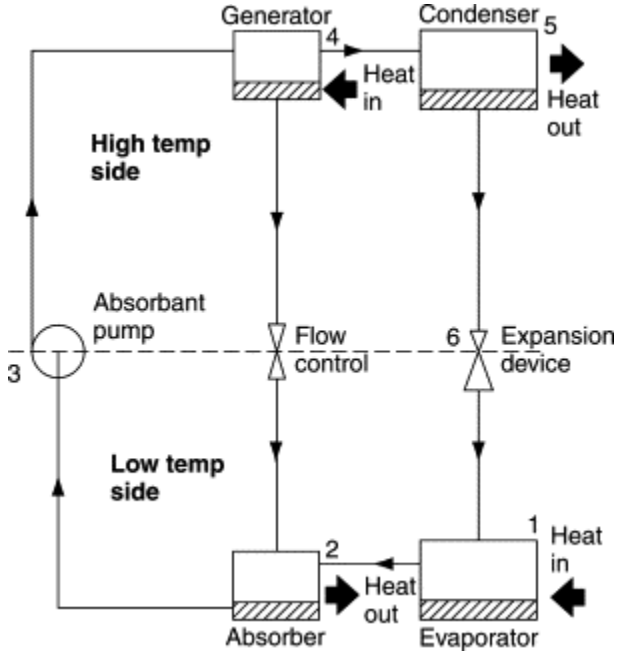

Fig. 1.2.: Absorption Refrigeration System Schematic [3]

Absorption chillers use a low-pressure refrigerant, typically ammonia or water, to extract heat from the evaporator as the refrigerant evaporates. The gaseous refrigerant then passes through to the absorber where it is absorbed by a second fluid producing a liquid saturated with refrigerant. The saturated solution is pumped through the absorbent pump to a higher pressure in the regenerator where heat is applied causing the refrigerant to evaporate out of the solution. The hot gaseous refrigerant proceeds to the condenser where it rejects heat to the surroundings condensing back into a liquid while the absorbent drops out of the regenerator through an expansion valve so it can reabsorb refrigerant from the evaporator [3]. The main advantages of using an absorption refrigeration system are that it requires less maintenance since the only moving parts are housed in the absorbent pump and that it is driven primarily by heat, a lower grade energy source compared to electricity. Natural gas tends to be a much cheaper source of energy than electricity so an absorption refrigeration could potentially offer lower operating costs for certain facilities depending on the specific rate structures. Heat from combined heat and power (CHP) systems

or waste heat from industrial process could be used to provide the heat required to drive the absorption refrigeration cycle, further reducing the system's operational costs. Disadvantages of absorption refrigeration system include a much lower coefficient of performance (0.7-1.5) compared to vapor compression systems (2-6), higher initial installation costs and a larger heat rejection demand to operate. Absorption chillers tend to be much less common compared to vapor compression chillers so the remainder of this research paper will focus on vapor compression chillers.

1.1.2 Vapor Compression Chillers

Most cooling systems, ranging from residential air conditions to large commercial and industrial chillers, utilize the vapor compression refrigeration process to supply a cooling load [4]. Figure 1.3 displays the stages in an ideal vapor compression cycle.

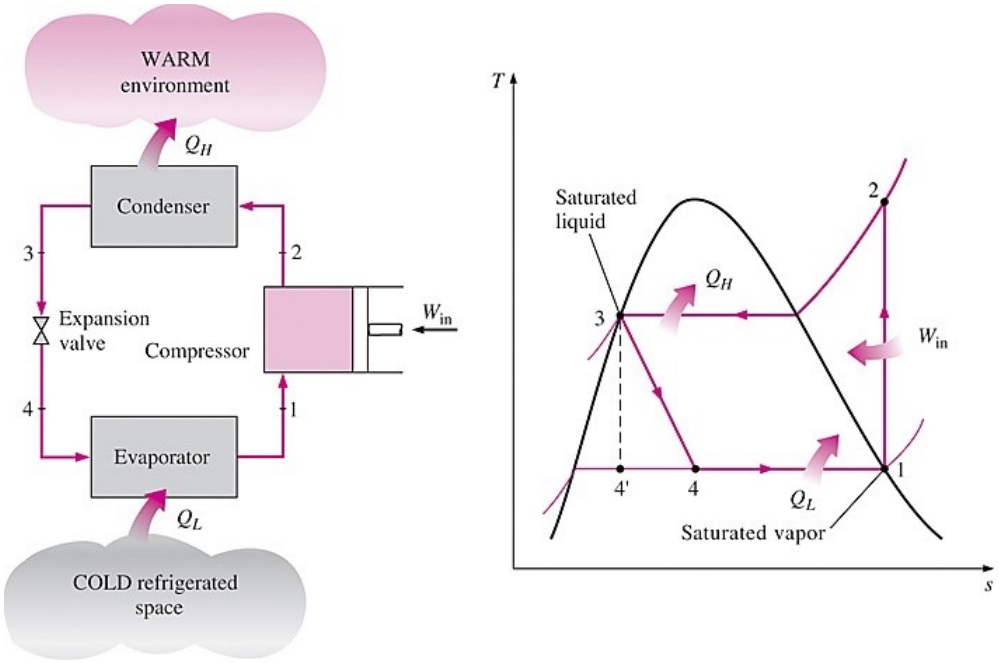

Fig. 1.3.: Ideal Vapor Compression Cycle [5]

In the ideal vapor compression cycle, a compressor drives a refrigerant to a superheated vapor at high pressure and temperature. The superheated refrigerant is

piped through the hot gas discharge line into the condenser where heat is transferred from the refrigerant to the condenser fluid until the refrigerant reaches a saturated liquid state. After passing through the condenser, the refrigerant expands through a thermal expansion valve to a low-pressure vapor-liquid mixture on the evaporator side of the chiller. The low temperature refrigerant absorbs heat from the evaporator fluid until it becomes a saturated vapor. Finally, the refrigerant returns to the compressor through the suction line completing the vapor compression cycle. The vapor compression cycle can be driven by a number of different method's of compression. Scroll, Screw, reciprocating and centrifugal compressors are all different commonly used compressor systems used to drive the refrigeration cycle. Scroll, screw and reciprocating compressors are all positive displacement compressors meaning they operate by reducing the intake volume to increase the fluid's pressure, while centrifugal compressors are dynamic compressors. Each type of compressor possesses unique operating characteristics and capacity modulation methods. Centrifugal and screw compressors are more prevalent in applications requiring large cooling loads, while scroll and reciprocating compressors find use in smaller functions.

Centrifugal Compressors

Figure 1.4 shows a diagram of the impeller chamber for a centrifugal compressor.

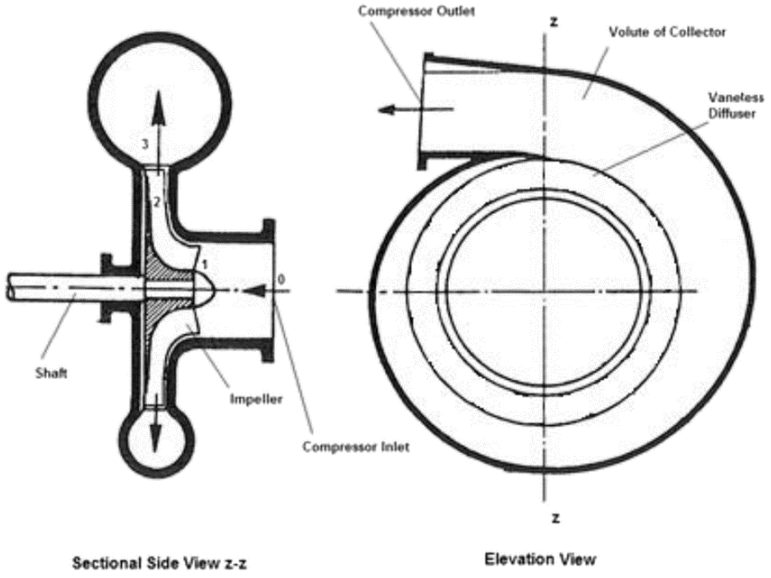

Fig. 1.4.: Centrifugal Compressor Diagram [6]

Centrifugal compressors operate using a rapidly rotating impeller that adds kinetic energy to a refrigerant. A diffuser converts the kinetic energy into static pressure resulting in the pressure rise across the compressor. Centrifugal compressors have several considerations that must be examined to keep the compressor from surging during low refrigerant flow rates and choking during high flow rates. Surge is a form of aerodynamic instability that occurs when the compressor's head is insufficient to overcome the pressure difference between the inlet and discharge points, causing refrigerant flow to reverse through the compressor. Choke on the other hand occurs at sufficiently high flow rates that compressor head drops significantly, which dramatically reduces the system's efficiency. Most centrifugal chillers possess sensors to monitor the internal status of the refrigerant and keep the compressor in a stable operating range. The capacity of centrifugal compressors can be modulated using inlet guide vanes, hot gas bypass, throttling valves and speed control using VFDs.

Reciprocating Compressors

Figure 1.5 displays the crankshaft and compression chamber of a reciprocating compressor.

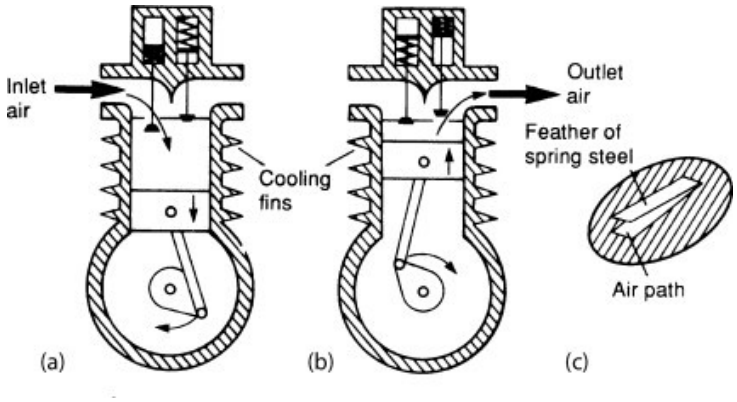

Fig. 1.5.: Reciprocating Compressor Diagram [7]

Reciprocating compressors were historically very popular, however in the past 50 years other compressor types have emerged as the preferred options for different applications [8]. The compressors intake refrigerant through the suction manifold into a compression chamber. A crankshaft drives a piston to compress the refrigerant to a higher pressure. Reciprocating compressors modulate their capacity using different combinations of valve unloaders, clearance pockets, bypass and motor speed control.

Scroll Compressors

Figure 1.6 displays the internal compressor chamber of a scroll compressor.

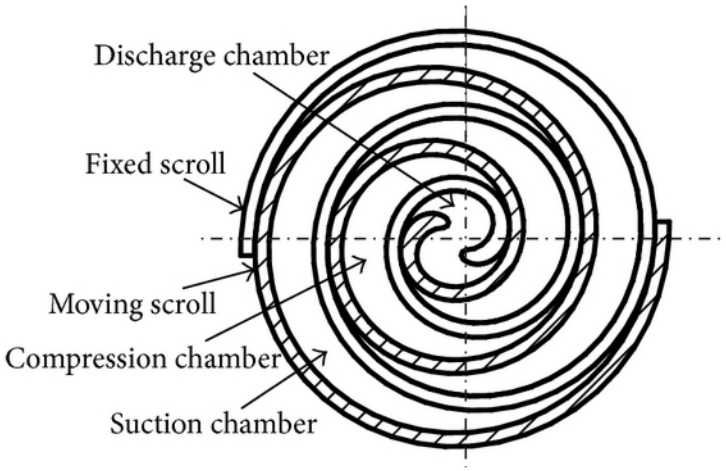

Fig. 1.6.: Scroll Compressor Diagram [9]

Scroll compressors use two identical spiral formed scrolls which are inverted and intermesh to form the compression chambers. The system uses a specially designed motor shaft to drive the dynamic scroll around the stationary scroll in an orbital motion. As the orbiting scroll moves it intakes low pressure gas on the outer end of the spiral and compresses the gas as it moves toward the discharge point in the center of the spiral scrolls. The compression process is continuous and requires multiple orbits to fully compress the gas, so at any point the scrolls contains multiple chambers of gaseous refrigerant at intermediate pressures. The capacity of scroll compressors can be modulated using staged compressors, slide valves, lift valves and variable speed control.

Screw Compressors

Figure 1.7 displays an internal compression chamber of a rotating screw compression system.

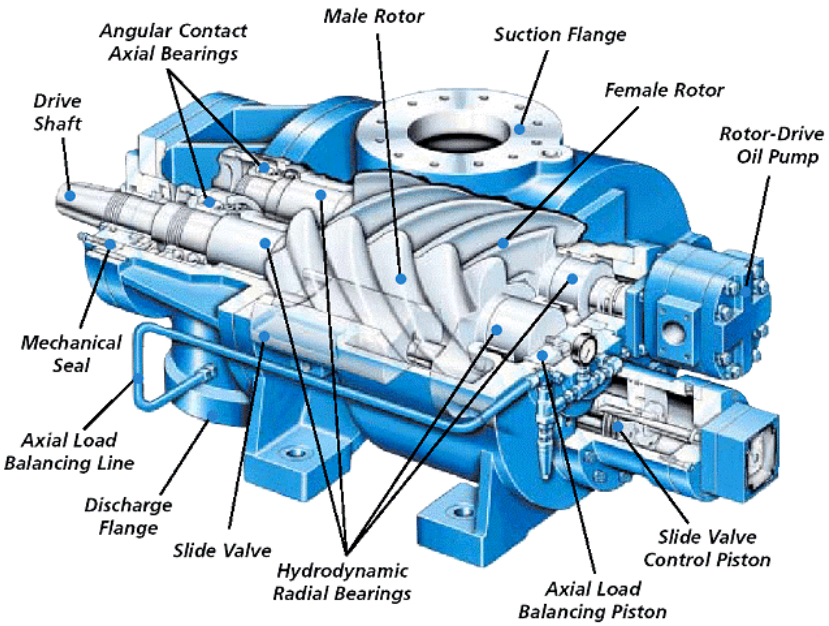

Fig. 1.7.: Screw Compressor Diagram [10]

Screw compressors consist of two rotors with intermeshing helical lobes. These rotors revolve against each other forming compression chambers that steadily decrease in volume as the rotors turn. They are common in commercial and industrial applications that require relatively large cooling loads. Screw compressors can modulate their capacity using internal slide valves, bypass methods and motor speed control. Speed control with a VFD is the most efficient method of capacity control for screw compressors [8].

1.1.3 Condenser Type

Air Cooled

Air cooled condensers are more commonly used to reject heat from chiller system supplying small to moderately sized cooling loads. Air cooled chillers use condenser fans to draw ambient air across a cooling coil containing hot refrigerant vapor. The air draws heat from the cooling coil condensing the refrigerant vapor. Using ambient

air to condense the refrigerant would imply that the capacity and efficiency of air-cooled chillers diminishes significantly as the outdoor air temperature increases. A higher ambient temperature increases the condenser temperature, which increases the lift across the compressor and reduces the capacity and efficiency of the system. Air cooled chillers can operate in below freezing without the same freeze protection requirements associated with operating cooling towers in sub-freezing conditions. As a result, air-cooled chillers, can be particularly useful in process cooling applications that require year-round cooling. The primary advantage of air-cooled chillers is that they eliminate the need for a cooling tower, condenser water pump and condenser piping which can significantly reduce the capital costs and maintenance requirements of the system.

Water Cooled

Water-cooled chillers circulate condenser water through a heat exchanger where it will draw heat from the hot refrigerant and subsequently expel the heat to the atmosphere through a cooling tower. Cooling towers can be natural or mechanical draft. Natural draft cooling towers circulate hot water through a tall hyperbolic tower to heat air at the bottom of the tower stack. The difference in air density between the heated and ambient air circulates air from the bottom of the tower to the top without the use of a cooling tower fan. They are more commonly used in industrial facilities with extremely large cooling loads. Mechanical draft cooling towers use fans to draw ambient air through the cooling tower fill. Condenser water is pumped through nozzles at the top of the tower that distribute the water over the tower fill. The interface between the air and water streams evaporates a fraction of the condenser water and transfers heat from the water to the air stream. Mechanical draft cooling towers can be classified as counter-flow or cross-flow based on the directional relationship between the relative air and water streams. Cross-flow cooling towers draw air horizontally perpendicular to the cascading water stream while counter-

flow cooling towers pull the air in a opposite parallel direction. The evaporative cooling process allows the condenser water stream to approach temperatures near the ambient wet-bulb temperature. Since wet-bulb temperatures are lower than ambient dry-bulb temperatures the refrigerant condensing temperature can be lower, which reduces chiller lift and improves system efficiency compared to air cooled chillers. Additionally, water is a much more effective fluid for transferring heat, which is why water cooled condenser systems are commonly found in moderate to large cooling systems where an air-cooled system wouldn't be as economical. Figure 1.8 displays a diagram of a typical mechanical draft counter-flow cooling tower.

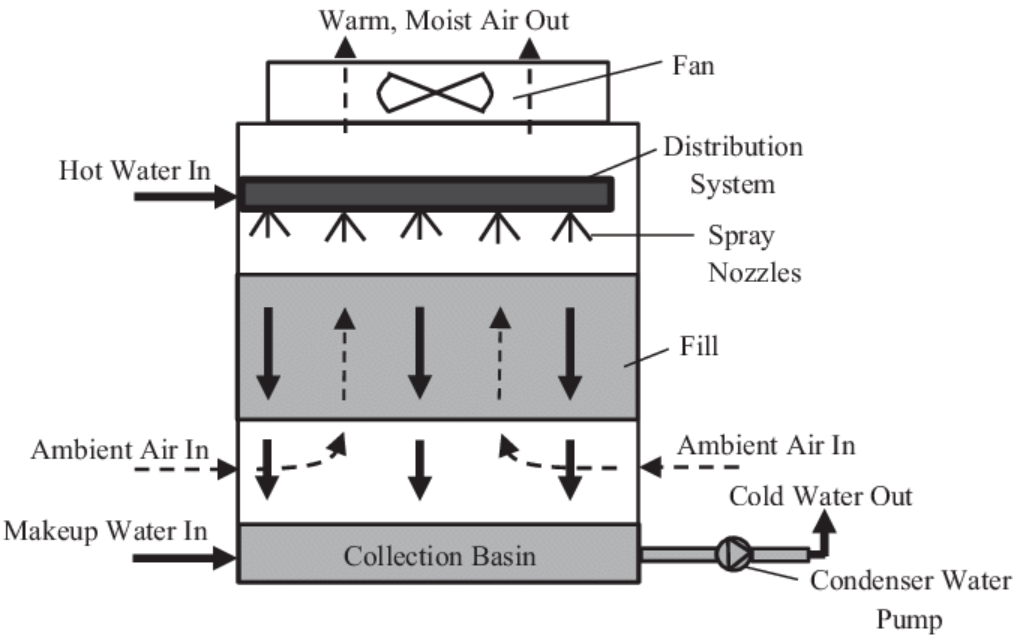

Fig. 1.8.: Counter-flow Cooling Tower Diagram [11]

There are several considerations involved with operating a cooling tower. The evaporation of water from the condenser water stream can lead to a build of dissolved solids, which will cause fouling in the cooling tower and condenser. Blowdown water is removed from the system to keep the concentration of dissolved solids from accumulating. Make-up water must be fed into the system to account for the water

evaporated from the cooling tower and the blowdown water removed from of the system. Chemical treatment of the water is often necessary to avoid scaling and prevent the growth of bacteria and algae in the system.

Evaporative Cooling

Figure 1.9 shows a schematic of a typical evaporatively cooled condenser system.

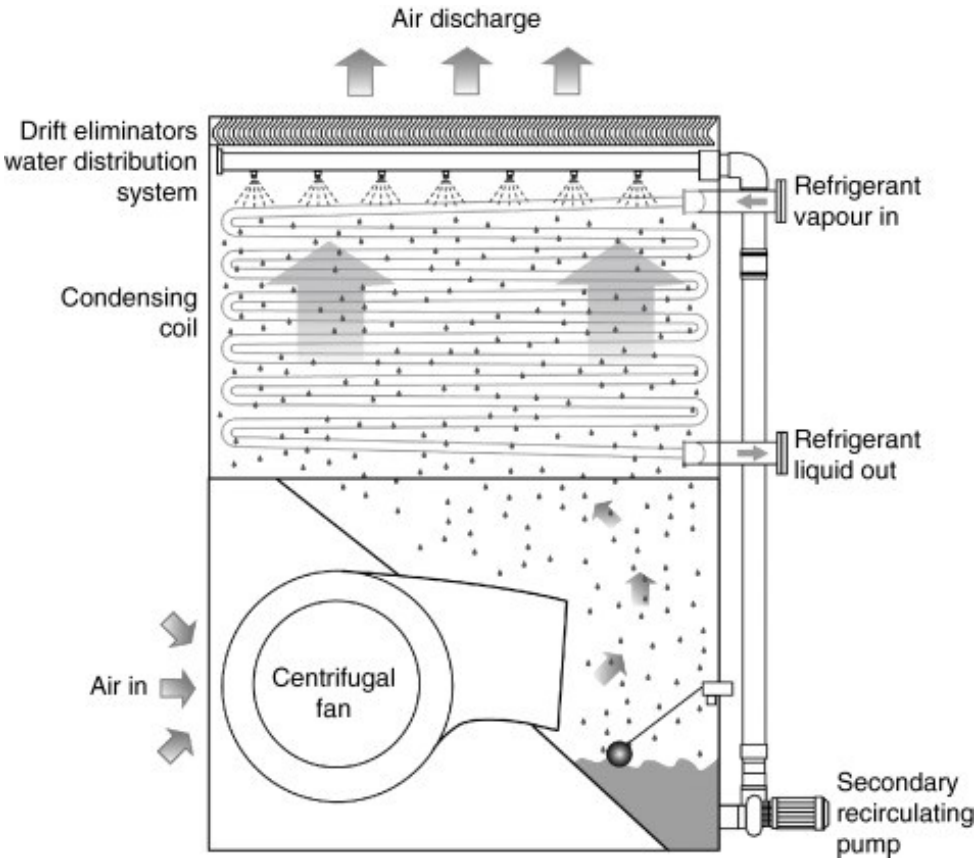

Fig. 1.9.: Evaporative Condenser Diagram [12]

Evaporative condensers closely resemble cooling tower systems in that they draw air through a cascading water stream. The fundamental difference between cooling towers and evaporative condensers is that an evaporative condenser evaporates water directly off the hot refrigerant piping while a cooling tower system transfers the re-

frigerant's heat to the water through a heat exchanger prior to the water entering the cooling tower. Due to the similarities in designs, evaporative condensers have many of the same operational considerations as cooling towers regarding treating the water used to cool the refrigerant piping.

1.1.4 Variable Frequency Drives

The emergence of progressively more affordable variable frequency drive technology has resulted in a shift in conventional control strategies for chilled water systems. This section aims to address how the addition of a variable speed drive on different pieces of equipment influences how a chilled water should be controlled in order to achieve energy savings. For brevity, the section will focus on variable speed applications for water cooled vapor compression chillers.

Vapor Compression Chillers

For a fixed entering condenser water temperature, a constant speed vapor compression chiller achieves peak efficiency near fully loaded conditions. On the other hand, variable speed driven chillers reach their peak efficiency at partially loaded conditions. Additionally, variable speed driven chillers exhibit a more dramatic improvement in efficiency at lower condenser water temperatures [13]. Figure 1.10 displays the coefficient of performance of variable speed and constant speed chillers as a function of their percent load for different inlet condenser water temperatures.

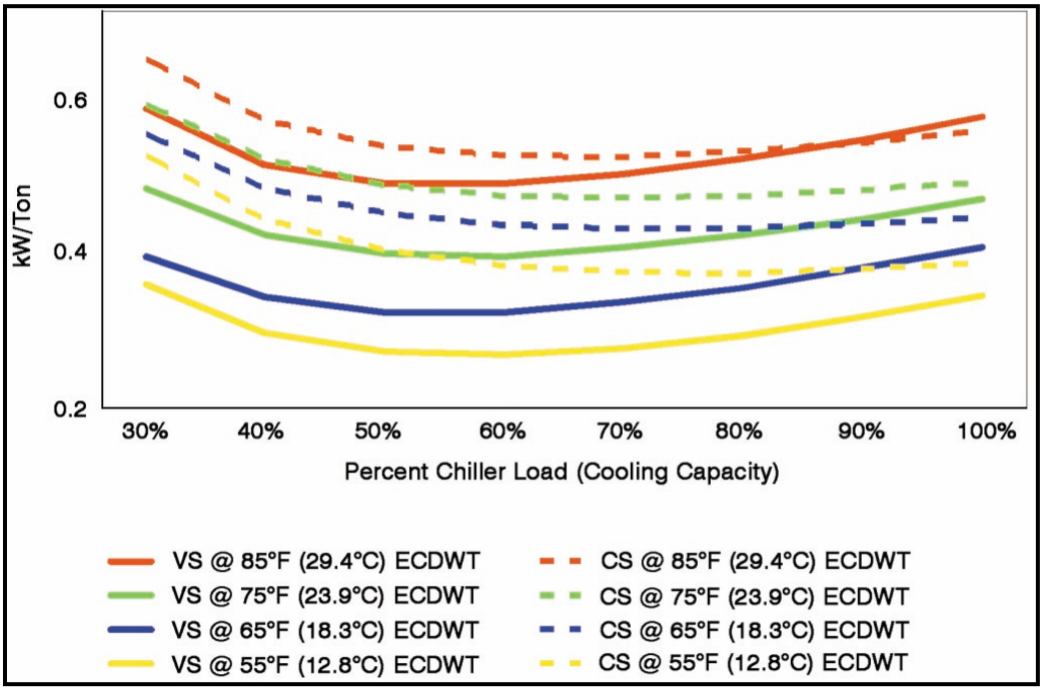

Fig. 1.10.: Performance Comparison of Fixed vs. Variable Speed Chillers [13]

The differences in the operational characteristics of constant speed and variable speed chillers changes how these chillers should be controlled to achieve energy savings. Chilled water plants with multiple fixed speed chillers traditionally stage chillers on one at a time only after exceeding full load. Since variable speed driven chillers reach peak efficiency at part load, a chiller water plant with multiple variable speed chillers should stage on chillers prior to full load to achieve optimum performance. Numerous studies have examined how to optimally stage variable speed chillers to operate in their region of maximum COP [14], [15]. Furthermore, the more pronounced effect that lower condenser water temperatures has on the efficiency of variable speed chillers also changes how the cooling tower fan and condenser water pump should be sized and controlled to reduce the energy consumption from the system.

Cooling Tower

Cooling tower fans can be single-speed, two-speed and VFD speed controlled. Cooling tower fan speed control with a VFD is one of the most common and cost-effective retrofits for chilled water systems. Cooling towers are generally sized to be able to provide cooling for the maximum cooling load and worst-case design conditions for a specific area. As a result, for most the year cooling towers operate at part-load of their design conditions. A VFD controlled cooling tower can generally operate the tower fan at speeds between 25-100%. Cooling tower fan power consumption closely resembles affinity laws in that the power consumption of the fan varies with the cubic of the fan's speed while the airflow rate changes approximately linearly with fan speed. The implication is that a tower operating at 50% speed can provide roughly 50% of the design airflow while using only 12.5% of the fan's power at full load. A common control strategy for cooling tower fans is to regulate the air flow to provide a constant setpoint condenser water temperature to the chiller regardless of the cooling load or ambient wet-bulb temperatures. Several studies have investigated the energy saving potential of resetting the condenser water temperature setpoint based on the tower approach [16], ambient wet-bulb temperatures [17], [18] and the overall system power consumption [19], [20]. Their findings indicate that operating a cooling tower to obtain the lowest possible condenser water temperature doesn't always result in energy savings due to the high fan power demand and that determining the optimal condenser water temperature setpoint can achieve varying degrees energy savings depending on the specific system and the climatic conditions of the region.

Chilled Water Distribution

The chilled water distribution system consists of all the pumps, piping, cooling coils and valves used to transmit water throughout the evaporator side of the chilled water system. Older chilled water designs will circulate a constant volume of water through the chillers and building regardless of the cooling load. During low load a

three-way valve will bypass chilled water around the cooling coils back to the chiller. Constant flow systems often waste pumping energy because bypassing the cooling load unnecessarily circulates chilled water without serving a cooling load. Variable flow applications are much more common on the evaporator side of the chiller and numerous studies have shown to they have the potential for attractive payback times and significant energy savings [21], [22], [23], [24]. Variable flow rate pumping configurations are classified by two main types of configurations, variable primary flow and constant primary-variable secondary flow. Variable primary flow systems use a single set of variable speed driven pumps to control the flow rate on the evaporator side of chilled water systems. Constant primary-variable secondary systems use two separate sets of pumps, one set of constant speed and a second set of variable speed driven pumps to control flow rate. Figures 1.11 and 1.12 show a setup of a variable primary and constant-primary variable-secondary pumping configuration.

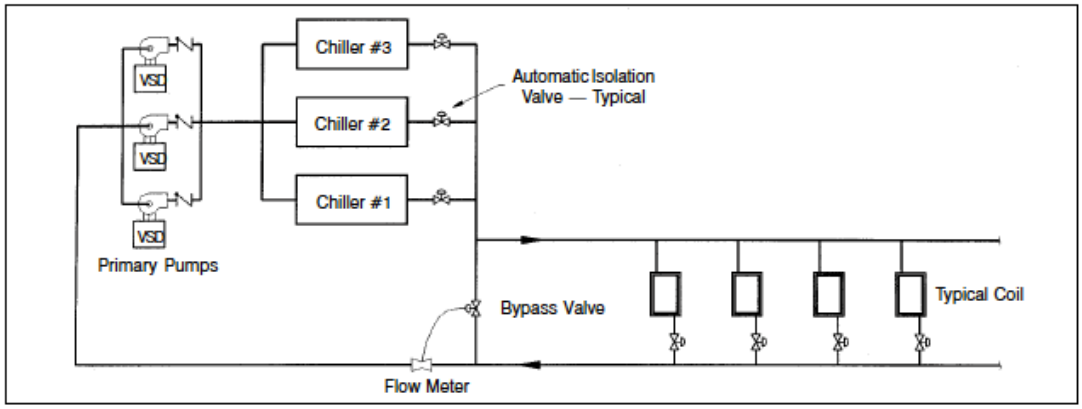

Figure 1: Primary-only system.

Fig. 1.11.: Variable Primary Flow Configuration [21]

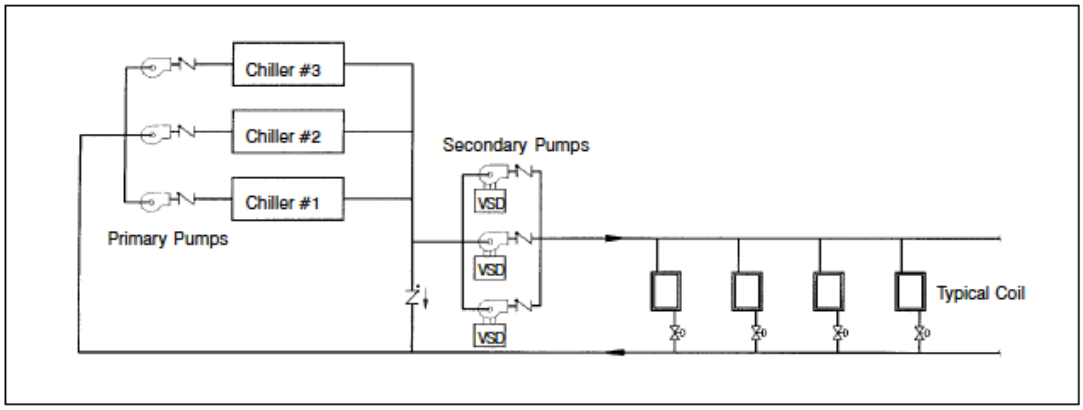

Figure 2: Conventional primary-secondary system.

Fig. 1.12.: Constant Primary Variable Secondary Configuration [21]

Several sources have considered the advantages and disadvantages of using variable primary vs. constant primary-variable secondary system configurations [21], [22], [25]. The consensus around these configurations appears to be that variable primary-only systems have lower installed and operating costs compared to primary-secondary systems. The advantage of primary-secondary systems is that the staging and bypass control are less complicated, and the system is overall less likely to fail [21]. The saving potential of variable flow pumping configurations depends upon the number of chillers serving the cooling load and the range of loads being met by the chillers.

Condenser Water Distribution

The condenser water distribution system consists of all equipment responsible for the circulation of water on the condenser side of water-cooled chillers. Variable flow in condenser water systems is uncommon in existing systems because the energy saving potential is not always clearly cost effective and the implementation requires more complex control strategies that are highly dependent on the configuration [26], [27]. Nevertheless, in the pursuit of improving plant efficiency and the growing academic interest in all-variable speed chilled water plants [13], [28], [14], variable speed applications for condenser water pumps has been an active topic of research. Lu Lu

et. Al used a genetic algorithm to optimize data from a pilot test plant and determine the optimal system setpoints for various loads and wet bulb temperatures [20]. Wang and Burnett developed an adaptive control method for speed control by adjusting the differential pressure setpoint in relation to the systems change in total power with respect to a change in pressure [29]. Wang and Ma developed a similar optimal control strategy for sequencing and speed control based on the resetting the pressure differential setpoint based on signals from control valves [30]. Yu and Chan suggested a load-based speed control method where the optimum speed of condenser water pumps and fans is adjusted relative to the cooling load [31].

2. LITERATURE REVIEW

2.1 Overview

The following section will focus on work that has been done in modeling different aspects of a chilled water system. The literature review will examine current methods for predicting a building's cooling load, modeling a cooling tower and modeling vapor compression chillers. The techniques found to be the most suitable to serving the goal of the research will be used to create a model of the overall system.

2.2 Cooling Load Prediction

Cooling Load prediction is an important component in developing online optimal control algorithms for HVAC systems. Cooling Load prediction methods generally fall into three categories: simulation, artificial intelligence and regression analysis. There are several simulation software packages that can forecast a building's cooling load if comprehensive building details are known. EnergyPlus, eQuest and TRNSYS are all reputable software for simulating building operating conditions. These simulation software all use detailed information involving building layout, construction, operating schedules, occupancy information and internal equipment to simulate a buildings cooling load [32], [33], [34]. These software are well validated and can achieve high accuracy for modeling a buildings cooling load, however they significantly work intensive and require detailed building information to develop. In addition, they are lacking in their ability to provide online optimal control of equipment. Artificial Neural Networks have been widely used in HVAC system modeling, optimization and for cooling load predictions [35], [36], [37], [38]. ANN's can attain high accuracy for cooling load predictions, however ANN's must be trained using large amounts of historical

cooling load and weather data in order to develop accurate cooling load predictions and are notably more difficult to develop compared to regression models. Regression models are another popular data-driven method researchers have investigated for simple building load prediction [39], [40], [41]. Regression models are trained using large datasets to develop coefficients for predicting a building's cooling load subject to a range of conditions. Regression methods can be less accurate then more complicated forms of analysis; however they don't require detailed building information, have lower computation requirements and are simpler to develop compared to simulation software and artificial neural networks. Regression based analysis encompasses a wide variety of techniques include multiple linear regression (MLR), multiple nonlinear regression, autoregression (AR) and autoregression with exogenous inputs (ARX). Multiple nonlinear regression modeling techniques have been shown to offer potentially superior prediction accuracy compared to multiple linear and autoregressive methods [40].

2.3 Cooling Tower Modeling

Dr. Fredrick Merkel developed one of the first practical methods for modeling cooling tower back in 1925 [42]. Merkel's model is based on relating the evaporative and sensible heat transfer for counterflow air and water streams. In order to solve the governing equations, the Merkel analysis makes several simplifying assumptions. Most notably it neglects water loss due to evaporation and assumes a Lewis number of unity. The method requires iterative numerical integration of two separate equations to determine output conditions of the air and water stream. The Merkel's model serves as the foundation for several more modern cooling tower modeling methods. Sutherland showed that Merkel's assumptions can underestimate tower volume by 5-15% [43]. Braun proposed an effectiveness model that expanded upon Merkel's method. Braun's effectiveness model assumes a linearized air saturation enthalpy with respect to temperature. The average slope between the inlet and outlet condi-

tions creates an air-side effectiveness term defined as the ratio of actual heat transfer to the maximum possible heat transfer where completely saturated air would exit the tower at the temperature of the entering condenser water. Braun's model still requires iterative computation with respect to the outlet water temperature but is generally considered an effective method for design and simulation [44]. Stoecker proposed an empirically determined polynomial approximation using the ambient wet-bulb and cooling tower supply temperature as input variables. The analysis assumes a constant airflow and water flow rate so it cannot account for variable speed driven condenser water pumps and cooling tower fans [45]. Modern cooling tower simulation algorithms often utilize empirically formed multi-parameter regression models. The CoolTools simulation algorithm is a third order, 35-parameter regression model that computes the tower approach as a function of wet-bulb temperature, tower range, water flow ratio and air flow ratio [46]. Regression models are well-noted for their speed and accuracy; however, erratic behavior can arise when attempting to extrapolate variables beyond the range of the available data.

2.4 Chiller Modeling

The ASHRAE Primary toolkit model consists of four components modeling the evaporator, condenser, compressor and expansion device. The model was developed to determine whether a chiller can meet a certain evaporator setpoint subject to a variety of inlet temperatures and flowrates [47]. Hydeman and Gillespie developed an electric chiller model for the DOE2 platform which consists of three regression curves that together can predict the power consumption of a chiller under various operating conditions [48]. The authors proposed two techniques of calibrating the DOE2 electric chiller model. The first method applies standard least-squares linear regression to large training datasets that fully encompass the range of operating conditions. The second method for calibrating the chiller performance curves is used when the data available is insufficient to develop the curve coefficients using the least squares method.

It relies on fitting the available data to a subset of curves from a library of well established chiller curves [49]. The reformulated electric chiller model builds on the previous method. The only fundamental differences between the methods is that the reformulated model utilizes the leaving condenser water temperature in place of the supply temperature and incorporates additional coefficients to the energy input as a function of part load ratio equation [50]. Gordon et al. developed one of the first chiller models that highlights condenser water flow rate as a possible control variable [51]. The analysis manipulates a previous thermodynamic chiller model developed for reciprocating chillers [52] to explicitly account for the effect variable condenser water flow has on heat exchanger thermal resistance. Jiang and Reddy proposed an adaptation to the model which assumes the entropy generated in the chiller is linear with respect to chiller load. The modification was shown to improve the model's accuracy for predicting chiller coefficient of performance for variable speed driven chillers [53].

2.5 Literary Gap

The emergence of increasingly affordable variable speed drives has changed conventional chilled water control strategies in order to achieve energy savings. An abundance of research has been done surrounding optimizing variable speed driven cooling tower fans and a variety of control strategies have been proposed to strive for optimal cooling tower fan operation. Similarly, variable speed driven evaporator pumps have been researched extensively and the energy saving potential of controlling evaporator water pumps has been well validated. Compared to constant speed chillers, variable speed driven chillers have been show to exhibit superior efficiency for partially loaded operation and demonstrate a more drastic improvement to efficiency for lower condenser water temperatures. What remains to be seen, is whether or not operating one or more variable speed condenser water pumps to provide controllable condenser water flow rate will result in energy savings and if there is indeed potential

to save energy, what would be an advantageous strategy to control the condenser water flow rate. The research that has been done in this area contains differing view points concerning whether or not the additional cost and complexity of introducing a variable flow condenser water is justified by the potential energy savings. It has been shown that the energy saving potential for controlling variable speed driven condenser water pumps is dependent on the particular system being examined and the climatic characteristics of the region in which the system is operated. The goal of this study is to develop a system model that can be routinely applied to various different chilled water systems to determine the energy saving potential of optimizing a system with variable speed driven condenser water pumps. Additionally, the study will aim to explore different proposed strategies for controlling both variable speed driven cooling tower fans and condenser water pumps.

3. CASE STUDY

A sketch-up drawing of the Eiteljorg Museum, the building used for the case study, can be seen in Figure 3.1.

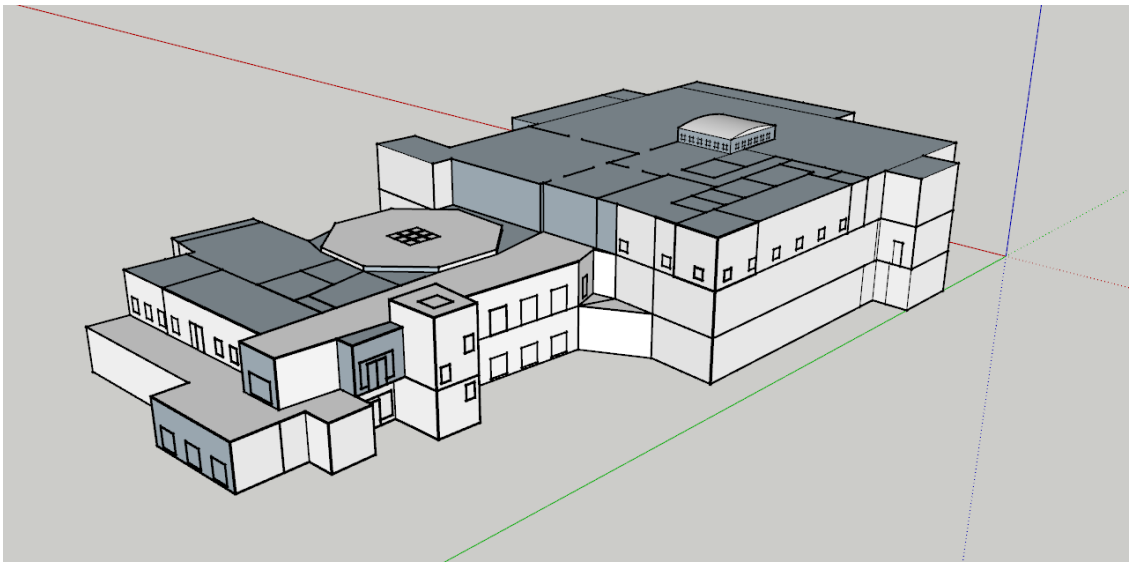

Fig. 3.1.: Sketchup Drawing of the Eiteljorg Museum

The Eiteljorg Museum in Indianapolis, IN is a 120,000 ft^2 building that houses a variety of western and Native American arts. As a museum, the facility has strict climate control requirements in order to maintain the integrity of the exhibits housed inside the building. For mixed collections a humidity level between 45-50% and temperature between 68-72°F (20-22.2°C) is recommended to prevent chemical reactions and biodegradation in the art installations [54]. The Eiteljorg's HVAC system operates to maintain an internal temperature of 70°F (21.1°C) and relative humidity level of approximately 50%. Since dehumidification is an important factor in maintaining the integrity of the museum's exhibits, the chilled water system operates to provide a constant chilled water temperature of 40°F (4.4°C) to the building's three

air handling unit's cooling coils. The museum utilizes a 300-ton Carrier 19XRV variable speed driven chiller to produce the buildings chilled water. An image of the Eiteljorg's chiller can be seen in Figure 3.2.

Fig. 3.2.: Eiteljorg's Carrier 19XRV 300 Ton Chiller

The chiller uses a centrifugal compressor to drive refrigerant R-134A to a high pressure and temperature on the shell side of the condenser. The refrigerant rejects heat into the condenser water running through the tube side of the heat exchanger. The condenser water is pumped through the condenser into one of the building's two VT1-307-0 Baltimore Aircoil Company cooling towers. One cooling tower services the chiller, while the other is used as a back-up in case the first tower requires maintenance. An image of the Eiteljorg's cooling towers can be seen in Figure 3.3.

Fig. 3.3.: Eiteljorg's VT-301-0 BAC Cooling Towers

The cooling tower fans are driven by 30HP motors connected to variable speed drives. The cooling tower fan is controlled to achieve and maintain an entering condenser water temperature of 65°F (18.3°C). Once the condenser water setpoint is reached, the cooling tower fan speed cycles between 25% and 100% to maintain the condenser water temperature. The condenser and evaporator water pumps are Bell & Gossett series 1510 driven by 15HP Baldor Reliance SuperE motors. The pump motors are also equipped with variable frequency drives; however, the building control system currently operates these pump motors at 100% speed continually. Data for the building's chilled water system were collected in 15-minute intervals from July 10th, 2019 to October 31st, 2019. Several different time periods within the data collection phase had to be erased due to either data corruption or a lack the complete set of required data. The data was collected using Onset UM120-006M data loggers, CTV-C

10-100 Amp current transducers, CTV-E 60-600 Amp current transducers, Fluke 1732 Three-Phase Power Loggers and a Fuji FCS Portable Ultrasonic Flowmeter. Table 3.1 gives an overview of the data that was collected from the Eiteljorg's system. Figure 3.4 shows a diagram of the Eiteljorg's chilled water system with the various data collection points on the different pieces of equipment.

Table 3.1.: Overview of Data Collection

Data Collected	Equipment Used
Cooling Tower Fan Amps	Onset UM-120-005M Data Logger & CTV-C Current Transducer
Cooling Tower Fan Power	Fluke 1732 Power Analyzer
Chiller Amps	Onset UM-120-005M Data Logger & CTV-E Current Transducer
Chiller Power	Fluke 1732 Power Analyzer
Condenser Pump Amps	Onset UM-120-005M Data Logger & CTV-C Current Transducer
Condenser Pump Power	Fluke 1732 Power Analyzer
Condenser Water Flow Rate	Fuji FCS Portable Ultrasonic Flowmeter
Condenser Entering & Exiting Water Temperature	Building Automation System
Evaporator Entering & Exiting Water Temperature	Building Automation System
Weather Data	NOAA Quality Controlled Datasets [55]

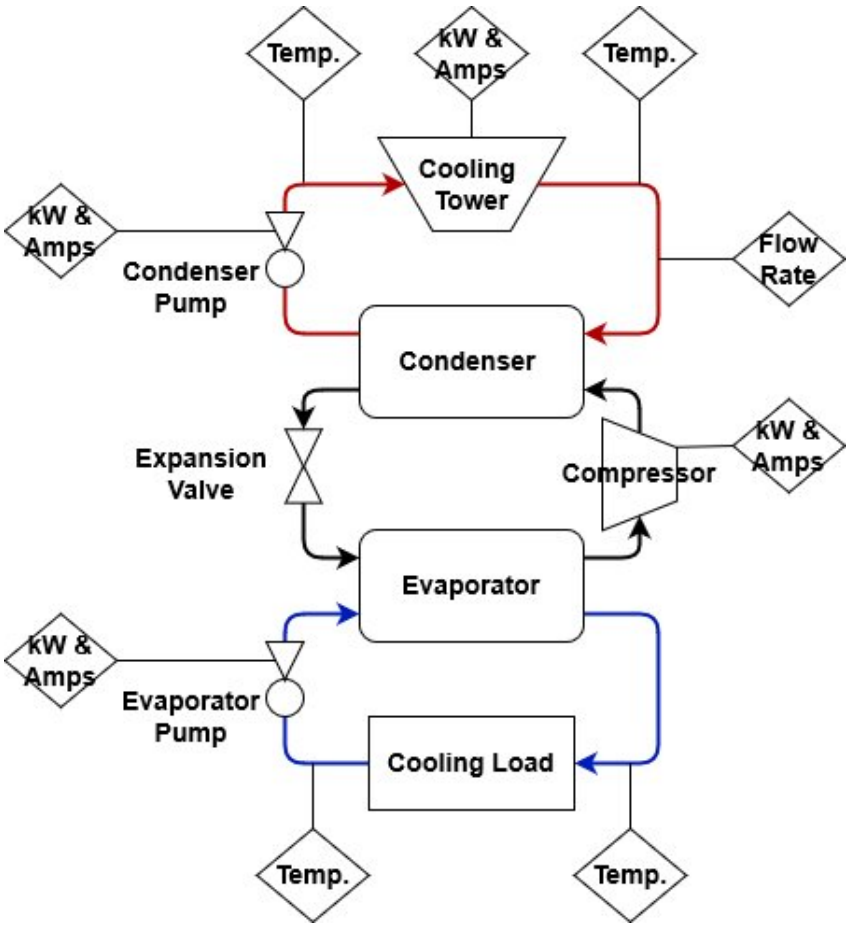

Fig. 3.4.: Eiteljorg Chilled Water Diagram & Data Collection Points

Entering and leaving condenser and evaporator water temperatures were collected using the building automation system. The HOBO data loggers and current transducers were attached to the cooling tower fan, chiller, chilled and condenser water pumps. The Fluke power logger was used to create a correlation between the motor line amps and power consumption for the chiller and cooling tower. The water flow rate of the condenser line was found to be a relatively constant value of 671 gpm (42.3 L/s). Although the chilled water pump is equipped with a variable speed drive, the building automation system operates the pump at 100% and the flow rate on the evaporator side of the chiller is regulated with a bypass valve. The flow rate of the chilled water line could not be ascertained with the portable ultrasonic flowmeter due

to insulation covering the chilled water piping. Due to the chilled water system's importance in maintaining the integrity of the museum's exhibits, the Eiteljorg's HVAC system operators were opposed to allowing changes to the chilled water system's current control strategies for data collection purposes. As a result, data could not be collected for various condenser water flow rates, cooling tower fan speeds or for entering condenser water temperatures lower than the setpoint temperature of 65°F (18.3°C). The data collected was used to develop component models of the condenser water pump, chiller and cooling tower with the goal of predicting how the system would perform with varying condenser pump and cooling tower fan speeds.

4. MODELING

4.1 Overview

Table 4.1 gives an overview of the inputs and outputs for each individual model. The respective outputs from each model feed into the other models to simulate the overall system. First the building's cooling load must be predicted to determine the load that must be met by the chiller. Second, a correlation between the condenser water pump input power and the resulting condenser water flow rate needs to be established. The condenser water flow rate can then be used as an input to both the cooling tower and chiller model. The outputs of the chiller and cooling tower model play into the other model which requires the overall system to be solved iteratively with respect to the inlet and outlet condenser water temperature.

Table 4.1.: Overview of Modeling Inputs & Outputs

Model	Inputs	Outputs
Cooling Load Prediction	Ambient Temperature, Relative Humidity, Solar Radiation, Occupied Hours, Day of Week	Building Cooling Load
Pump Model	Full Load Pump Power, Full Load Pump Flow Rate, Curve Coefficients	Condenser Water Flow Rate
Cooling Tower Model	Ambient Temperature, Relative Humidity, Air Mass Flow Rate, Water Mass Flow Rate, Tower Constants, Tower Inlet Water Temperature, Initial Guess for Tower Outlet Water Temperature	Tower Outlet Water Temperature
Chiller Model	Cooling Load, Max Cooling Load, Tower Outlet Water Temperature, Regressed Coefficients, Condenser Water Flow Rate, Initial Guess for Condenser Outlet Water Temperature	Chiller COP
Combined Model	Cooling Load, Chiller COP, Chiller Power, Tower Inlet Water Temperature, Condenser Water Flow Rate	Chiller Power, Condenser Outlet Water Temperature

4.2 Cooling Load Prediction

Determining a building's cooling load generally requires the evaporator flow rate and the temperature difference across the evaporator. Without data for the water flow rate on the evaporator side of the chiller, the cooling load had to be determined using the temperature difference across the condenser and the condenser water flow rate by

deducting the compressor's power from condenser water load. The calculated cooling load is subject to a large degree of variation with minimal change in temperature difference across the condenser. In order to reduce noise in the calculated cooling load, the one-hour moving average of the load was substituted for the 15-minute discreet load. Figure 4.1 shows how the one hour moving average of the cooling load reduces the noise in the system's measured values.

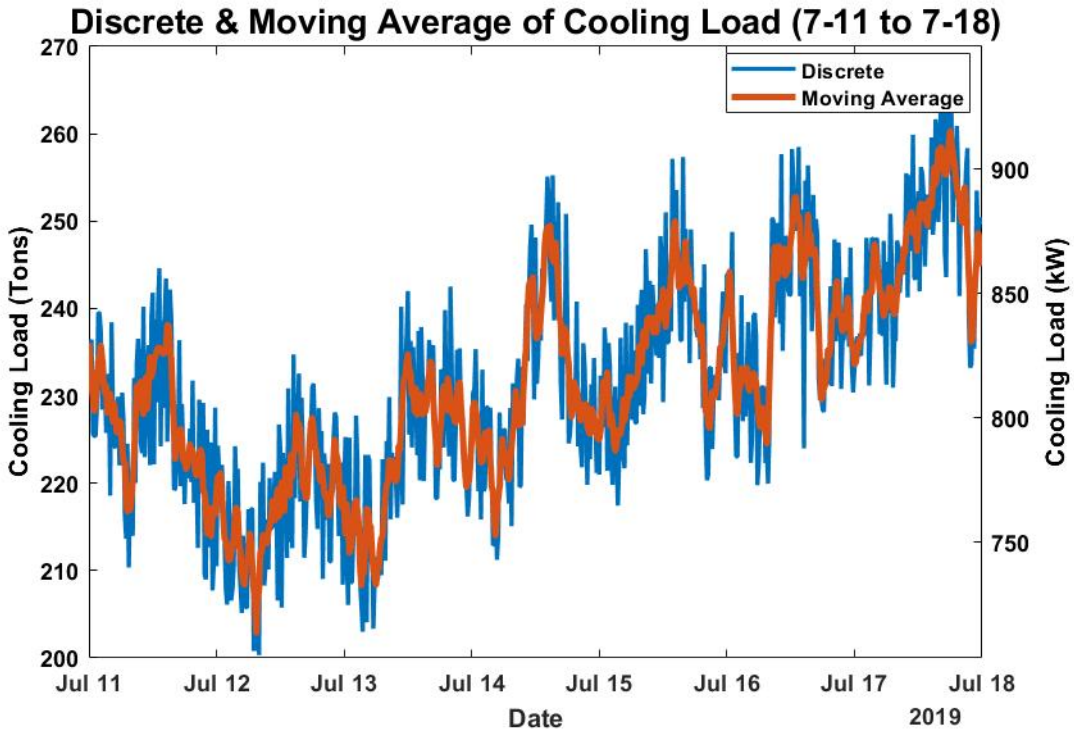

Fig. 4.1.: Discrete & Moving Average of Cooling Load

Replacing the discreet cooling load with the moving average creates a clearer view of how the building's cooling load changes over time and will help improve the model's predictive capabilities. The next step in the process is to decide what form of cooling load prediction modeling would be most applicable to the situation. Without detailed information pertaining to the building's infrastructure, using a simulation software predict the cooling load would not be suitable. Instead a multiple non-linear regression algorithm was chosen for the load prediction model because it can achieve

good correlation for various building types with low computation requirements and without exceedingly detailed building information. Table 4.2 shows the inputs and the data sources for the variables included in the cooling load prediction regression model.

Table 4.2.: Cooling Load Prediction Model Inputs & Data Sources

Input	Data Source
Occupied Hours	Building Schedule
Solar Radition	NOAA Quality Controlled Datasets [55]
Temperature	NOAA Quality Controlled Datasets [55]
Relative Humidity	NOAA Quality Controlled Datasets [55]
Cooling Load	Calculated from: BAS data, Condenser Water Flow Rate & Chiller Power
Day of Week	Data Timestamp
Regression Coefficients	Regression of Collected Data

The environmental variables that have been shown to have the greatest influence over a building's cooling load are the dry-bulb temperature, relative humidity and solar irradiance [40]. The weather data used to train the regression model was obtained from the National Oceanic and Atmospheric Administration's quality-controlled datasets [55]. The sub-hourly dataset contains 5-minute data for a wide range of variables collected with USCRN and USRCRN weather stations across the country. The only set containing solar irradiance data for the state of Indiana was collected from a USCRN station in Bedford, Indiana. Although Bedford is roughly 70 miles south of Indianapolis, the weather data from this station was assumed to be similar enough to Indianapolis' weather to incorporate the data into the regression model. To account for occupancy related loads, Boolean variables were added to incorporate each day of the week and to distinguish between occupied and unoccupied hours. Additionally, it has been shown that adding a term for the cooling load from

two hours prior to the current time step can greatly improve the regression model's accuracy [40]. Eq. 4.1 shows the initial multiple non-linear regression equation that was developed. In addition to the individual variables, a second order term for the temperature and an interaction term between the temperature and humidity were added to the regression equation. The Least Squares method was used to determine the coefficients for the regression modeling.

$$\begin{aligned} Q_L = a_1 * (Occupied) + a_2 * (T) + a_3 * (RH) + a_4 * (SolarRad.) + \\ a_5 * (T^2) + a_6 * (T * RH) + a_7 * (Q_{L,2HR}) + a_8 * (Mon.) + a_9 * (Tue.) + \\ a_{10} * (Wed.) + a_{11} * (Thur.) + a_{12} * (Fri.) + a_{13} * (Sat.) + a_{14} * (Sun.) + b \end{aligned} \tag{4.1}$$

After performing an analysis on the initial regression model, any variable found to have p-value of greater than 0.05 was determined to be statistically insignificant to the model and the variable was removed from the cooling load prediction model. Eq. 4.2 shows the final regression model used after statistically insignificant variables were removed. Table 4.3 shows the regression coefficients determined through the least square's method. Figure 4.2 displays the predicted cooling load from the regression analysis with the measured cooling load for a week in July. Figure 4.3 shows the measured vs. the predicted cooling load for the whole dataset.

$$\begin{aligned} Q_L = a_1 * (Occupied) + a_2 * (SolarRad.) + a_3 * (T^2) + a_4 * (T * RH) + \\ a_5 * (Q_{L,2HR}) + a_6 * (Sat.) + b \end{aligned} \tag{4.2}$$

Table 4.3.: Cooling Load Regression Coefficients

Coefficients	a1	a2	a3	a4	a5	a6	b
English Units	Tons	$\frac{Tons}{\frac{Btu}{(ft^2 \times hr)}}$	$\frac{Tons}{(^\circ F)^2}$	$\frac{Tons}{(^\circ F \times \%)}$	$\frac{Tons}{Tons}$	$\frac{1}{Tons}$	Tons
Values	-1.444	0.02645	0.1922	0.001951	0.7946	1.0411	22.18
SI Units	kW	$\frac{kW}{\frac{W}{m^2}}$	$\frac{kW}{(^\circ C)^2}$	$\frac{kW}{(^\circ C \times \%)}$	$\frac{kW}{kW}$	$\frac{1}{kW}$	kW
Values	-5.3878	0.02872	2.1264	0.02644	0.7915	3.7416	104.54

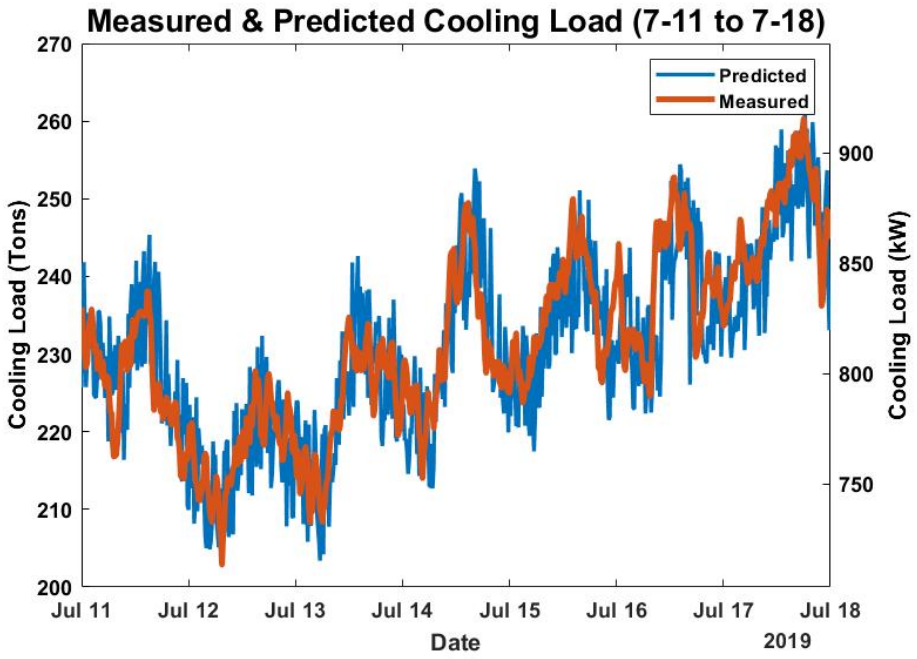

Fig. 4.2.: Measured & Predicted Building Cooling Load

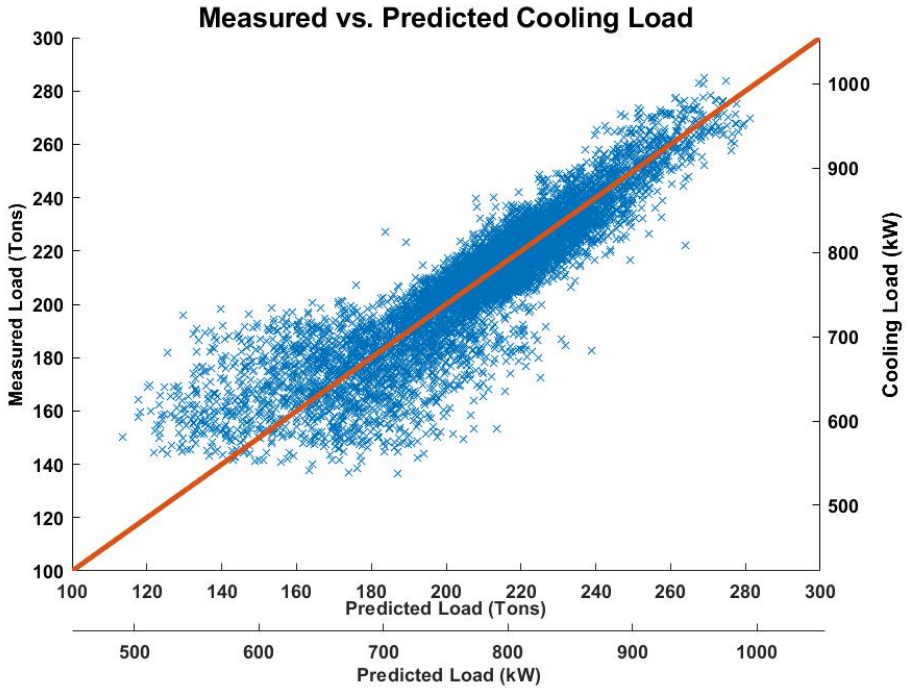

Fig. 4.3.: Measured vs. Predicted Cooling Load

Substituting the moving average for the discreet values greatly increased the final regression model's correlation from a R^2 of 0.7545 to a R^2 of 0.9302. The RSME (a statistical indicator of the average difference between predicted and observed values in a model) of the final regression model was calculated to be 6.883 tons. To validate the regression model, every third time point was removed from the dataset to create two unbiased datasets that both span the range of environmental conditions registered over the data collection period. The dataset containing two-thirds of the data was used to train the regression model and predict the cooling load for the validation dataset. The results showed that both the training dataset and the validation dataset possessed the same prediction capabilities as the model developed using the entire dataset. Figure 4.4 shows the measured vs. predicted cooling loads for the training and validation datasets.

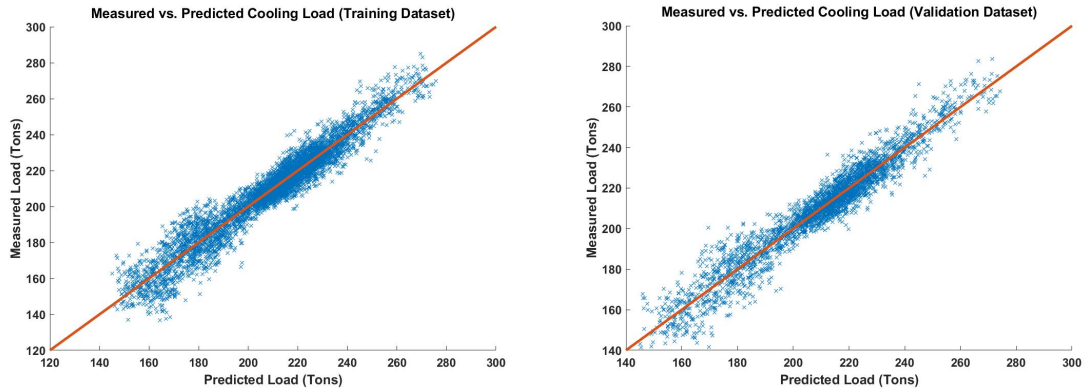

(a) Training Dataset

(b) Validation Dataset

Fig. 4.4.: Measured vs. Predicted Cooling Load for Training & Validation Datasets

4.3 Pump Modeling

The condenser water flow rate is an important factor in optimizing the system's overall energy consumption because it affects the performance of both the chiller and the cooling tower. A relationship between the pump's power consumption and the condenser water flow needed to be determined, however since the condenser water

pump only operates at full capacity, using empirical measurements of the relationship at multiple pump speeds could not be achieved. The National Renewable Energy Laboratory developed a simple method to estimate the relationship between water flow rate and pump power for a broad range of system configurations known as the default curve method. The method uses a polynomial expression and predetermined correlation coefficients relating the pump's power consumption to the condenser water flow rate [56]. The default curve method was developed for the expressed purpose of evaluating the energy saving potential of a VFD controlled centrifugal pump over a broad range of system configurations for which empirical relationships could not be determined, therefore the method was found to be suitable for the required application. Table 4.4 shows the inputs and the data sources for the condenser pump default curve model.

Table 4.4.: Pump Model Inputs & Data Sources

Inputs	Data Source
Full Load Flow Rate	Fuji FCS Ultrasonic Flowmeter
Full Load Pump Power	Fluke 1732 Power Analyzer
Correlation Coefficients	NREL VFD Evaluation Protocol [56]

The only values required for the default curve method are the full load condenser pump power, full load flow rate and the correlation coefficients for a VFD controlled centrifugal pump. Eq. 4.3 shows the relationship between pump power and flow rate using the correlation coefficients for a VFD controlled centrifugal pump. The terms for both flow and power are input as the percentage of the value to its maximum.

$$Flow = 0.219762 - 0.874784 * Power + 1.652597 * (Power)^2 \tag{4.3}$$

The measurements of the water flow rate and condenser pump power with the pump running at full speed were 671 gpm (42.3 L/s) and 11.2 kW respectively. The values represent the maximum for both the water flow rate and the pump's power consump-

tion for the given configuration. Inputting these max load values into the default curve method correlation develops an estimate of the relation between the condenser water flow rate and the condenser water pump power over the range of applicable operating conditions. The relationship that was developed can be in seen Eq. 4.4.

$$\begin{aligned}
[English]\ \frac{\dot{V}_w}{671gpm} &= 0.219762 - 0.874784 * (\frac{P_p}{15hp}) + 1.652597 * (\frac{P_p}{15hp})^2 \\
[SI]\quad \frac{\dot{V}_w}{42.33L/s} &= 0.219762 - 0.874784 * (\frac{P_p}{11.2kW}) + 1.652597 * (\frac{P_p}{11.2kW})^2
\end{aligned} \tag{4.4}$$

The chiller's condenser is a two-pass shell and tube heat exchanger which has a minimum water flow rate of 367 gpm (23.7 L/s). Figure 4.5 shows the pump's power vs. flow rate with the red line indicating the minimum flow rate that should be pumped through the chiller.

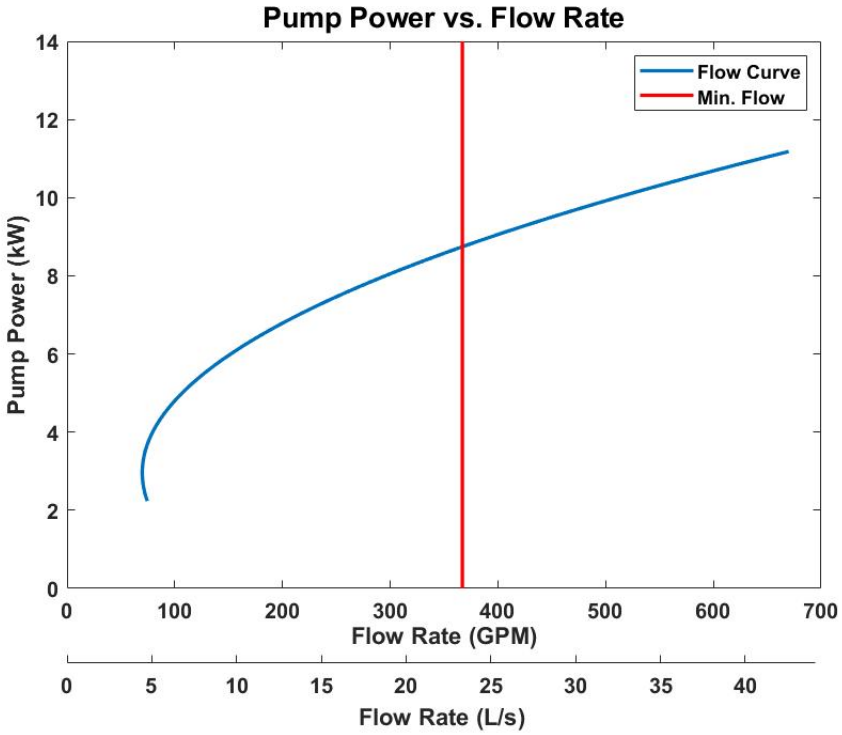

Fig. 4.5.: Pump Power vs. Flow Rate

The minimum flow rate in the heat exchanger is set to keep the tube side water flow rate from becoming laminar. Laminar flow would greatly reduce the heat transfer between the refrigerant and the condenser water. To keep the flow rate through the heat exchanger turbulent, the pump's power should be kept above 11.8 HP (8.8 kW).

4.4 Cooling Tower Modeling

Long term data for the cooling tower fan's line amps was collected using an Onset UM120-006M data logger and a CTV-C 10-100-amp current transducer. The cooling tower fan power and line amps were measured using the Fluke 1732 three-phase power analyzer at fan speeds of 25%, 50%, 75% and 100%. The data collection process was designed to adhere to the recommendations from NREL's VFD evaluation protocol of fans in luie of long-term true power measurements [56]. The measurements were used to determine the relationship between the cooling tower's fan speed, the motor's line amps and power consumption. The correlations were used in luie of true long-term power measurements because for an online adaptive control system monitoring the cooling tower's line amps would be cheaper than using a device to constantly monitor the fan's true power consumption. The correlation between motor line amps and the motor power consumption can be seen in Figure 4.6. Figure 4.7 shows the relationship between the fan speed and the motor power consumption and graphs the relationship in comparison to affinity laws. The fan's power consumption in relation to speed was found to closely mirror affinity. A second order polynomial relationship was used to related fan power consumption and amps to the cooling tower's fan speed and subsequently to the cooling tower airflow rate. Actual airflow measurements of cooling tower fans are difficult to obtain so the cooling tower's the airflow rate was assumed to vary linearly in relation to fans speed as according to affinity laws. The design air flow rate of the cooling tower operating at full fan speed is 74,350 CFM (35.1 m^3/s).

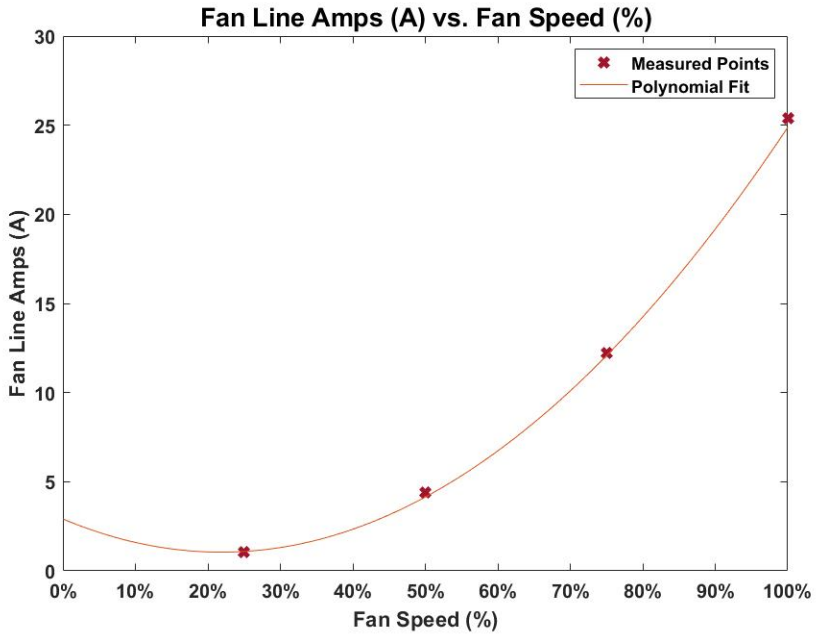

Fig. 4.6.: Cooling Tower Fan Line Amps vs. Fan Speed (%)

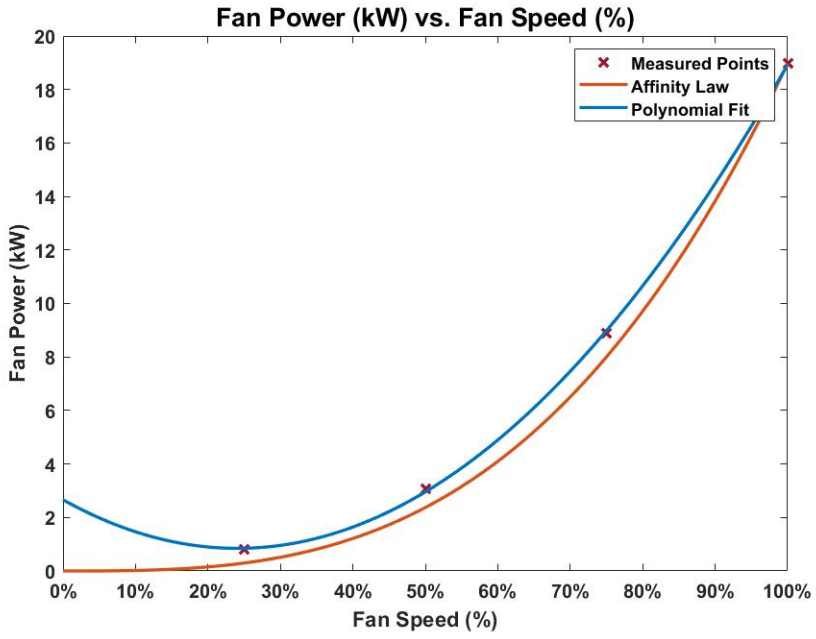

Fig. 4.7.: Cooling Tower Fan Power vs. Fan Speed(%)

The building automation system controlling the cooling tower fan operates the fan speed at 100% until the tower supply water temperature reaches a setpoint of 65°F (18.3°C). Once the temperature setpoint has been reached the cooling tower cycles between 25% and 100% fan speed to maintain the tower supply temperature approximately at the setpoint temperature. During the warmer months the cooling tower fan speed constantly ran at full speed, however once the ambient wet bulb temperature fell during the cooler months the fan began cycling to maintain the setpoint temperature. Figure 4.8 and Figure 4.9 display the differences in the cooling tower fan's operational behavior during warmer and colder months of the cooling season.

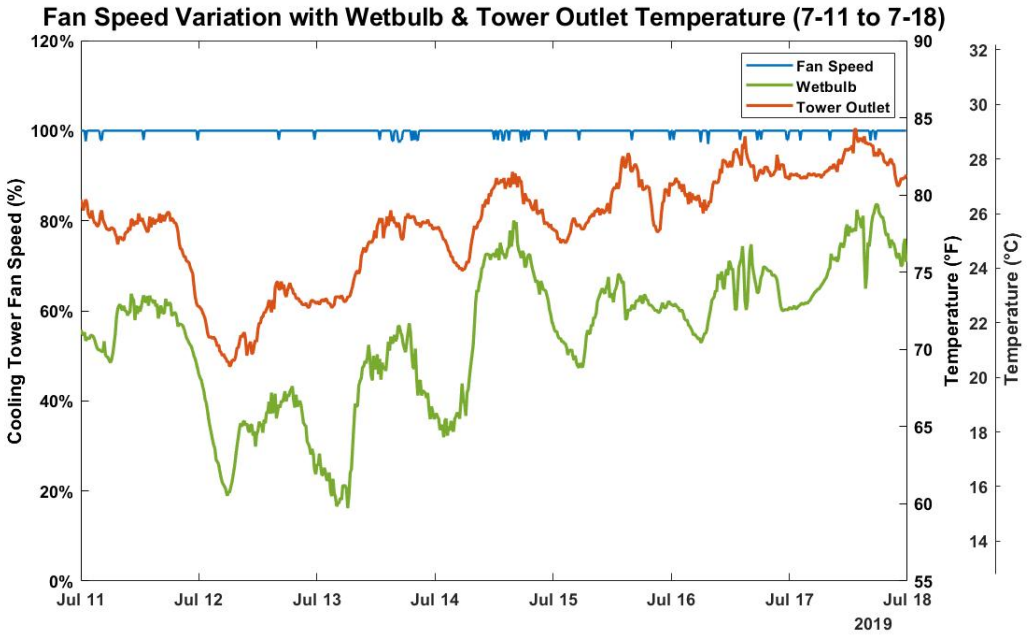

Fig. 4.8.: Cooling Tower Speed vs. Wetbulb & Tower Outlet Temperature (Jul.)

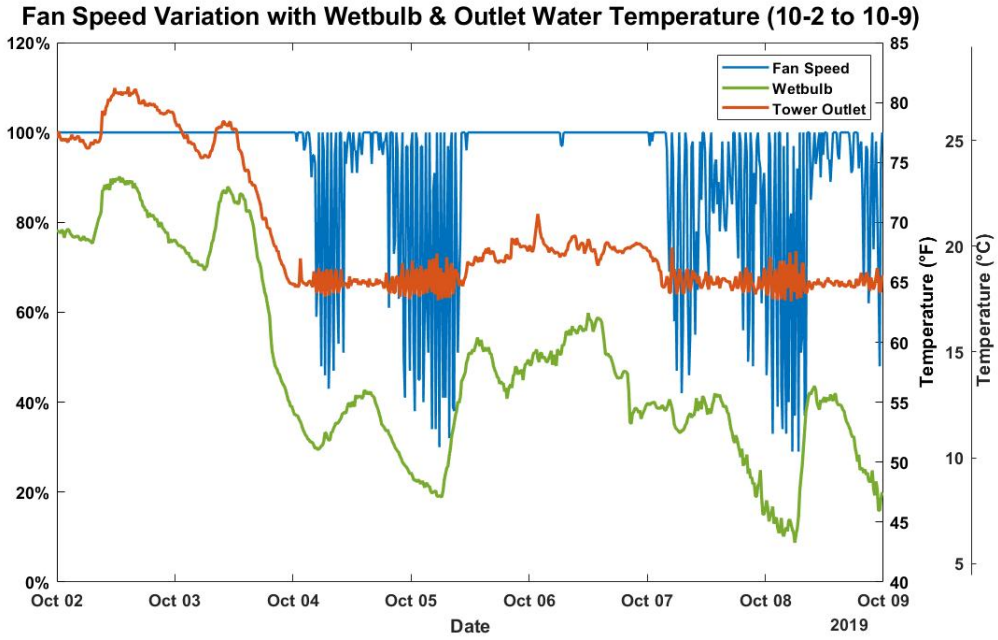

Fig. 4.9.: Cooling Tower Speed vs. Wetbulb & Tower Outlet Temperature (Oct.)

The cycling of the cooling tower made processing and modeling the cooling tower data more difficult because during these periods the system is constantly fluctuating. The sharp variation in the tower fan's speed would lead to inconsistent results in a system that is assumed to be in a relatively steady state condition. The intermittent nature of the fan during the periods where it cycles brought about the removal of the data from 9/27-10/30 for training the cooling tower model. As a result, the entire cooling tower dataset is comprised of only one value for both the air and water volumetric flow rates. EnergyPlus models cooling towers using either the CoolTool's algorithm or the YorkCalc correlation, both of which are simply high-order multi-parameter regression models that incorporate water flow rate, airflow rate, wet-bulb temperature and tower range as input variables to calculate the tower approach [32]. Regression models can be very accurate; however, they are erratic when extrapolating input variables beyond the range of operating conditions used to train the model. Without a large amount of training data that encompasses the entire range of operating conditions, empirically based regression models could not be used to model

the cooling tower. Instead, the NTU-effectiveness model was selected because it can achieve accurate estimations for outlet water temperatures without the extensive data requirements and without complicated tower information. Table 4.3 details the inputs required for the NTU-effectiveness model and how the values were obtained.

Table 4.5.: Cooling Tower Model Input Data Sources

Input	Data Source
Ambient Temperature	NOAA Quality Controlled Datasets [55]
Relative Humidity	NOAA Quality Controlled Datasets [55]
Fan Power	Fluke 1732 Power Analyzer
Air Mass Flow Rate	Affinity Laws & Tower Specifications
Condenser Water Flow Rate	Condenser Water Pump Model
Tower Inlet Water Temperature	Mass & Energy Balance
Tower Outlet Water Temperature	Initial Guess & Cooling Tower Model
Tower Constants	Regression of Performance Data
Psychrometric Data	Psych:Psychrometric Calculator [57]

4.4.1 Physical Equations

Figure 4.10 shows a diagram for the mass and energy balance done on an incremental volume of cooling tower. The mass and energy balance is the basis of the physical equations used to determine the tower's outlet water temperature.

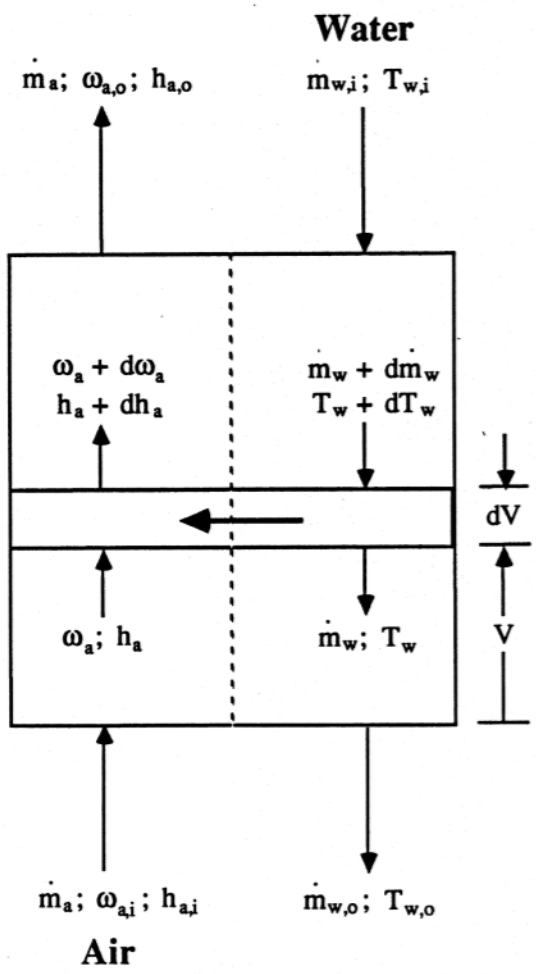

Fig. 4.10.: Mass & Energy Balance on Incremental Tower Volume [44]

The physical equations used to develop the NTU-Effectiveness model were first proposed by Merkel [42]. The relationships presented are derived from performing a mass and energy balance on an incremental tower volume and numerically integrating the equations over the entire tower volume. The psychrometric variables required to solve the physical equations were calculated using Psych, an opensource psychrometric calculator developed by UC Davis' Western Cooling Efficiency Center [57]. The psychrometric calculator can calculate a range of properties for moist air using equations established in the ASHRAE 2005 Fundamentals Handbook [58]. The equations as presented strongly reflect those presented by Braun [44]. Assuming there is

negligible heat transfer from the tower walls, a steady state energy balance for an incremental volume of the tower can be given by Eq. 4.5.

$$\begin{aligned} \dot{m}_a dh_a &= d(\dot{m}_w h_{f,w}) \\ &= \dot{m}_w dh_{f,w} + h_{f,w} d\dot{m}_w \end{aligned} \tag{4.5}$$

The steady state mass balance on the fluid streams presents the relationship for the incremental water loss in the tower due to evaporation into the air stream as seen in Eq. 4.6.

$$\begin{aligned} d\dot{m}_w &= \dot{m}_a d\omega_a \\ \dot{m}_w &= \dot{m}_{w,i} - \dot{m}_a(\omega_{a,o} - \omega_a) \end{aligned} \tag{4.6}$$

Using the steady state mass and energy balance and assuming a constant specific heat for water and a zero enthalpy reference temperature of zero degrees, the change in water temperature across an incremental tower volume can be determined using Eq.4.7.

$$dT_w = \frac{dh_a - C_{p,w}(T_w - T_{ref})d\omega_a}{[\frac{\dot{m}_{w,i}}{\dot{m}_a} - (\omega_{a,o} - \omega_a)]C_{p,w}} \tag{4.7}$$

The enthalpy of the air stream increases at the rate at which energy is transferred from the water through both sensible and latent heat exchange. Thus the incremental change in air enthalpy is given by Eq. 4.8.

$$\dot{m}_a dh_a = h_C A_V dV(T_w - T_a) + h_{g,w}\dot{m}_a d\omega_a \tag{4.8}$$

Using the humidity ratio to represent the mass fraction of water vapor in the air stream, the mass transfer rate of water vapor into the air stream is given by Eq. 4.9.

$$\dot{m}_a d\omega_a = h_D A_V dV(\omega_{s,w} - \omega_a) \tag{4.9}$$

The Lewis Number is the dimensionless number defined as the ratio between thermal diffusivity and mass diffusivity. It is used as a parameter to describe fluid flows containing both heat and mass transfer. The Lewis number used to characterized cooling tower fluid flows is defined as seen in Eq. 4.10.

$$Le = \frac{h_c}{h_D C_{pm}} \tag{4.10}$$

Where h_c is the convection heat transfer coefficient, h_D is the mass transfer coefficient and C_{pm} is the constant pressure specific heat of moist air. Substituting the relationship for the mass transfer of water to air into the incremental enthalpy balance of the air stream and implementing the definition of the Lewis number creates the relationship shown in Eq. 4.11.

$$\begin{aligned} \dot{m}_a h_a &= h_D A_V dV[LeC_{pm}(T_w - T_a) + (\omega_{s,w} - \omega_a)h_{g,w}] \\ &= Leh_D A_V dV[(h_{s,w} - h_a) + (\omega_{s,w} - \omega_a)(\frac{1}{Le} - 1)h_{g,w}] \end{aligned} \tag{4.11}$$

For a cooling tower the overall number of heat transfer units in the tower is defined by Eq. 4.12.

$$Ntu = \frac{h_D A_V V_T}{\dot{m}_a} \tag{4.12}$$

Implementing the definition for a cooling tower's Ntu, the incremental change in the humidity ratio and the incremental change in air enthalpy across the cooling tower volume can be given by Eq 4.13 and Eq. 4.14.

$$\frac{d\omega_a}{dV} = -\frac{Ntu}{V_T}(\omega_a - \omega_{s,w}) \tag{4.13}$$

$$\frac{dh_a}{dV} = -\frac{LeNtu}{V_T}[(h_a - h_{s,w}) + (\omega_a - \omega_{s,w})(\frac{1}{Le} - 1)h_{g,w}] \tag{4.14}$$

The outlet air and water stream conditions can be solved for a given inlet conditions, number of units and Lewis number by iteratively integrating the equations over the tower volume. Merkel's cooling tower model neglects water loss from evaporation and assumes a Lewis number of unity to simplify the analysis [42]. The simplifications allow one to define the incremental change in air enthalpy and water temperature with respect to tower volume as given in Eq. 4.15 and Eq. 4.16.

$$\frac{dh_a}{dV} = -\frac{Ntu}{V_T}(h_a - h_{s,w}) \tag{4.15}$$

$$\frac{dT_w}{dV} = \frac{\dot{m}_a(\frac{dh_a}{dV})}{\dot{m}_w C_{pw}} \tag{4.16}$$

The Ntu-effectiveness model is another physical model which predicts a tower's outlet water temperature given the inlet water temperature and flow rate and the inlet

air temperature, humidity and flow rate. The model builds on Merkel's analysis by assuming a linear variation in air saturation enthalpy with respect to temperature and incorporating water loss due to evaporation [44]. Figure 4.11 shows an example of a linearly estimated derivative of air saturation enthalpy with respect to temperature.

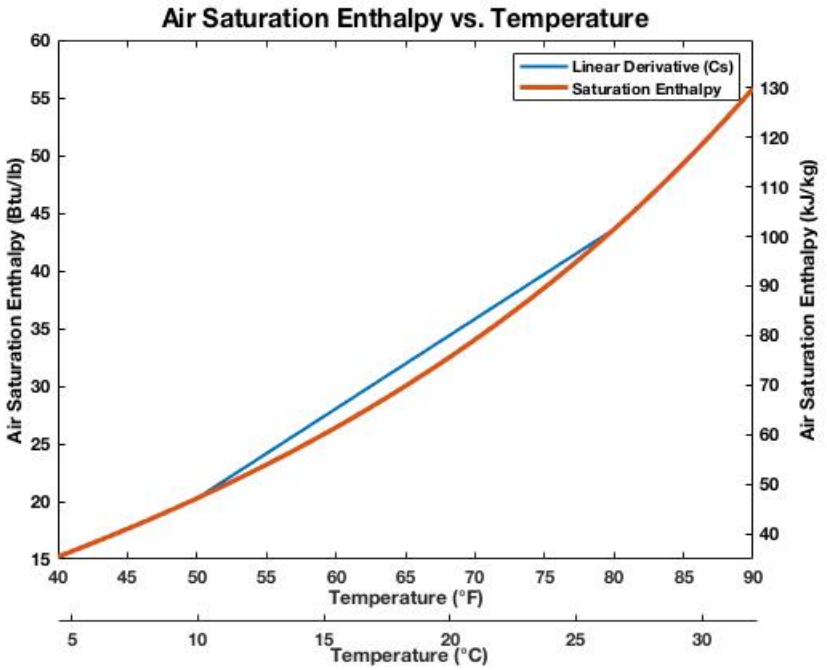

Fig. 4.11.: Saturation Air Enthalpy vs. Temperature

The linearly estimated derivative of the saturation air enthalpy with respect to temperature is calculated as seen in Eq. 4.17. To determine C_S, an initial guess is needed for the outlet water temperature, which is where the model becomes iterative with respect to the outlet water temperature.

$$\begin{aligned} C_S &= [\frac{dh_s}{dT}]_{T=T_w} \\ C_S &\approx \frac{h_{s,w,i} - h_{s,w,o}}{T_{w,i} - T_{w,o}} \end{aligned} \tag{4.17}$$

Braun's Ntu effectiveness model reevaluates Merkel's term for the incremental change in air enthalpy with respect to tower volume (Eq. 4.14) in terms of only air enthalpies by introducing the linearly estimated derivative of saturated air enthalpy calculated

at the inlet water temperature and an initial guess for the tower outlet water temperature. Eq. 4.18 shows how the relationship between the incremental change in enthalpy with respect to tower volume changes with the introduction of C_S.

$$\frac{dh_{s,w}}{dV} = \frac{\dot{m}_a C_S(\frac{dh_a}{dV})}{\dot{m}_w C_{p,w}} \tag{4.18}$$

The heat rejection rate of the tower is evaluated by defining an air side effectiveness term as the ratio to the actual heat transfer to the maximum heat transfer possible. The maximum air-side heat transfer occurs if the air stream leaving the tower is fully saturated at the temperature of the inlet water stream. Eq. 4.19 shows the relationship between the air-side effectiveness and the overall heat transfer in the cooling tower.

$$\dot{Q} = \epsilon_a \dot{m}_a (h_{s,w,i} - h_{a,i}) \tag{4.19}$$

The air side effectiveness term is defined with the number of transfer units and a term that incorporates the ratio between the air and water mass flow rates and the ratio between the linearly estimated derivative between the saturated air enthalpy and temperature and the constant pressure specific heat of water. Eq. 4.20 displays the term used to relate the mass flow ratios for determining the air-side effectiveness. Eq 4.21 shows how the effectiveness is evaluated from the mass ratio term and the number of transfer units.

$$m^* = \frac{\dot{m}_a(C_S)}{\dot{m}_{w,i}(C_{pw})} \tag{4.20}$$

$$\epsilon_a = \frac{1 - exp(-Ntu(1-m^*))}{1 - m^* exp(-Ntu(1-m^*))} \tag{4.21}$$

Executing energy balances on the air and water streams results in relations that can be solved for the exit air enthalpy and the exiting water temperature as seen in Eq. 4.22 & Eq. 4.23.

$$h_{a,o} = h_{a,i} + \epsilon_a (h_{s,w,i} - h_{a,i}) \tag{4.22}$$

$$T_{w,o} = \frac{\dot{m}_{w,i}(T_{w,i}) C_{p,w} - \dot{m}_a (h_{a,o} - h_{a,i)}}{\dot{m}_{w,o} C_{p,w}} \tag{4.23}$$

In order to incorporate the water loss from evaporation into the analysis, an effective saturated air enthalpy is defined using the inlet and outlet air conditions and the number of heat transfer units as seen in Eq. 4.24.

$$h_{s,w,e} = h_{a,i} + \frac{h_{a,o} - h_{a,i}}{1 - exp(-Ntu)} \tag{4.24}$$

From the effective saturated air enthalpy, an effective saturated humidity ratio is determined using psychrometric relations between the enthalpy and the humidity ratio for completely saturated air. The humidity ratio for the exit air stream can then be calculated using the relation presented in Eq. 4.25.

$$\omega_{a,o} = \omega_{s,w,e} + (\omega_{a,i} - \omega_{s,w,e})exp(-Ntu) \tag{4.25}$$

The exiting water flow rate can then be determined using a mass balance on the inlet water flow rate by deducting the mass flow rate of water evaporated into the air stream as seen in Eq. 4.26.

$$\dot{m}_{w,o} = \dot{m}_{w,i} - \dot{m}_a(\omega_{a,o} - \omega_{a,i}) \tag{4.26}$$

The final piece of information necessary to proceed with the calculations is to determine a correlation for a cooling tower's Ntu. Braun's method manipulates a correlation between the air and water mass flow rates, tower volume, mass transfer coefficient and the surface area of water droplets per unit volume of cooling tower shown in Eq. 4.27.

$$\frac{h_D A_V V_T}{\dot{m}_w} = c[\frac{\dot{m}_w}{\dot{m}_a}]^n \tag{4.27}$$

Multiplying both sides of the correlation by the ratio between the mass flow rate of water and the mass flow rate of air and using the definition of the number of transfer units creates a simple correlation for determining the number of transfer units in a cooling tower as seen in Eq. 4.28.

$$Ntu = c[\frac{\dot{m}_w}{\dot{m}_a}]^{1+n} \tag{4.28}$$

The values for c and n are empirically determined constants that are specific to a particular cooling tower. The values of c and n can be determined with a straight-line

correlation of a log-log plot of Ntu versus the mass flow rate ratio of water to air where the slope is equal to (n+1) and the intercept equal to log(c). The dataset collected had no variation in the air or water mass flow rate ratio, so performance data published by the Baltimore Aircoil Company for the VT1-307-0 cooling tower was used to introduce datapoints with varying water flow rates [59]. Using performance data alone was found to slightly over predict cooling tower performance so the dataset was combined with selected datapoints from the collected dataset. The selected points were chosen to span the range of wet bulb temperatures for which the data was collected and so that half of the dataset is made up of the published performance data and half from the collected data for the tower.The log-log plot of Ntu vs. the mass flow ratio can be seen in Figure 4.12.

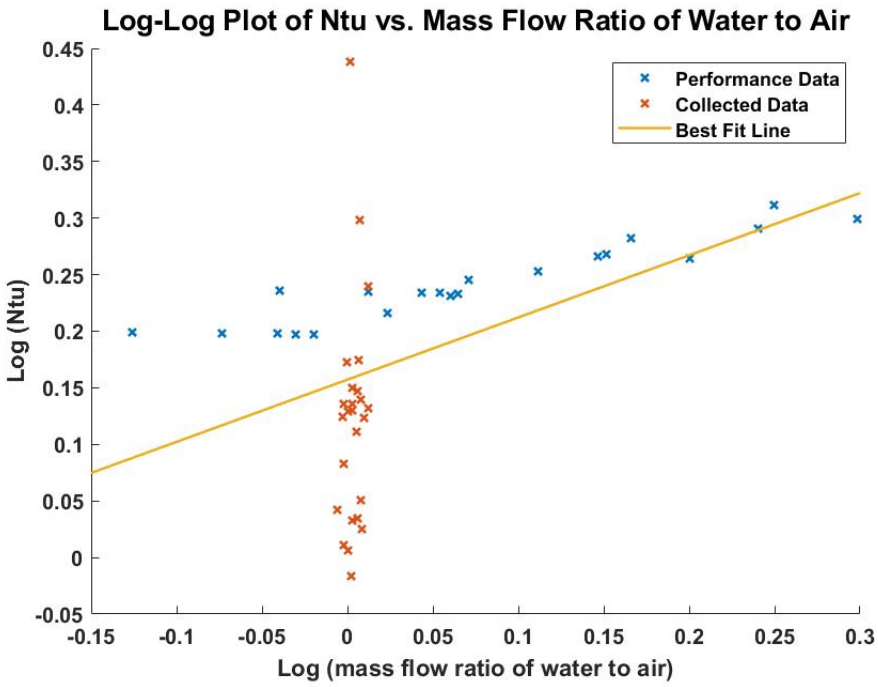

Fig. 4.12.: Log-Log Plot of Ntu vs. Mass flow Ratio of Water to Air

In Figure 4.12, the data collected from the Eiteljorg's system is centered around a single value for the log of the mass flow ratio, while the published performance data spreads across the x-axis. The combination of these datasets enables the calculation

of the cooling tower constants and removes the model's tendancy to overpredict the cooling tower's effectiveness. The tower constants, R^2 and RSME for performance data alone and for the combined dataset can be seen in Table 4.4. Figure 4.13 shows the measured vs. predicted tower outlet water temperature using the coefficients determined from the combined dataset. Figure 4.14 shows the measured and predicted tower outlet water temperature for a week in July.

Table 4.6.: Cooling Tower Constants

Constant	C	n	R^2	RSME
Performance Data	1.66379	-0.7017	0.917	1.343
Combined Dataset	1.43714	-0.4378	0.929	1.186

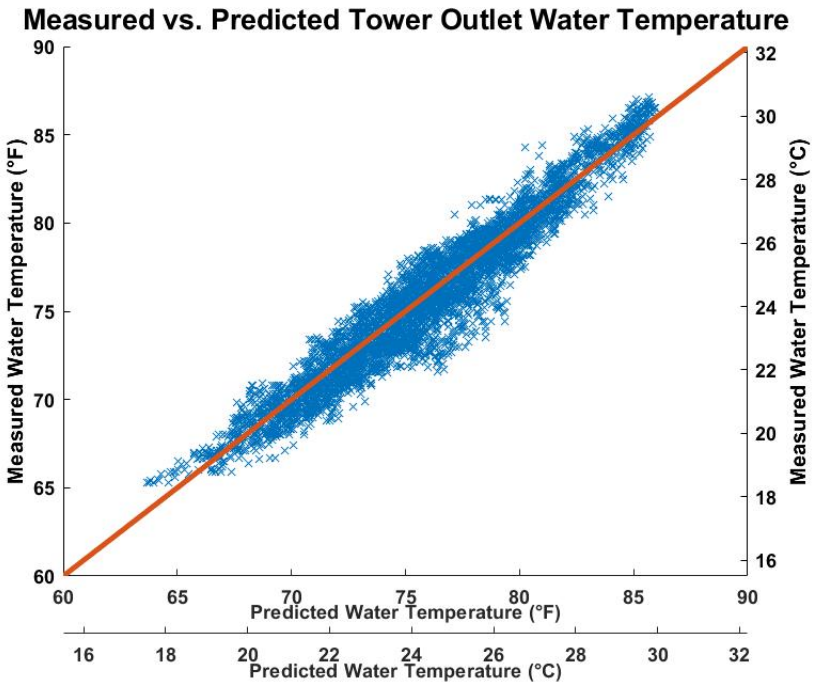

Fig. 4.13.: Measured vs. Predicted Tower Outlet Water Temperature

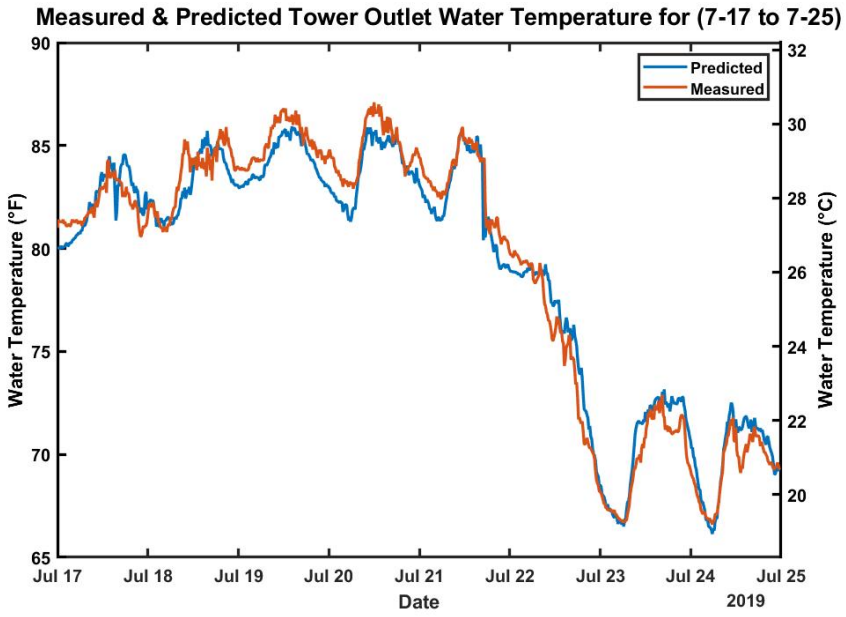

Fig. 4.14.: Measured & Predicted Tower Outlet Water Temperature

Solving the Ntu-effectiveness model is iterative with respect to the outlet water temperature and requires an initial guess to solve for C_s. Using the ambient wet bulb temperature as the preliminary estimate for the outlet water temperature was observed to converge in roughly a single iteration. By the third iteration, the R^2 increased slightly from 0.929 to 0.938 while the RSME remained relatively constant.

4.5 Chiller Modeling

The chiller performance data was collected using a combination of an Onset UM120-006M HOBO data logger with a CTV-E 60-600 Amp current transducers and a Fluke 1732 three phase power analyzer. The data logger was used to collect long-term current data for a single phase of the chiller, while the Fluke power analyzer was used to create a correlation between the chiller's power consumption and the line amps through each of the three phases. Utilizing both data sources allowed the chiller's power consumption to be determined for the entire data collection period without requiring multiple power analyzers for an excessively long time period.

The primary consideration when analyzing potential chiller models was the model's ability to incorporate condenser water flow rate as an optimization variable. Most models with the ability to account for variable condenser water flow rate require large datasets that span the entire range of the chiller's operating conditions. Without the freedom to manipulate the system's flow rate, data could only be collected for the flow rate of 671 GPM (42.33 L/s) meaning the selected model would need to be able to extrapolate the chiller's operating character under different condenser flow rates. EnergyPlus offers well-developed default curve coefficients for the reformulated electric chiller model for different types of chillers of various sizes. Upon applying the default curve coefficients to the collected dataset it was found the that the correlation between the default curve model and the collected data set was substandard. Chillers tend to have unique internal control mechanisms which generate distinctive performance characteristics so the generalized default curve method couldn't accurately mimic the specific operating characteristics of the Eiteljorg's chiller. The Gordon and Ng thermodynamic chiller model was determined to be the most appropriate method due to the limited range of available data and the ability to regress physical parameters from the collected dataset. Several modifications to the original model have been made over the years, one of which emphasizes variable condenser water flow rate as a control variable. Table 4.5 shows the inputs required for the Gordon NG chiller model and the source of the input data.

Table 4.7.: Chiller Model Input Data Sources

Input	Data Source
Chiller Power	Fluke 1732 Power Analyzer
Cooling Load	Cooling Load Prediction Model
Max Cooling Load	Chiller Specifications
Chiller COP	Cooling Load & Chiller Power
Condenser Water Flow Rate	Condenser Pump Model
Condenser Outlet Water Temperature	Initial Guess, Mass & Energy Balance
Condenser Inlet Water Temperature	Cooling Tower Model
Regression Coefficients	Regression of Collected Data

The original Gordon and NG thermodynamic model can be seen in Eq. 4.29 [52]

$$\frac{T_{evap,o}}{T_{cond,i}}[1+\frac{1}{COP}] = 1 + \frac{T_{evap,o}\Delta S_{int}}{Q_L} + \frac{L}{Q_L}[\frac{T_{cond,i}-T_{evap,o}}{T_{cond,i}}] + \frac{Q_L R}{T_{cond,i}}[1+\frac{1}{COP}] \tag{4.29}$$

Given the evaporator outlet water temperature, condenser inlet water temperature and the cooling load, the model predicts the chillers COP using three unknown parameters. The internal rate of entropy generation (ΔS_{int}), rate of heat loss/gain from the environment (L) and the total heat exchanger thermal resistance (R), are regressed using measured performance data. Once these values are obtained Eq. 4.29 can be algebraically rearranged to solve for the chiller's COP using only the evaporator outlet water temperature, condenser inlet water temperature and the cooling load. Studies have shown that the assumption of a constant rate of internal entropy generation can lead to inaccuracy when attempting to model variable speed driven chillers [50], [53]. Jiang and Reddy proposed a modification to the model that incorporates a term to make the rate of internal entropy generation linear with respect to the cooling load. The modified thermodynamic equation can be seen in Eq. 4.30.

$$\frac{T_{evap,o}}{T_{cond,i}}[1+\frac{1}{COP}] = 1 + \frac{T_{evap,o}(\Delta S_{int,1} + \Delta S_{int,2}\frac{Q_L}{Q_{max}})}{Q_L} + \frac{L}{Q_L}[\frac{T_{cond,i} - T_{evap,o}}{T_{cond,i}}] + \frac{Q_L R}{T_{cond,i}}[1+\frac{1}{COP}] \tag{4.30}$$

The addition of the linear term for the internal entropy generation ($\Delta S_{int,2}$) has been shown to improve the model's accuracy for predicting the coefficient of performance, specifically for variable speed driven chillers. Figure 4.15 shows the measured vs. predicted chiller efficiency using the Gordon model with the modification proposed by Jiang and Reddy.

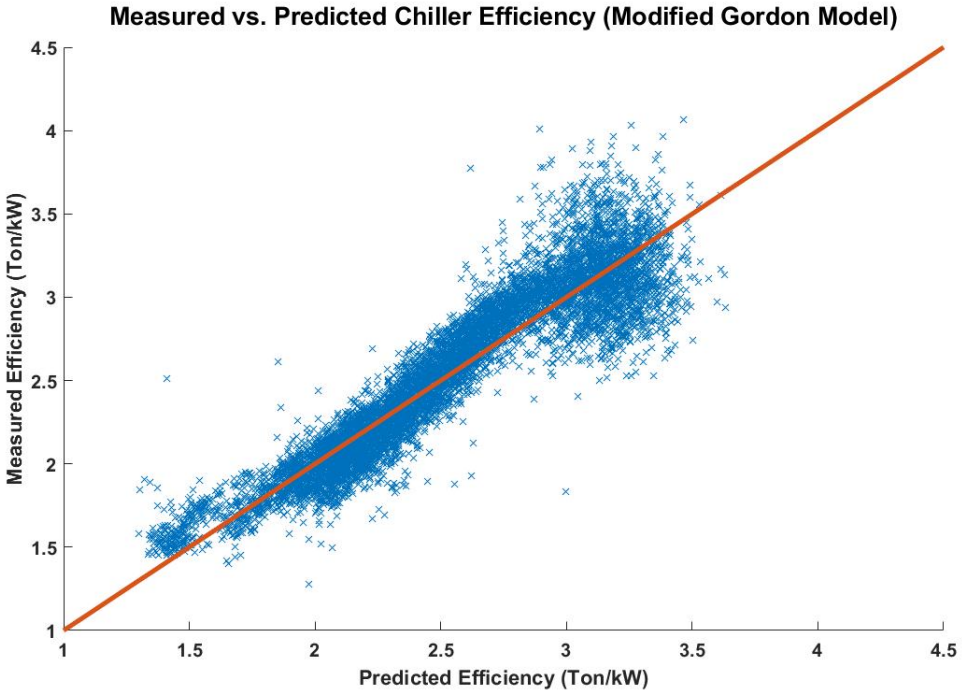

Fig. 4.15.: Measured vs. Predicted Chiller Efficiency (Modified Gordon Model)

Gordon et.al. proposed a separate modification to the original model which manipulates the heat exchanger resistance term to incorporate condenser water flow rate as a control variable. The modification brakes the heat exchanger thermal resistance into two separate pieces representing the thermal resistance of the evaporator and

condenser separately. The resistances were then defined in terms of the coolant's volumetric flow rate ($\dot{V}_w$), specific heat (C), density (ρ) and the heat exchanger effectiveness (E) as seen in Eq. 4.31.

$$R = R_{cond} + R_{evap} = \frac{1}{(\dot{V}_w \rho C E)_{cond}} + \frac{1}{(\dot{V}_w \rho C E)_{evap}} \tag{4.31}$$

Assuming the refrigerant can be characterized with an effective isothermal temperature, the heat exchanger effectiveness show in Eq. 4.32 can be rewritten as shown in Eq. 4.33.

$$E = 1 - exp(-\frac{UA}{\dot{V}_w \rho C}) \tag{4.32}$$

$$E = 1 - exp(-\frac{K}{\dot{V}_w^{\ 0.2}}) \tag{4.33}$$

Where K represents a positive constant value that describes a specific heat exchanger. Incorporating the modification into the original equation results in the variable condenser flow rate Gordon model visible in Eq. 4.34.

$$\begin{aligned} \frac{T_{evap,o}}{T_{cond,i}}[1 + \frac{1}{COP}] = 1 + \frac{T_{evap,o}\Delta S_{int}}{Q_L} + \frac{L}{Q_L}[\frac{T_{cond,i} - T_{evap,o}}{T_{cond,i}}] + \\ \frac{Q_L}{T_{cond,i}}[1 + \frac{1}{COP}] \times [\frac{1}{\dot{V}_w \rho C[1 - exp(-\frac{K}{\dot{V}_w^{\ 0.2}})]} + R_{evap}] \end{aligned} \tag{4.34}$$

The model now determines the chiller coefficient of performance as a function of four parameters, the internal rate of entropy generation (ΔS_{int}), rate of heat loss/gain from the environment (L), the heat exchanger thermal resistance for the evaporator (R_{evap}) and the heat exchanger constant (K). The four parameters can be determined using non-linear regression of measured data collected at various condenser water flow rates. Obtaining chiller data from multiple flow rates could not be accomplished. However, for the centrifugal chiller Gordon et.al used to validate the proposed model, they found that the constant K was effectively large enough that the condenser heat

exchanger resistance term could be estimated to be a function of just the condenser volumetric flow ($\dot{V}_w$), fluid specific heat (C) and fluid density (ρ) as seen in Eq. 4.35.

$$R_{cond} = \frac{1}{(\dot{V}_w \rho C)_{cond}} \tag{4.35}$$

Presuming that the heat exchanger constant K is sufficiently large enough to ignore enables one to predict how a chiller will operate under various condenser flow rates without collecting performance data from different flow rates. In order to progress with modeling the system's chiller, the assumption that the coefficient of performance is relatively uninfluenced by the constant K had to be made despite the inability to validate the assumption with the data that was collected from the Eiteljorg's system. Eq. 4.36 displays the variable condenser flow rate chiller model proposed by Gordon et.al. [51].

$$\begin{aligned} \frac{T_{evap,o}}{T_{cond,i}}[1 + \frac{1}{COP}] = 1 + \frac{T_{evap,o}\Delta S_{int}}{Q_L} + \frac{L}{Q_L}[\frac{T_{cond,i} - T_{evap,o}}{T_{cond,i}}] + \\ \frac{Q_L}{T_{cond,i}}[1 + \frac{1}{COP}] \times [\frac{1}{\dot{V}_w \rho C} + R_{evap}] \end{aligned} \tag{4.36}$$

The model is again a function of three unknown parameters ($\Delta S_{int}, L, R_{evap}$). The values of these parameters were determined using multiple linear regression of the chiller performance data collected. Once the parameters have been regressed, Eq. 4.32 can then be algebraically rearranged to solve for the chiller's COP from the performance data collected. Figure 4.16 shows the measured vs. predicted chiller efficiency from the variable condenser water flow rate Gordon model.

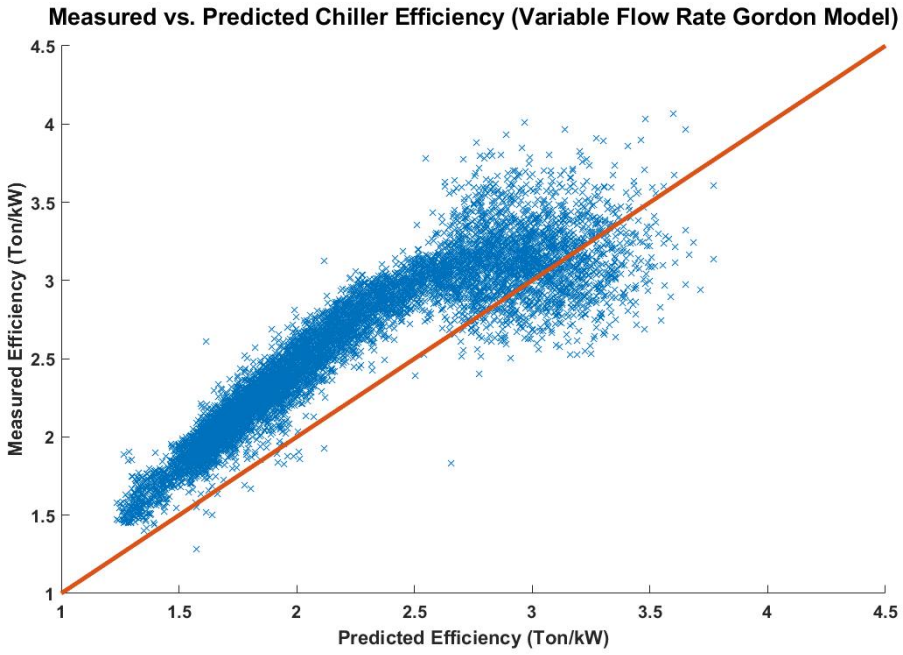

Fig. 4.16.: Measured vs. Predicted Chiller Efficiency (Variable Flow Rate Gordon Model)

The variable flow model was found to consistently underestimate the chiller's COP for the middle and lower ranges of the measured COP and possess statistically substandard RSME and R-square values compared to the modified chiller model. The deviation of the accuracy between the models suggest that, as Jiang and Reddy suggested, the addition of the linearly varying internal entropy generation is important to improve the model's predictive capabilities for variable speed driven chillers. A complementary model was developed that would incorporate both modifications for variable flow rate and linear entropy generation to the original thermodynamic relationship. Eq. 4.37 is the result of combining both modifications in one equation. Figure 4.17 shows the measured vs. predicted chiller efficiency for the model possessing both modifications.

$$\frac{T_{evap,o}}{T_{cond,i}}[1+\frac{1}{COP}] = 1 + \frac{T_{evap,o}(\Delta S_{int,1} + \Delta S_{int,2}\frac{Q_L}{Q_{max}})}{Q_L} + \frac{L}{Q_L}[\frac{T_{cond,i} - T_{evap,o}}{T_{cond,i}}] + \frac{Q_L}{T_{cond,i}}[1+\frac{1}{COP}] \times [\frac{1}{\dot{V}_w \rho C} + R_{evap}] \tag{4.37}$$

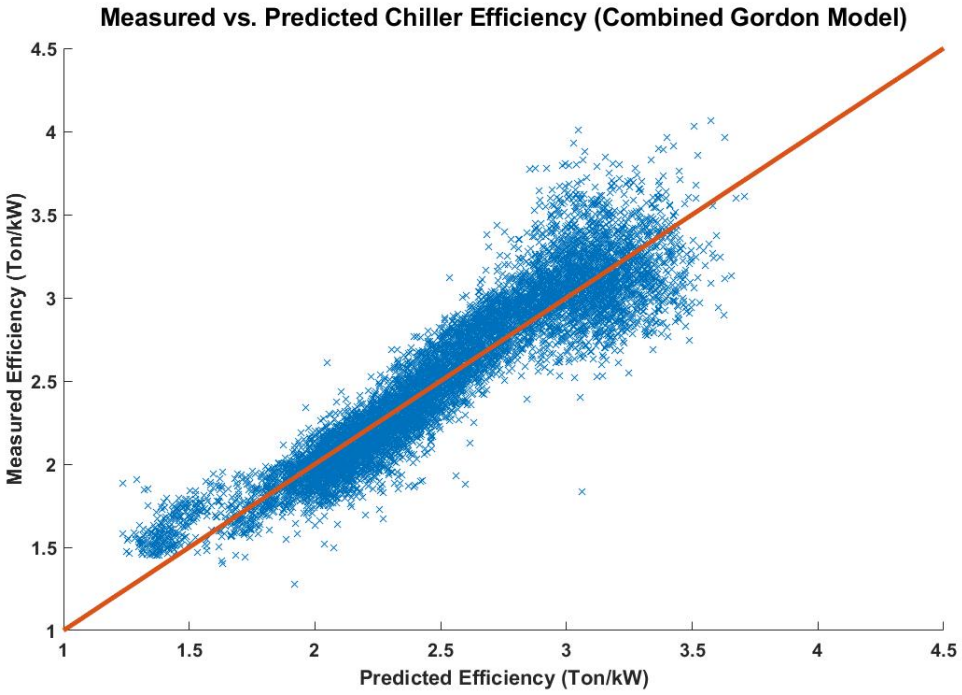

Fig. 4.17.: Measured vs. Predicted Chiller Efficiency (Combined Gordon Model)

In their models, Jiang and Reddy and Gordon et. al used the condenser inlet water temperature to represent the condition in the condenser, however in the final modeling effort it was found that this assumption leads the model to preferentially favor reducing the condenser water flow rate. Reducing the flow rate through the chiller and cooling tower significantly increases the condenser's outlet water temperature while the inlet condenser water temperature can remain relatively unchanged due to an increase in the cooling tower's effectiveness. Using the inlet condenser water temperature in the final model created the surface plot of the overall power consumption with varying fan and pump speeds seen in Figure 4.18. The surface plot shows

how the combined power demand from the chiller, cooling tower and condenser pump varies with changes in the cooling tower fan speed and condenser pump power. From the figure you can see that the modeled system power has a slight gradient toward reducing the condenser water pump's power input.

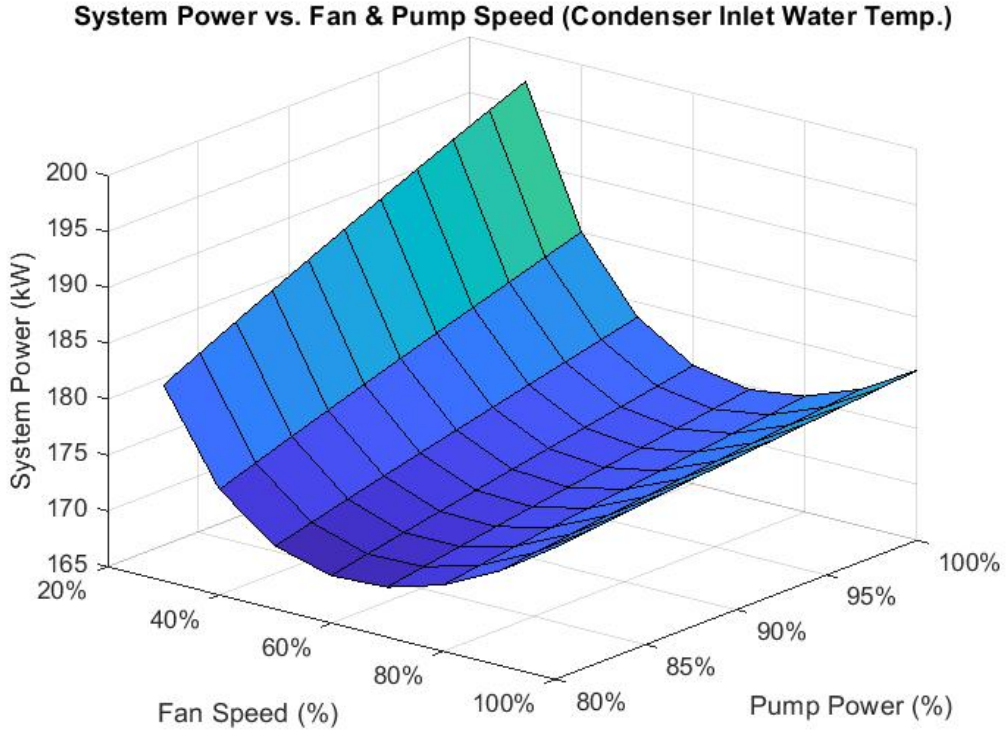

Fig. 4.18.: System Power vs. Fan Speed & Pump Power (Inlet Water Temperature)

Figure 4.18 would suggest that reducing the condenser water flow rate reduces the system power demand because it doesn't take into account the effect an increased condenser outlet water temperature would have on the system. Other authors recommend using the outlet condenser water temperature to model chillers with variable flow applications [13], [50]. They suggest that using the outlet condenser water temperature is a better indicator of the condenser's state because it better compensates for variable condenser flow rates. Implementing the outlet condenser water temperature into the chiller model reverses the system power demand's relationship to

condenser pump power. The model now indicates that a fully loaded condenser pump is most advantageous for the overall system power demand. Figure 4.19 shows the how replacing the condenser inlet water temperature with the outlet temperature affects the modeled system power consumption and how it varies with fan and pump speed.

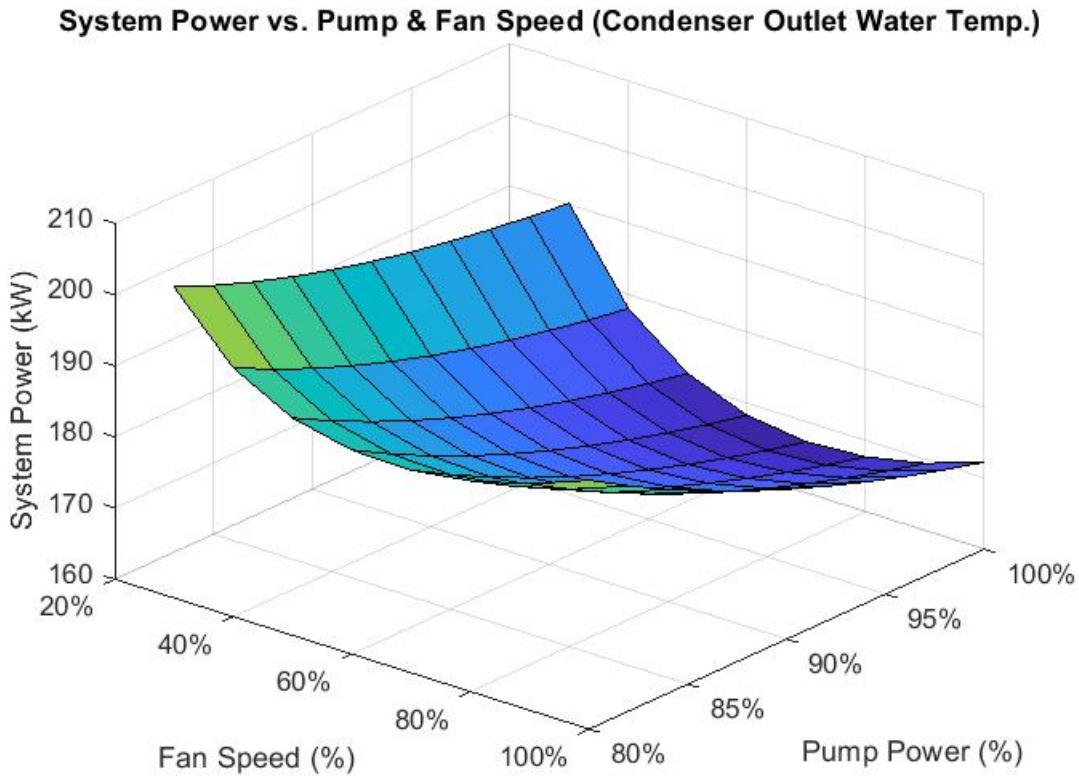

Fig. 4.19.: System Power vs. Fan Speed & Pump Power (Outlet Water Temperature)

The dichotomy between the system's relationship to the condenser water flow rate significantly affects how the model recommends optimal fan and pump speeds. Using the inlet water temperature, the model consistently recommends reducing the flow rate through the condenser, while using the outlet water temperature consistently recommends running the pump at full speed. In order to address the contradiction,

the average value of the inlet and outlet water temperature was used in the chiller model because the average temperature would be the most accurate representation of the overall condition throughout the condenser. Using the average condenser water temperature requires that the model be solved iteratively with respect to the outlet condenser water temperature. Since the cooling tower model must also be iteratively solved with respect to the inlet water temperatures the combined model becomes iterative with respect to both variables. The surface plot of how the modeled power demand, using the average condenser water temperature, is affected by varying the fan speed and pump power can be seen in Figure 4.20.

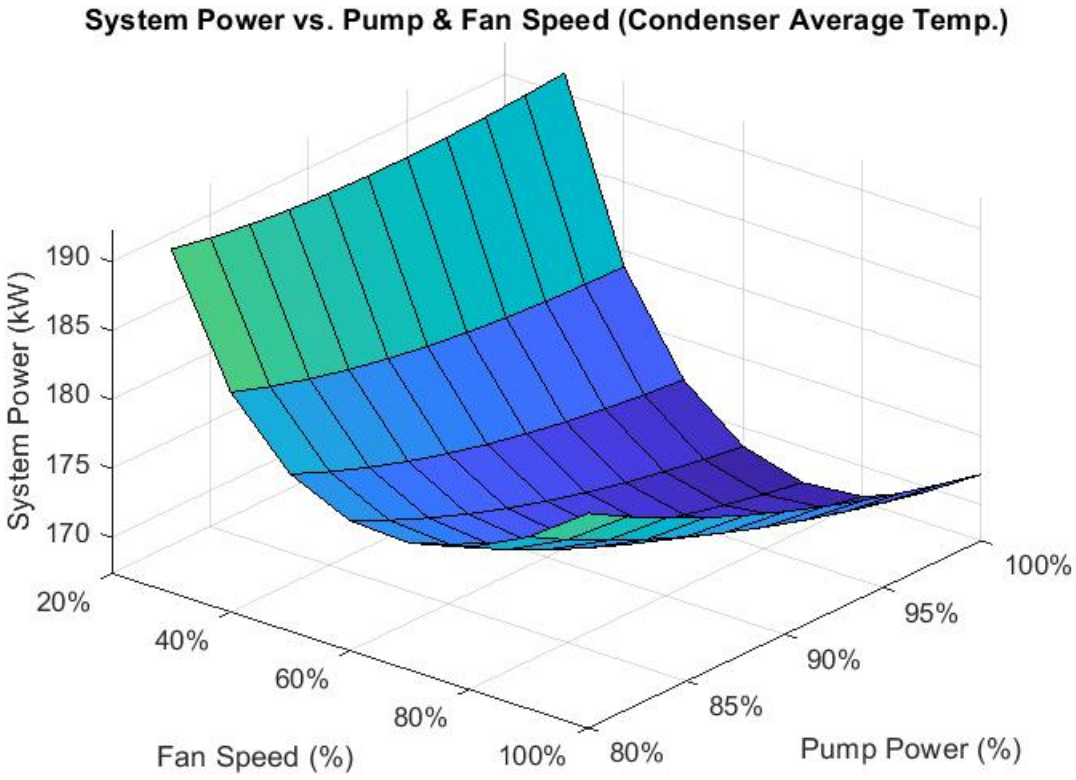

Fig. 4.20.: System Power vs. Fan Speed & Pump Power (Average Water Temperature)

Determining the parameters for the final chiller model was achieved through multiple linear regression of the chillers performance data by performing least squares to determine the unknown variables as seen in Eq. 4.38.

$$\frac{T_{evap,o}}{T_{cond,avg}}[1+\frac{1}{COP}] = 1+\frac{T_{evap,o}}{Q_L}(b_1+b_2\frac{Q_L}{Q_{max}})+b_3[\frac{T_{cond,avg}-T_{evap,o}}{Q_L T_{cond,avg}}]+ \\ \frac{Q_L}{T_{cond,avg}}[1+\frac{1}{COP}]\times[\frac{1}{\dot{V}_w\rho C}+b_4] \tag{4.38}$$

The regression is performed such that Eq. 4.38 becomes linear with respect to the unknown coefficients as seen in Eq. 4.39.

$$y = b_1x_1 + b_2x_2 + b_3x_3 + b_4x_4 \tag{4.39}$$

Where,

$$\begin{aligned} y &= \frac{T_{evap,o}}{T_{cond,avg}}[1+\frac{1}{COP}]-1-\frac{Q_L}{T_{cond,avg}}[1+\frac{1}{COP}]\times\frac{1}{\dot{V}_w\rho C}, \\ x_1 &= \frac{T_{evap,o}}{Q_L}, \\ x_2 &= \frac{T_{evap,o}}{Q_{max}}, \\ x_3 &= \frac{T_{cond,avg}-T_{evap,o}}{T_{cond,avg}Q_L}, \\ x_4 &= \frac{Q_L}{T_{cond,avg}}[1+\frac{1}{COP}] \end{aligned} \tag{4.40}$$

Once the coefficients have been determined, the chiller's coefficient of performance can be estimated with the required cooling load, evaporator outlet water temperature, condenser inlet water temperature and the four parameters calculated through the linear regression. Solving for the coefficient of performance requires algebraically rearranging the model as expressed by Eq.4.41.

$$COP = \frac{\frac{T_{evap,o}}{T_{cond,avg}}-\frac{Q_L}{T_{cond,avg}}\times\frac{1}{\dot{V}_w\rho C}-b_4\frac{Q_L}{T_{cond,avg}}}{1+b_1\frac{T_{evap,o}}{Q_L}+b_2\frac{T_{evap,o}}{Q_{max}}+b_3\frac{T_{cond,avg}-T_{evap,o}}{T_{cond,avg}Q_L}+b_4\frac{Q_L}{T_{cond,avg}}+\frac{Q_L}{T_{cond,avg}}\frac{1}{V_w\rho C}-\frac{T_{evap,o}}{T_{cond,avg}}} \tag{4.41}$$

The final chiller model exhibits better accuracy than the variable flow rate Gordon model and it incorporates condenser water flow rate as a control variable for the system. Again, the absence of chiller data subject to multiple flow rates inhibits

the ability to validate the proposed model's accuracy when suggesting reduced condenser water flow rates. Figure 4.21 shows the modeled chiller's efficiency versus the building's cooling load for various average condenser water temperatures. Figure 4.22 shows a surface plot of the final model's relationship between the chiller's efficiency versus the building's cooling load and the average condenser water temperature.

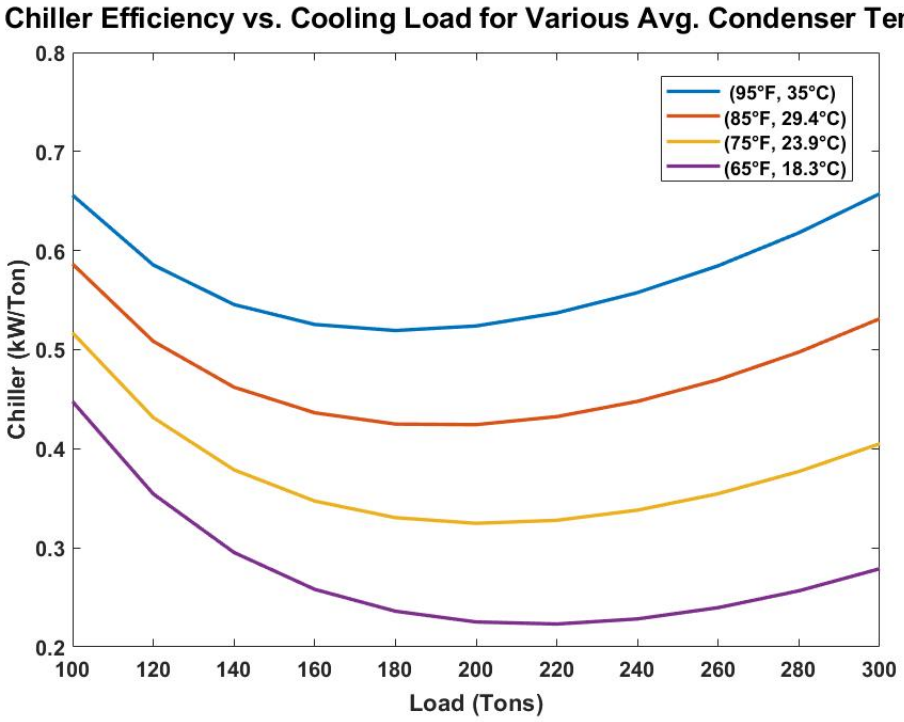

Fig. 4.21.: Chiller Efficiency vs. Cooling Load for Various Avg. Condenser Temp.

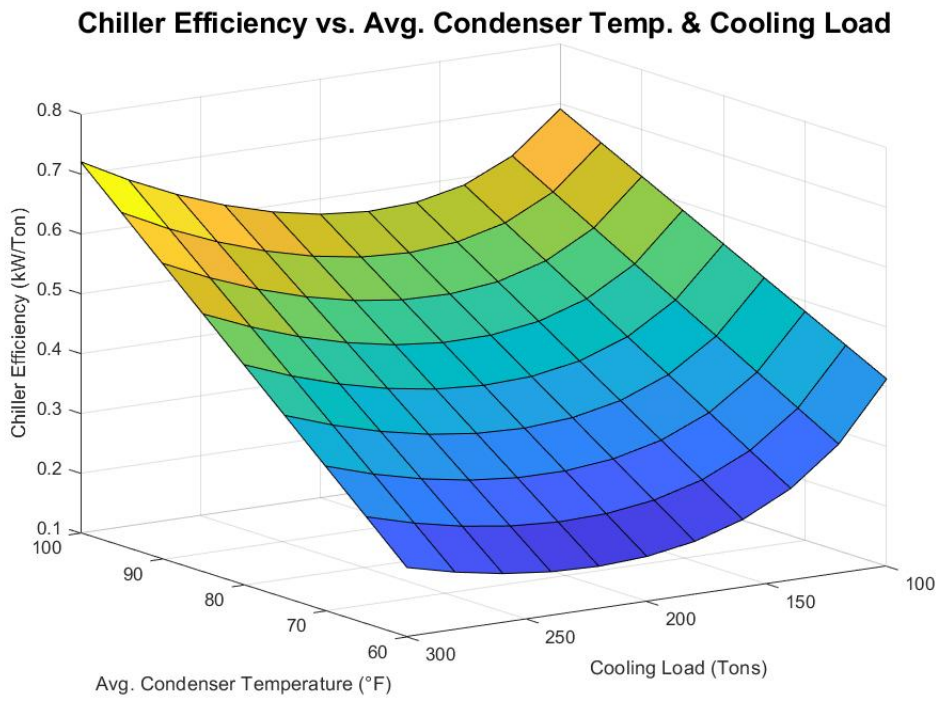

Fig. 4.22.: Chiller Efficiency vs. Avg. Condenser Temp. & Cooling Load

4.6 Combined Model

The inputs and outputs of the individual models were connected to each other to develop a model of the complete condenser water system. To begin with, the multiple non-linear regression model was used to predict the building's cooling load for the data collection period using each time point's day, time and weather conditions as input variables. The predicted building cooling load was supplied to the chiller model's input for the required chiller cooling load. The measured cooling load data could have been used in place of the predicted load, however the ability to predict a building's cooling load is useful for forecasting, online optimization and demand management of a chilled water network. Given the importance a cooling load prediction algorithm would have on the actual optimization of a chilled water system, incorporating the prediction algorithm in lieu of the measured cooling load seemed practical. The condenser water pump model was simply used to relate the power

consumption of the pump to the condenser water flow rate. The flow rate is provided as an input to both the cooling tower and chiller model. Although the condenser water pump only constitutes a small portion of the condenser water system's overall energy consumption, the water flow rate through the chiller and cooling tower can have a pronounced effect on the system's total performance. The chiller model uses the coefficients previously regressed from the data set to predict the chiller coefficient of performance using the required cooling load, exiting chilled water temperature, entering condenser water temperature and the condenser water flow rate as input variables. The chiller currently operates to provide a constant chilled water temperature of 40°F (4.4°C) in order to maintain an acceptable level of humidity in the museum environment. Resetting the chilled water temperature setpoint could have the capacity to reduce the chillers energy consumption, however due to the setpoint's importance in preserving the museum's strict environmental climate, manipulating the system's chilled water temperature setpoint will not be investigated. With that consideration, a constant chilled water temperature of 40°F (4.4°C) was used as the input for the chiller's outlet evaporator water temperature. The chiller's projected energy consumption is determined using the estimated coefficient of performance from the model and the building's predicted cooling load as shown in Eq. 4.42.

$$P_{c,k}(kW) = \frac{Q_{L,k}(tons)}{COP_k(tons/kW)} \tag{4.42}$$

An energy balance is performed on the condenser water stream to determine the water temperature exiting the chiller. Using the chiller's predicted power consumption and the building's cooling load, the water temperature exiting the chiller can be determined with Eq. 4.43.

$$\begin{aligned} [English]\, T_{cond,o,k} &= \frac{P_{c,k} \times 2544.4 \frac{Btu}{hp \times hr} + Q_{L,k} \times 12,000 \frac{Btu/hr}{ton}}{\dot{V_{w,k}}(gpm) \times 8.33 \frac{lb}{gal} \times 1 \frac{BTU}{lb^\circ F} \times 60 \frac{min}{hr}} + T_{cond,i,k} \\ [SI] \quad T_{cond,o,k} &= \frac{P_{c,k} \times + Q_{L,k}}{\dot{V_{w,k}}(L/s) \times 1 \frac{kg}{L} \times 4.181 \frac{kJ}{kg^\circ C}} + T_{cond,i,k} \end{aligned} \tag{4.43}$$

The energy balance on the water stream provides the cooling tower and chiller model with the condenser outlet water temperature; however, the cooling tower model

also must provide the chiller model with the condenser inlet water temperature necessary for determining the chiller's COP and outlet water temperature. The circular reference requires that the model be solved iteratively with respect to both the condenser inlet and outlet water temperature. After linking the components together, the individual models interact such that the output from one model affects the inputs and outputs of the other models. The overall condenser water system has been modeled and the energy consumption of the system can be minimized using a suitable optimization algorithm. Figure 4.23 shows a flow chart of how the inputs and outputs of each model interact with one another.

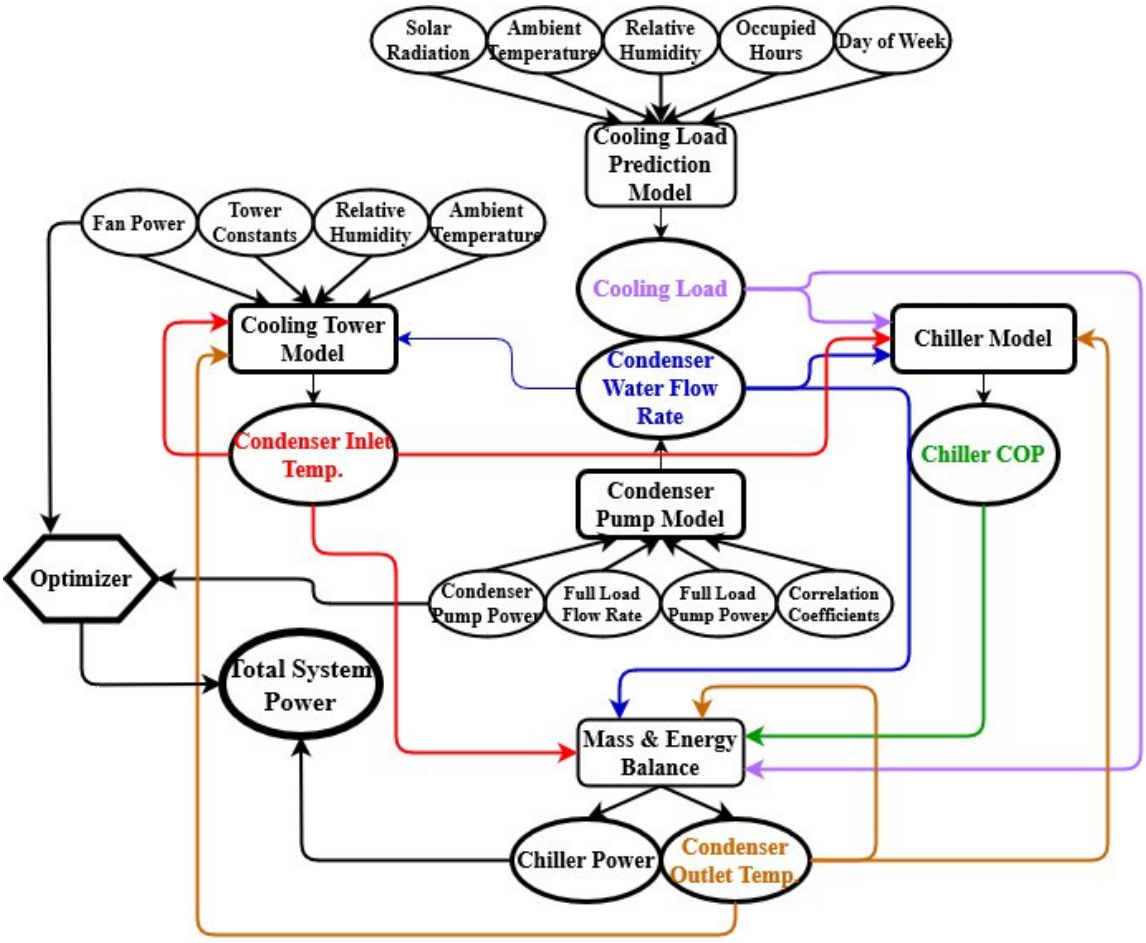

Fig. 4.23.: Flow Chart of Component Model Interactions

Figure 4.24 shows the modeled and the measured chiller power consumption for a week in July. Figure 4.25 shows the modeled and the measured condenser inlet and outlet water temperatures for a week in July for the combined component models. The figures serve as indicators for how accurately the overall system is modeled.

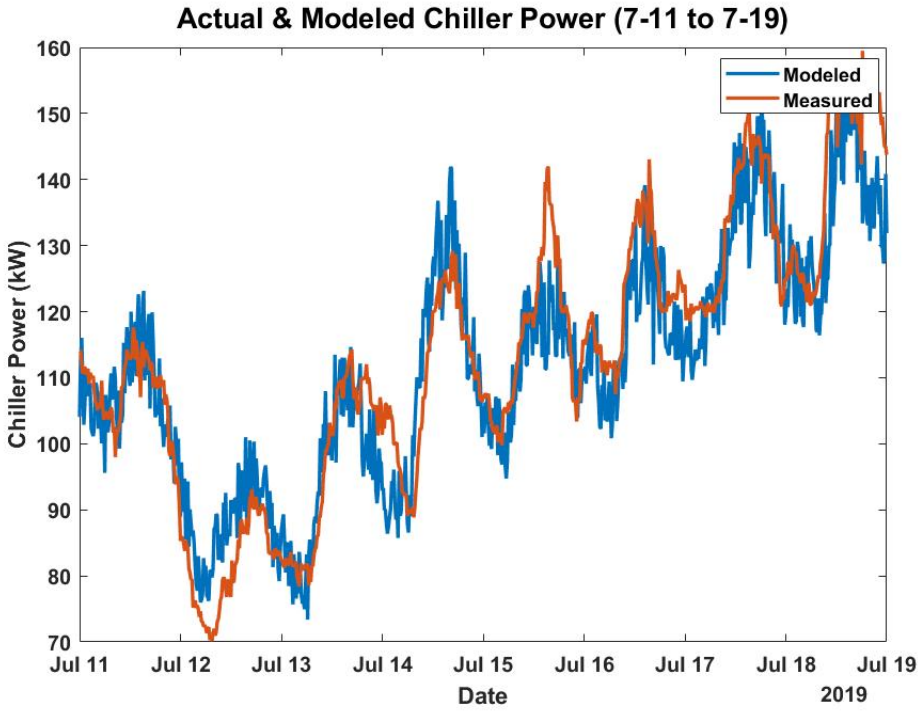

Fig. 4.24.: Actual & Modeled Chiller Power (7-11 to 7-19)

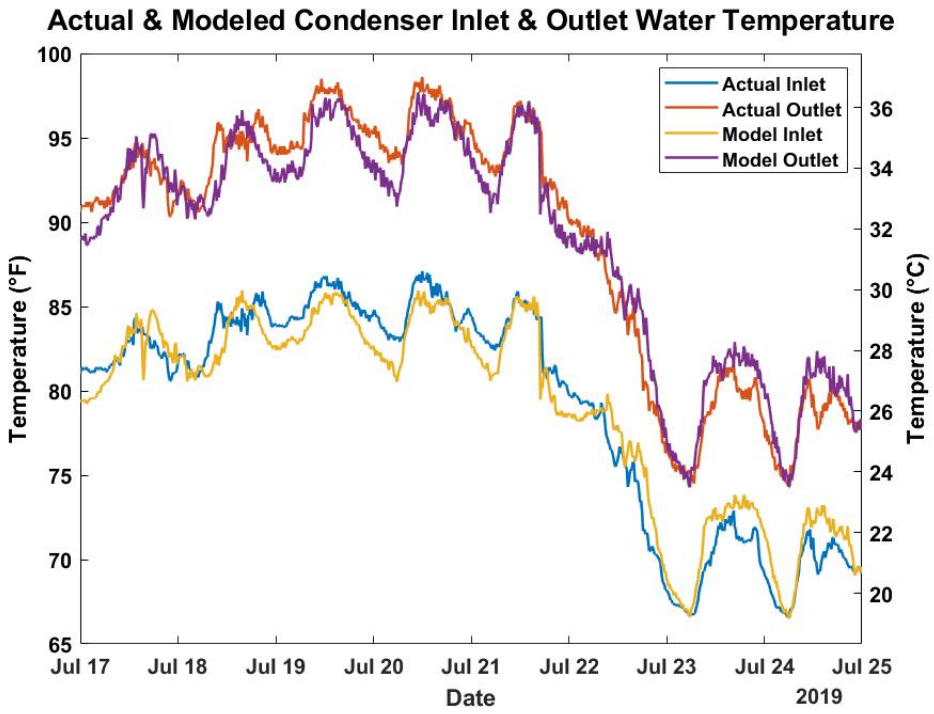

Fig. 4.25.: Acutal & Modeled Condenser Inlet & Outlet Water Temperature

4.7 Optimization

The objective of the optimization is to minimize the system's overall power consumption by manipulating the fan speed and pump motor power as optimization variables. The fan speed is constrained between the fan's minimum and maximum speed of 25% and 100%. The pump power is constrained between the minimum value of 8.8kW and 11.2kW. The minimum pump power is required to provide the minimum flow rate of 367 gpm (23.1 L/s) to maintain turbulence in the chiller condenser. The optimization sequence was run for two separate weeks worth of data. The first was a week in July with high wet-bulb temperature and cooling loads and another week in October with more mild temperatures and lower cooling loads. The two weeks were meant to span the range of ambient conditions and cooling loads that would be experienced during the buildings cooling season. Determining the proper optimization algorithm requires understanding the relationship between the objective

function and the optimization variables. Since the objective function is iterative with respect to two variables a population-based algorithm such as a particle swarm or genetic algorithm would require iterating each member of the population at every step of the optimization process. As a result, population-based optimization methods would require a large amount of time and computational power to run for even a portion of the dataset. Due to the convex relationship between the objective function and the optimization variables, a gradient algorithm would be more ideal to determine the system's optimal operating conditions. The algorithm chosen to minimize the condenser water system's energy consumption was the Frank-Wolfe algorithm. The Frank-Wolfe algorithm, also known as the reduced gradient algorithm, was first proposed by Marguerite Frank and Philip Wolfe in 1956 [60]. The method is used to optimize constrained smooth nonlinear programs where the derivative of the of the objective function is not directly available. The algorithm creates a linear approximation of the objective function and moves the solution towards the function's minimizer. The algorithm follows the form shown in Figure 4.26.

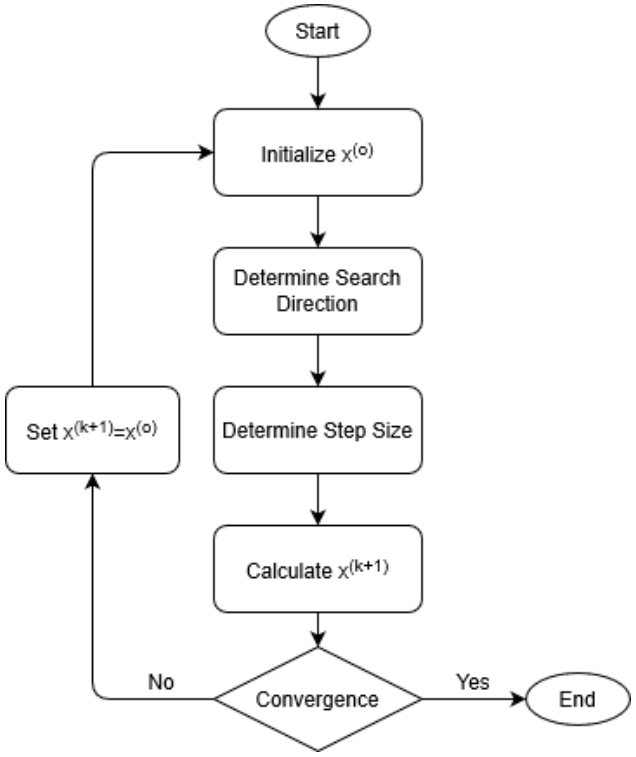

Fig. 4.26.: Optimization Flow Chart

$$minf(x)$$
$$\text{subject to}$$
$$x \in \Omega$$

1. Initialize: $x^{(o)}$

2. Determine search direction: (p_k)

$$min(z_k(y)) = f(x_k) + \nabla f(x_k)^T(y - x_k)$$

3. Determine step length: (α_k)

$$\alpha_k = \frac{2}{2+k} \text{ or minimize } f(x_k + \alpha_k p_k)$$
$$\text{subject to } \alpha_k \in [0, 1]$$

4. Next step:

$$x_{k+1} = x_k + \alpha_k p_k$$

5. Check stopping criteria

$$if|(x_{k+1} - x_k)| < \epsilon \text{ then stop}$$
$$\text{else } x_k = x_{k+1} \text{ return to 1.}$$

5. RESULTS & DISCUSSION

The combined system model was run for four different control scenarios to compare the energy consumption of the condenser system with various operational strategies. Table 5.1 describes the respective pump and fan control strategy for each scenario. The scenarios were selected to compare the individual benefits of optimizing different pieces of equipment in the chilled water system.

Table 5.1.: Control Strategy Scenarios

Scenario	Pump Control Strategy	Fan Control Strategy
1	Full Load	Full Load
2	Full Load	65°F Condenser Water Setpoint
3	Full Load	Optimized
4	Optimized	Optimized

For scenario 1, the cooling tower fan and condenser water pump both run at full load constantly. Scenario 2 represents the Eiteljorg's current control strategy in which the cooling tower fan cycles between 25-100% to achieve and maintain the condenser water setpoint of 65°F. Scenario 2 acts as the baseline for comparing the performance of the different scenarios. The data collected from the Eiteljorg's chilled water system was directly used to represent scenario 2. Scenario 3 operates the condenser water pump at fully load and seeks to optimize the system's energy consumption by controlling the cooling tower fan speed. Scenario 4 seeks to optimize the system's power consumption by controlling both the cooling tower fan speed and the condenser water pump's power consumption. The optimization procedure for scenario 3 & 4 was run from July 11^{th} to July 19^{th}, September 1^{st} to September

$9^{th}$and from October 21^{st} to October 29^{th}. The periods were specifically chosen to determine the optimal system operating points for a range of building cooling loads and ambient wet-bulb temperatures in order to compare the results of the different scenarios over a range of external conditions. Figure 5.1 compares the system power consumption for scenarios 1 & 2 from July 11^{th} to July 19^{th} and Figure 5.2 shows the system power consumption for scenarios 1 & 2 from September 1st to September 9th. For a perfect model, the power consumption in Figure 5.1 and 5.2 would be equal since the cooling tower fan ran fully loaded and had not yet begun to cycle. However, error lead to slightly different power consumption between the modeled scenario and the collected data. Figure 5.3 displays the system power consumption for scenarios 1 & 2 for the period from October 21^{st} to October 29^{th}. At this point in the cooling season, the building management system would cycle the cooling tower fan between it's minimum and maximum speed to maintain the condenser water temperature at approximately 65°F. The power consumption for Scenario 1 was found to be in general larger than that in Scenario 2 over the period in October. The results would indicated that as suggested by [16], [17], [18], [19], [20], driving down the condenser water temperature to the lowest possible value won't result in energy savings due to the high cooling tower demand.

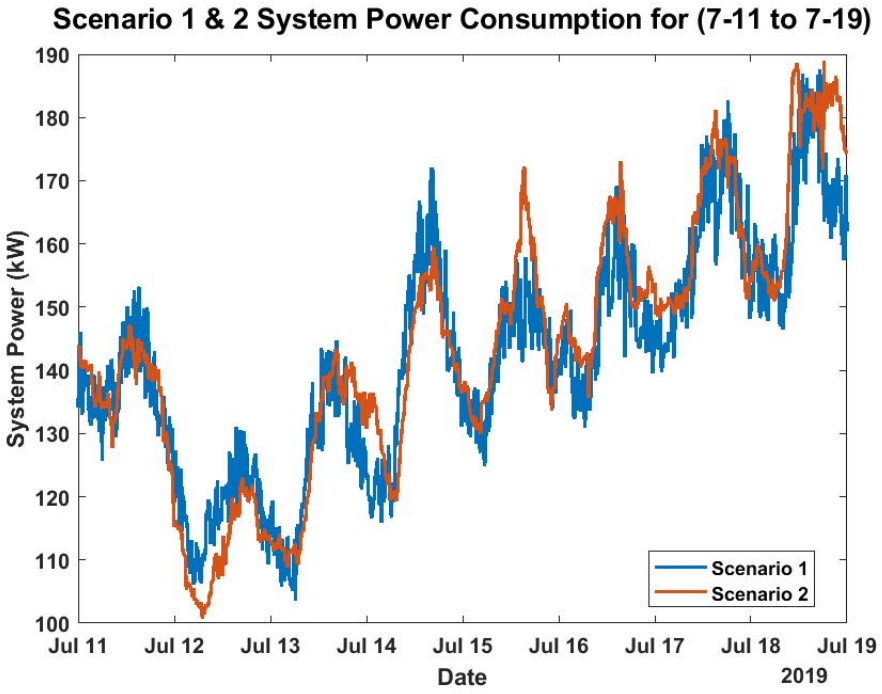

Fig. 5.1.: Scenario 1 & 2 System Power Consumption (7-11 to 7-19)

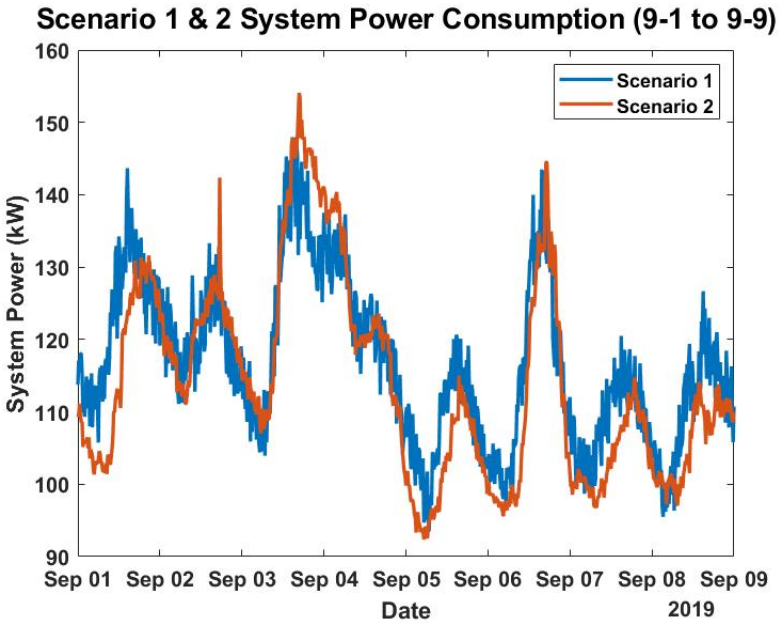

Fig. 5.2.: Scenario 1 & 2 System Power Consumption (9-1 to 9-9)

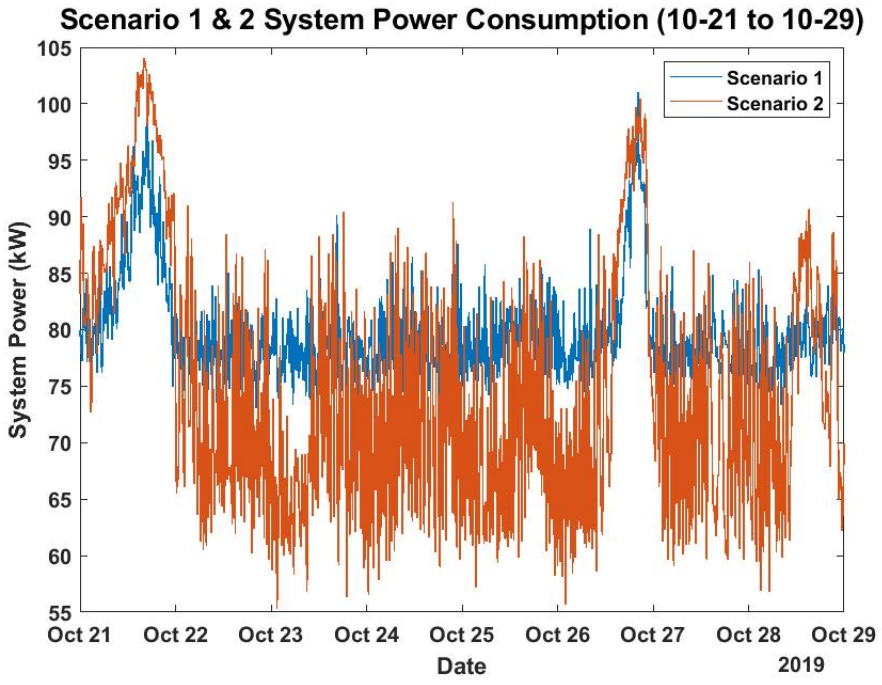

Fig. 5.3.: Scenario 1 & 2 System Power Consumption (10-21 to 10-29)

Figure 5.4, Figure 5.5 and Figure 5.6 compare the system power demand over the periods in July, September and October respectively. The results from each of the figures would indicate that there is consistent potential to save energy through optimizing the cooling tower fan speed.

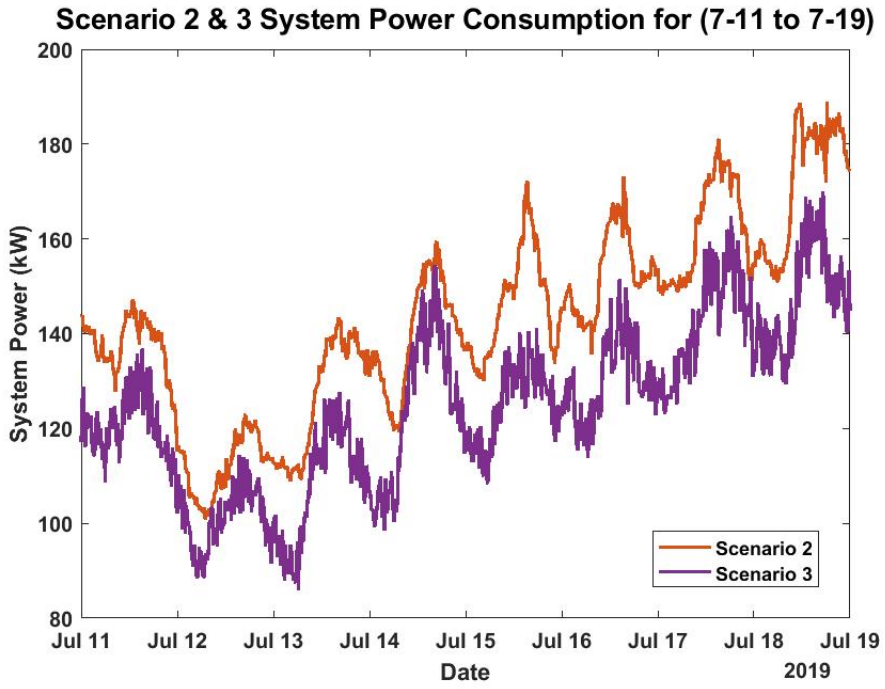

Fig. 5.4.: Scenario 2 & 3 System Power Consumption (7-11 to 7-19)

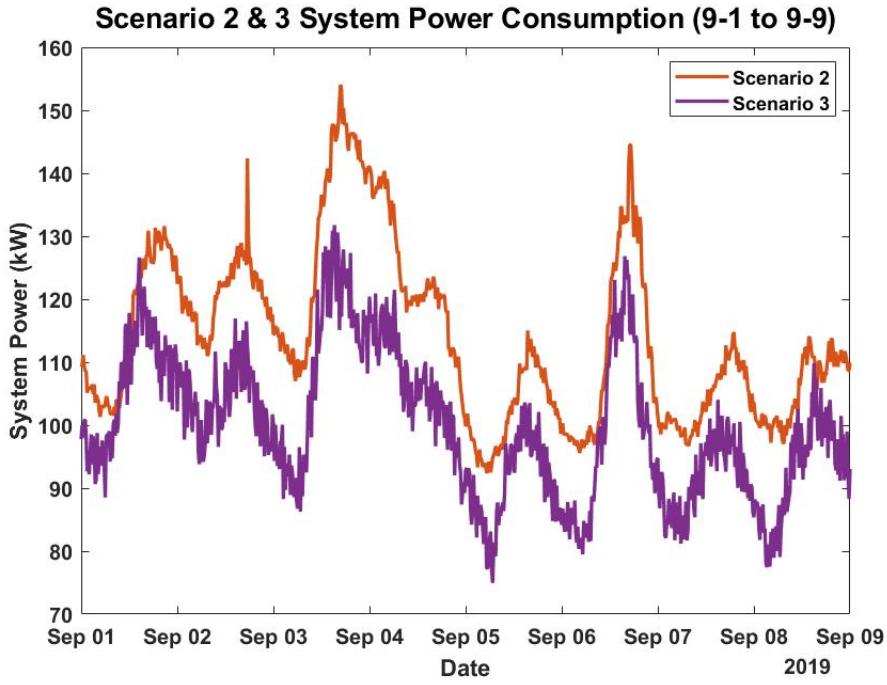

Fig. 5.5.: Scenario 2 & 3 System Power Consumption (9-1 to 9-9)

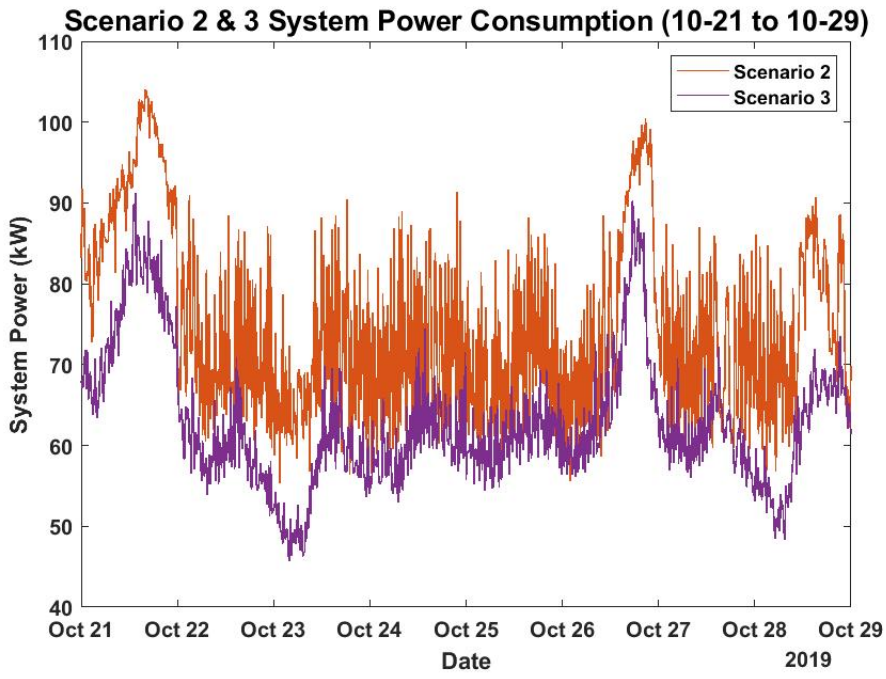

Fig. 5.6.: Scenario 2 & 3 System Power Consumption (10-21 to 10-29)

Figure 5.7, Figure 5.8 and Figure 5.9 compare the system power consumption for Scenario 3 & 4 for the period in July, September and October respectively. The system power consumption for Scenarios 3 & 4 was found to be almost exactly equal for all three weeks. The results would indicate that there is very little potential to save energy through optimizing the condenser water flow rate of the chilled water system.

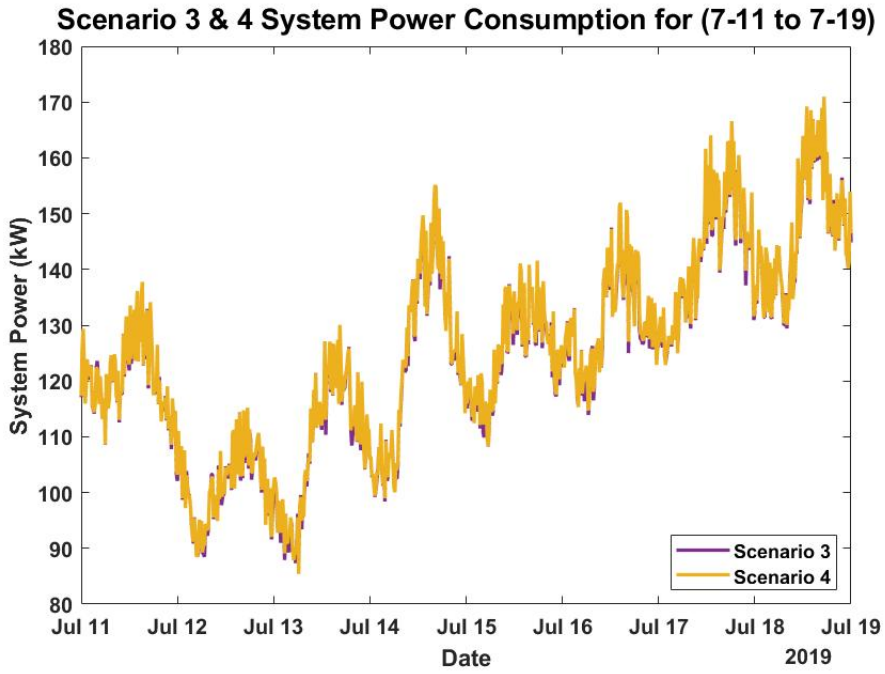

Fig. 5.7.: Scenario 3 & 4 System Power Consumption (7-11 to 7-19)

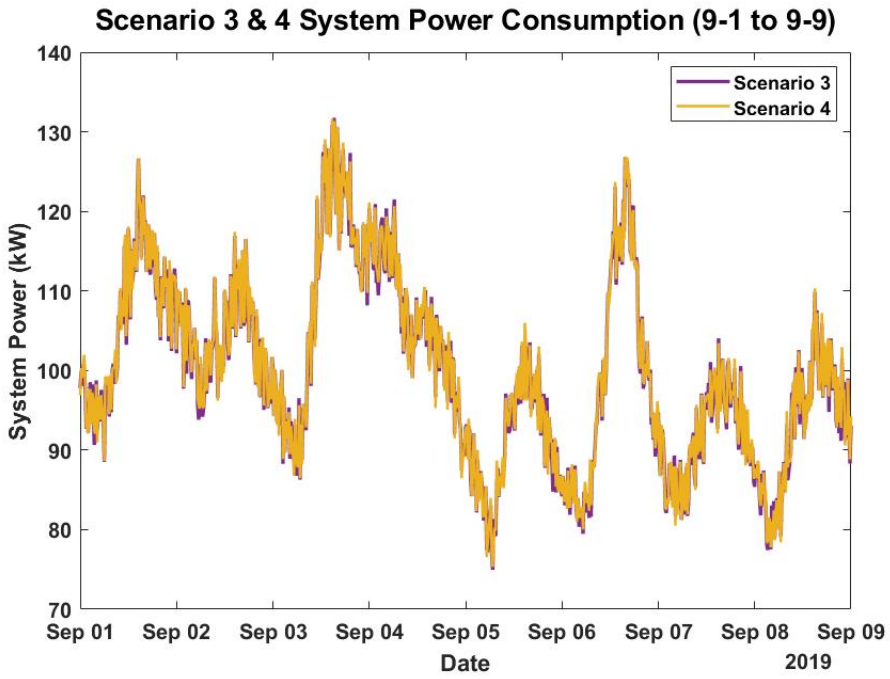

Fig. 5.8.: Scenario 3 & 4 System Power Consumption (9-1 to 9-9)

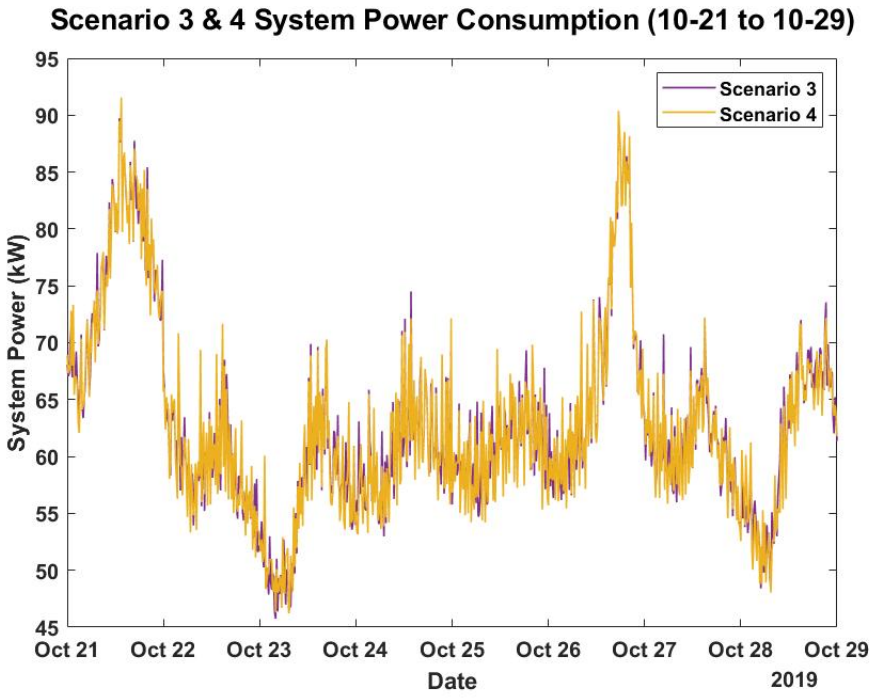

Fig. 5.9.: Scenario 3 & 4 System Power Consumption (10-21 to 10-29)

Integrating the condenser water system's power demand over the three optimization periods offers an estimate for each scenario's energy consumption during high, medium and low load conditions. Figure 5.10, Figure 5.11 and Figure 5.12 shows bar graphs of each scenario's total energy consumption of the overall system and of each individual piece of equipment for the three time periods. Table 5.2 shows the percent change in energy consumption relative to scenario 2 as the baseline.

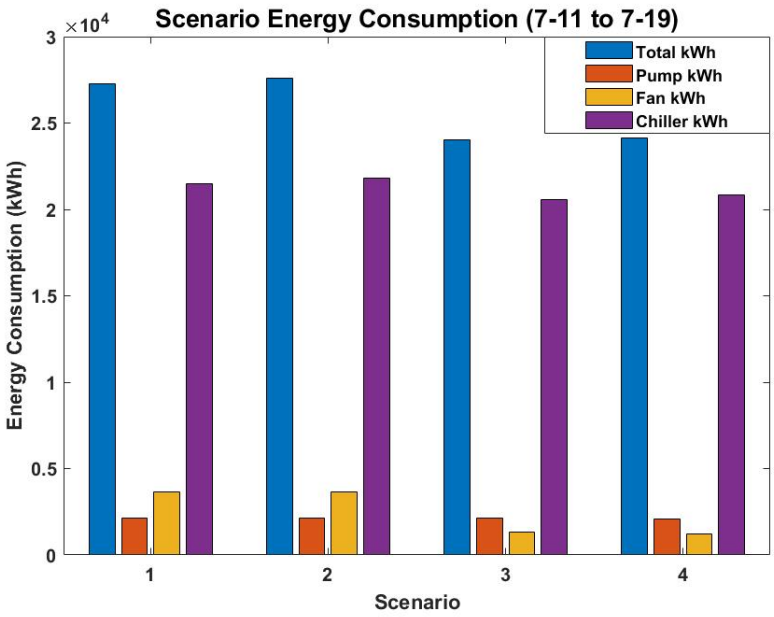

Fig. 5.10.: Scenario Energy Consumption (7-11 to 7-19)

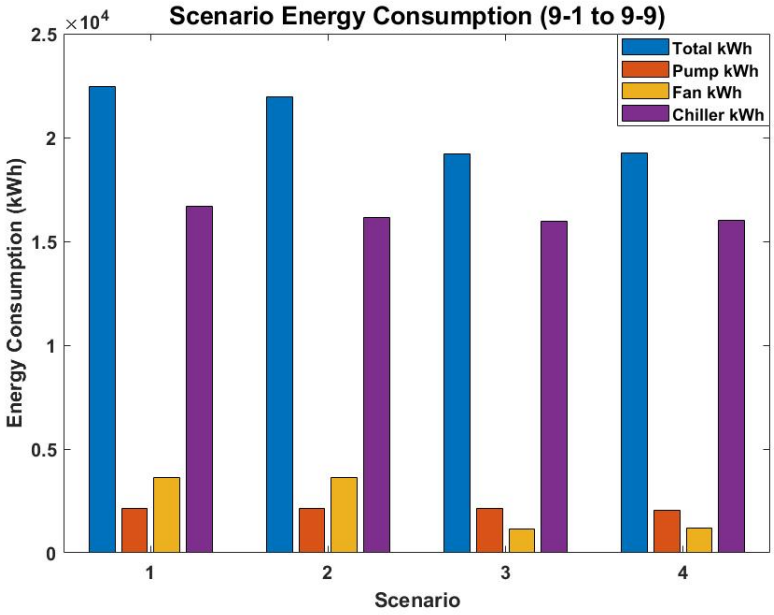

Fig. 5.11.: Scenario Energy Consumption (9-1 to 9-9)

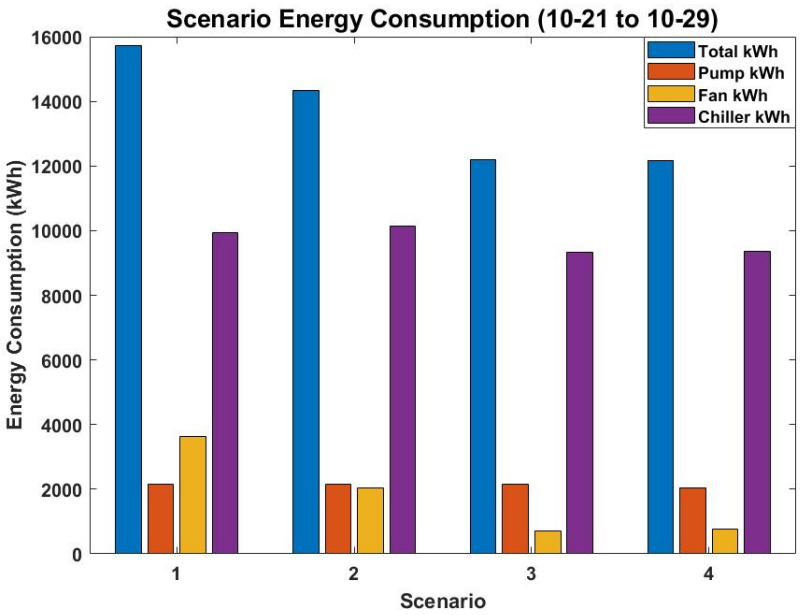

Fig. 5.12.: Scenario Energy Consumption (10-21 to 10-29)

Table 5.2.: Control Scenarios Energy Savings Compared to Baseline

Scenario	% Savings(7/11-7/19)	% Savings(9/1-9/9)	% Savings(10/21-10/29)
1	1.12%	-2.42 %	-9.73%
2	-	-	-
3	12.96%	12.41%	14.92%
4	12.58%	12.23%	15.01%

The results of the optimization procedure suggest that for a condenser water system serving a single chiller there is almost no energy saving potential to controlling the condenser water flow rate with VFD, but significant potential to save energy through optimizing the cooling tower fan. The findings are indicative only to the specific system analyzed. For another chilled water system with a higher condenser water flow rate there could be more potential to save energy through controlling the condenser water flow rate with a VFD.

5.1 Control Strategies

The results for scenario 3 were analyzed to find if there exists a simple control strategy for optimizing the cooling tower fan. The simplest strategy would be to control the cooling tower fan speed directly from the ambient wet-bulb temperature. Figure 5.13 shows the optimized cooling tower fan speed vs. the ambient wet-bulb temperature. The poor correlation between the variables would suggest that controlling the cooling tower fan directly according to the ambient wet-bulb temperature isn't an excellent control strategy.

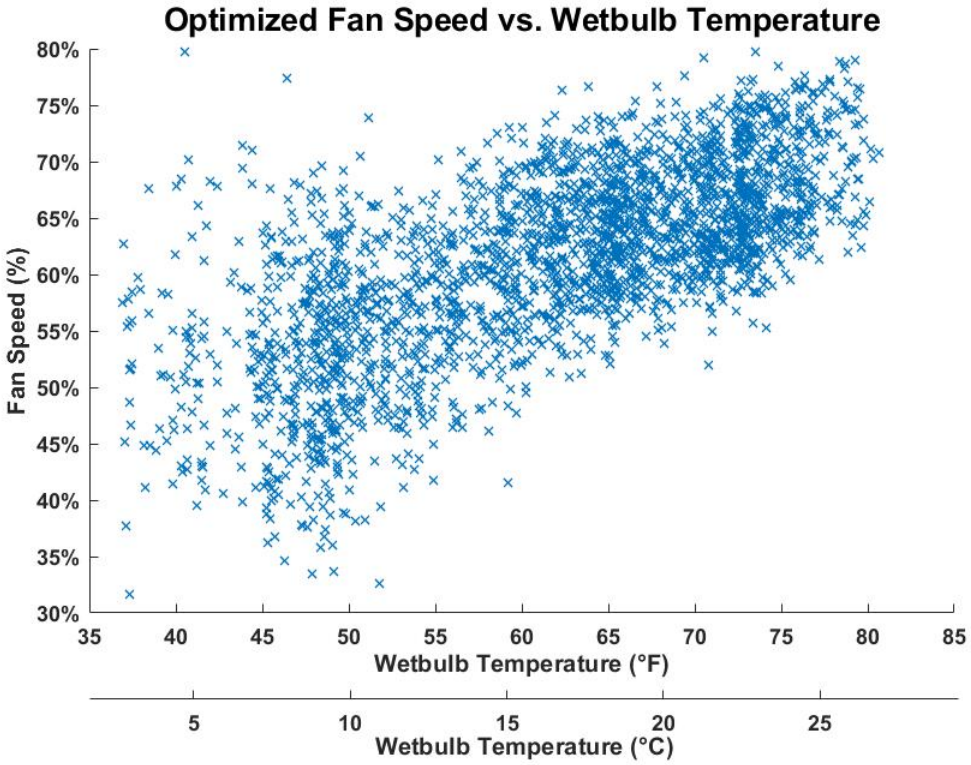

Fig. 5.13.: Optimal Fan Speed vs. Wet-bulb Temperature

Liu and Chuah suggested resetting the condenser water temperature setpoint based on the optimal approach temperature for a cooling tower [16]. The approach is defined as the temperature difference between the tower outlet water temperature and the ambient wet-bulb temperature. Following the control strategy proposed by

Liu and Chuah, the approach temperature determined from the optimized cooling tower fan speed was compared to the ambient wet-bulb. Figure 5.14 shows the optimized cooling tower's approach vs. the ambient wet-bulb temperature.

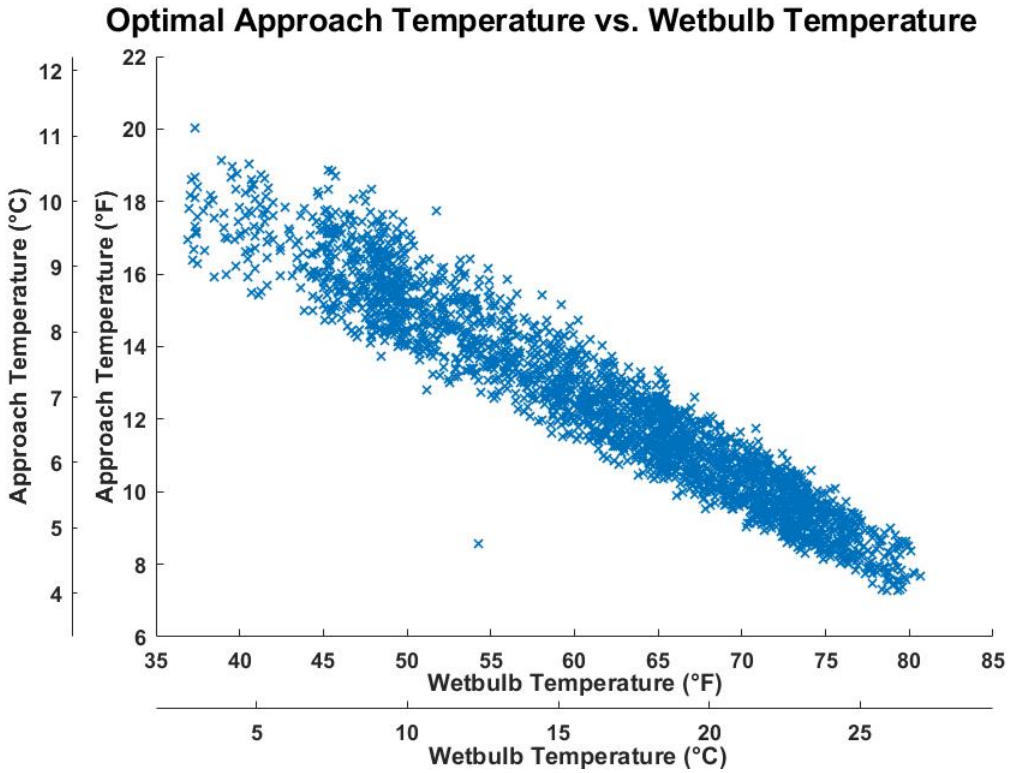

Fig. 5.14.: Optimal Approach vs. Wet-bulb Temperature

The correlation between the variables would suggest that resetting the condenser water temperature setpoint based on the optimal approach would be an advantageous control strategy. The difficulty with the indirect control technique is in determining the appropriate cooling tower fan speed to achieve the optimal tower approach. The model would need to operate the cooling tower fan speed with the object of attaining a specific tower outlet water temperature, which may or may not be an improvement over optimizing the system in real-time.

5.2 Potential Improvements

The goal of this research was to determine the energy saving potential of optimizing pieces of chilled water system equipment furnished with a variable frequency drives. To accomplish this goal, a series of component models were developed and linked together to simulate the overall system operation. In every system component, the ability to model and validate the different modules was severely limited by the lack of data spanning the range of possible operational conditions. For instance the reformulated EIR electric chiller model has been shown to potentially achieve higher accuracy compared to the Gordon chiller model, however the empirical nature of the regression model would have limited the ability to model different condenser water flow rates and inlet condenser water temperatures lower than the setpoint temperature. Similarly the CoolTools cooling tower algorithm could feasibly achieve higher accuracy than the Ntu-effectiveness model, but as a high order regression model it cannot be used to recommend operational setpoints outside the range for which the data was collected. As a result, the lack of data available for multiple condenser water flow rates would have undermined the goal of the research. Finally, the pump was modeled using a simple polynomial correlation which could not be experimentally validated. An empirical relationship developed from collecting data over a range of condenser pump speed would almost certainly be more accurate for modeling the condenser water flow rate as a function of pump power. Another potential improvement stems from the cooling load prediction model. The regression model developed was found to more accurately predict the building's cooling load when the load exceeds 200 tons. Below that the variation between the measured and predicted load grew substantially. An ANN or software simulation could potentially offer an improved prediction for low and high cooling loads. Additionally, creating a separate regression model with coefficients tailored toward low load scenarios could potentially improve the model's accuracy for predicting the buildings cooling load for cases when the cooling load was found to be below a

certain range. Additionally, the weather data used for the cooling tower model and cooling load prediction model was collected from a weather station roughly 70 miles south of Indianapolis. Although the ambient conditions at the sampling location would likely not vary heavily from those at the location of the case study, implementing environmental data taken directly at the facilities site could potentially result in improvements in the accuracy of both the cooling load prediction model and the cooling tower model. Another goal of the research was to determine a simple control strategy that could be used to control the equipment. Since there was found to be very little energy saving potential of controlling the condenser water pump for this system, control strategies for controlling the condenser water pump were not explored. On the other hand, optimizing the cooling tower fan speed was found to offer significant energy saving potential. The preferred control strategy derived from the optimization involved setting an optimal tower approach based off the ambient wet-bulb temperature. The correlation found was high, however the cooling tower would still need to be modeled to determine the appropriate fan speed required to achieve the optimal approach temperature. As a result, the proposed control strategy may or may not be straight forward enough to be considered an improvement over optimizing collected data in real-time.

5.3 Discussion

The study accomplished the goals of developing a personalized system model for a chilled water system and analyzing the energy saving potential of utilizing VFDs to control different pieces of equipment in the condenser water system. Data was collected from the chilled water system at a local museum to serve as a case study for the analysis. The museum's chilled water system is exceedingly important in maintaining the integrity of the exhibits housed inside the museum. Due to the importance in maintaining a stable internal climate in the museum, facility personnel were unwilling to allow changes to the system's current control strategies.

As a result, data could not be collected for various condenser water flow rates, cooling tower fan speeds or for inlet condenser water temperatures lower than 65°F (18.3°C). The lack of data ranging the span of possible operating conditions heavily influenced the modeling techniques that could be used to model the system components and impeded the ability to completely validate the models. A multiple non-linear regression model was developed to predict the building's cooling load subject to a range of environmental and occupancy related variables. To model the chiller, a variation of the Gordon NG thermodynamic chiller model was developed that would incorporate modifications to account for variable condenser water flow rate and improve it's accuracy for modeling variable speed driven chillers. The cooling tower was modeling using the Ntu-effectiveness model trained with a mix of collected data and performance data published by the Baltimore Aircoil Company. The condenser water pump was modeled using default curve method, a polynomial correlation relating the pump's power demand to the flow rate based on data collected from the respective variables full load values. These component models were linked together with mass and energy balances on the condenser water stream to model the system as a whole. The overall condenser water system model aims to meet the building's predicted cooling load given the ambient temperature, relative humidity and user defined inputs for the condenser pump power and cooling tower fan speed. A reduced gradient optimization algorithm was used to minimize the overall energy consumption required to meet the building's cooling load by manipulating the input values for the cooling tower fan speed and condenser pump power. There is one concern from the modeling efforts which stems from the relationship between the optimization algorithm's effect on the chiller's energy consumption. Reducing the cooling tower fan and condenser water pump power demand in scenario 3 & 4 should theoretically produce a slight increase in the chiller's power consumption, however the results showed a marginal decrease in the chiller's energy consumption. The discrepancy is justifiable for the period between October 21^{st} and October 29^{th} because the condenser water temperature can fall

below 65°F. On the other hand, for the periods between July 11 th and July 19^{th} and September 1^{st} and September 9^{st}, the optimization algorithm resulted in a 1-5% decrease in the chiller energy consumption. The distinction could be related to an under-prediction of the building's cooling load, an over-prediction of the cooling tower's effectiveness or a fractional internal error within the chiller model.

5.4 Conclusion

After developing the system model, the results showed that the composite model could accurately simulate the chilled water system's operating conditions. The optimization procedure found that for the system analyzed, the energy saving potential of optimizing the cooling tower fan could save approximately 12-15% of the systems overall energy consumption. On the contrary, the energy saving potential of optimizing the condenser water pump with the cooling tower fan was insignificant. The findings suggest that for the system analyzed there was almost no advantage to speed control optimization of both the cooling tower fan and the condenser water pump. Finally, the results of the cooling tower optimization scenario were analyzed to ascertain if there exists a simple method to control the cooling tower fan to achieve energy savings. It was found that controlling the cooling tower fan speed directly based on the ambient wet-bulb temperature resulted in a substandard correlation between the optimized fan speed and the wet-bulb temperature. On the other hand, the correlation found between the optimized tower's approach and the wet-bulb temperature was significantly better. The difficulty with the indirect control method is the system would still need to be modeled in order to determine the appropriate cooling tower fan speed to attain the recommended tower approach and whether or not this would be an improvement over real time optimization of the modeled system is uncertain.

REFERENCES

REFERENCES

[1] Annual energy outlook (2019). US Energy Information Administration. [Online]. Available: www.eia.gov/outlooks/aeo/pdf/aeo2019.pdf. (accessed: 01.24.2019)

[2] Commercial building energy consumption survey (2012): Table (30b.) cooling energy sources. US Energy Information Administration. [Online]. Available: https://www.eia.gov/consumption/commercial/data/2012/bc/cfm/b30.php (accessed: 01.29.2019)

[3] D. Snow, *Plant Engineers Reference Book*, 2nd ed., 2003.

[4] Overview of chiller compressors. CED Engineering. [Online]. Available: https://www.cedengineering.com/userfiles/Chiller Compressors.pdf. (accessed: 02.12.2019)

[5] C. Boles, *Thermodynamics: An Engineering Approach,(2006).* McGraw Hill, New York, NY.

[6] S. Elmoselhy, F. Elmoselhy, W. Hesham, and R. Hesham, "Validated analytical modeling of supercharging centrifugal compressors with vaneless diffusers for h2 bio-diesel dual-fuel engines with cooled egr," *International Journal of Hydrogen Energy*, 2017.

[7] A. Parr, *Hydraulics and Pneumatics: A Technician's and Engineer's guide*, 3rd ed. Butterworth-Heinemann, 2011.

[8] E. Broerman, T. Manthey, J. Wennemar, and J. Hollingsworth, *Compression Machinery for Oil and Gas*, 2019, ch. 6, pp. 253–307.

[9] T. Liu and Z. Wu. (2015) Modeling of top scroll profile using equidistant-curve approach for a scroll compressor.

[10] S. Sarangi, "Experimental and computational studies on oil injuected twin-screw compressor," 2020.

[11] P. Li, H.Qiao, Y. Li, J. Seem, J. Winkler, and X. Li, "Recent advances in dynamic modeling of hvac equipment. part 1:equipment modeling," *HVACR*, 1997.

[12] G. F. Hundy, *Refrigeration, Air Conditioning and Heat Pumps*. Butterworth-Heinemann, 2016.

[13] T. Hartman, "All-variable speed centrifugal chiller plants," *ASHRAE Journal*, vol. 43, pp. 43–53, 2001.

[14] F. Yu and K. Chan, "Environmental performance and economic analysis of all-variable speed chiller systems with load-based speed control," *Applied Thermal Engineering 29*, pp. 1721–1729, 2009.

[15] B. M. Seo and K. H. Lee, "Detailed analysis on part load ratio characteristics and cooling energy saving of chiller staging in an office building," *Energy and Buildings*, vol. 119, pp. 309–322, 2016.

[16] C.-W. Liu and Y.-K. Chuah, "A study on an optimal approach temperature control strategy of condensing water temperature for energy saving," *International journal of refrigeration*, vol. 34, no. 3, pp. 816–823, 2011.

[17] B. Ahn and J. Mitchell, "Optimal control development for chilled water plants using a quadratic representation," *Energy and Buildings*, vol. 33, no. 4, pp. 371–378, 2001.

[18] G. C. Briley, "Increasing operating efficiency," *ASHRAE Journal*, vol. 45, no. 5, p. 73, 2003.

[19] H. Crowther and J. Furlong, "Optimizing chillers & towers," *ASHRAE Journal*, vol. 46, no. 7, p. 34, 2004.

[20] L. Lu, C. Wenjian, S. C. Yeng, X. Lihua, and L. Shujiang, "Hvac system optimization-condenser water loop," *Energy Conversion and Management 45*, pp. 613–630, 2004.

[21] S. T. Taylor, "Optimizing design and control of chilled water plants: Part 1:chilled water distribution system selection," *ASHRAE Journal 53*, pp. 14–25, 2011.

[22] W. P. Bahnfleth, "Comparative analysis of variable and constrant primary-flow chilled water plant performance," *HPAC Engineering*, 2001.

[23] W. P. Bahnfleth and E. Peyer, "Variable primary flow chilled water systems: potential benefits and application issues," *Energy Efficiency Research, Arlington, Virginia: Air-Conditioning, Heating, and Refrigeration Institute*, 2004.

[24] I. Dubov, "Chilled water plant efficiency," *ASHRAE journal*, vol. 45, no. 6, p. 37, 2003.

[25] S. T. Taylor, "Primary-only vs.primary-secondary variable flow systems," *ASHRAE Journal 44*, pp. 25–29, 2002.

[26] S. Taylor, "Optimizing design and control of chilled water plants: Part 2: Condenser water system design," *ASHRAE Journal 53*, pp. 26–36, 2011.

[27] J. Liu, "Energy savings potential of variable condenser water flow systems," *ASHRAE Transactions*, vol. 118, p. 380, 2012.

[28] J. Hail, D. Hatley, and R. Underhill, "Optimization of variable speed chiller plants: Frank m. johnson jr. federal building and u.s. courthouse," Pacific Northwest National Laboratory, 2016.

[29] S. Wang and J. Burnett, "Online adaptive control for optimizing variable-speed pumps of indirect water-cooled chilling systems," *Applied Thermal Engineering*, vol. 21, no. 11, pp. 1083–1103, 2001.

[30] Z. Ma and S. Wang, "Energy efficient control of variable speed pumps in complex building central air-conditioning systems," *Energy and Buildings 41*, pp. 197–205, 2009.

[31] F. Yu and K. Chan, "Optimization of water-cooled chiller system with load-based speed control," *Applied Energy 85*, pp. 931–950, 2008.

[32] Energyplus engineering reference. US Department of Energy. [Online]. Available: https://energyplus.net/sites/all/modules/custom/nrelcustom/pdfs/pdfsv9.2.0/EngineeringReference.pdf. (accessed: 02.26.2019)

[33] T. Version, "15.0–user manual," *Solar Energy Laboratory, University of Wisconsin, Madison und Transsolar, Stuttgart*, 2013.

[34] D. A. York and C. C. Cappiello, "Doe-2 engineers manual (version 2. 1a)," Lawrence Berkeley Lab., CA (USA); Los Alamos National Lab., NM (USA), Tech. Rep., 1981.

[35] Q. Li, Q. Meng, J. Cai, H. Yoshino, and A. Mochida, "Predicting hourly cooling load in the building: a comparision of support vector machine and different artificial neural networks," *Energy Conversion and Management 50*, pp. 90–96, 2009.

[36] A. E. Ben-Nakhi and M. A. Mohamed, "Cooling load prediction for buildings using general regression neural networks," *Energy Conservation and Management*, 2004.

[37] Z. Hou, Z. Lian, Y. Ye, and Y. Xinjian, "Cooling-load prediction by the combination of rough set theory and an artificial neural-network based on data-fusion technique," *Applied Energy*, vol. 83, pp. 1033–1046, 2006.

[38] H. Huang, L. Chen, and E. Hu, "A neural network-based multi-zone modelling approach for predictive control system design in commercial buildings," *Energy and buildings*, vol. 97, pp. 86–97, 2015.

[39] C. Fan, X. Fu, and Z. Yang, "A short-term building cooling load prediction method using deep learning algorithms," *Applied Energy*, vol. 195, 2017.

[40] C. Fan and Y. Ding, "Cooling load prediction and optimal operation of hvac systems using a multiple nonlinear regression model," *Energy and Buildings*, vol. 197, 2019.

[41] G. Qiang, T. Zhe, D. Yan, and Z. Neng, "An improved office building cooling load prediction model based on multivariable linear regression," *Energy and Buildings*, vol. 107, pp. 445–455, 2015.

[42] F. Merkel, "Verdunstungskuhlung," *VDI Forschungsarbeiten*, 1925.

[43] J. W. Sutherland, "Analysis of mechanical-draught counterflow air/water cooling towers," *Journal of Heat Transfer 105*, pp. 576–583, 1983.

[44] J. E. Braun, "Methodologies for the design and control of central cooling plants," Ph.D. dissertation, 1988.

[45] W. F. Stoecker, "Procedures for simulating the performance of components and systems for energy calculations," 1975.

[46] D. J. Benton, C. F. Bowman, M. Hydeman, and P. Miller, "An improved cooling tower algorithm for the cooltools simulation model," *ASHRAE Transactions 108*, 2002.

[47] J. Bourdouxhe, M. Grodent, and J. Lebrun, "Hvac1 toolkit: Algorithms and subroutines for primary hvac system energy calculations," *ASHRAE*, 1997.

[48] M. Hydeman, K. Gillespie, and R. Kammerud, "*PG&E*'s cooltools project: A toolkit to improve evaluation and operation of chilled water plants," 1997.

[49] M. Hydeman and K. L. Gillespie, "Tools and techniques to calibrate electric chiller component models," *ASHRAE transactions 108*, vol. 1, pp. 733–741, 2002.

[50] M. Hydeman, N. Webb, P. Sreedharan, and S. Blanc, "Development and testing of a reformulated regression-based electric chiller model," *ASHRAE Transactions 108*, vol. 2, pp. 1118–1127, 2002.

[51] J. Gordon, K. Ng, H. Chua, and C. Lim, "How varying condenser coolant flow rate affects chiller performance:thermodynamic modeling and experimental confirmation," *Applied Thermal Engineering*, 2000.

[52] J. Gordon and K. Ng, "Thermodynamic modeling of reciprocating chillers," *Journal of Applied Physics*, 1994.

[53] W. Jiang and T. A. Reddy, "Reevaluation of the gordon-ng performance models for water-cooled chillers," *ASHRAE Transactions 109*, 2003.

[54] G. Thomson, *The museum environment*, 2nd ed. Butterworth-Heinemann, 2013.

[55] H. Diamond, T. Karl, M. Palecki, C. Baker, J. Bell, R. Leeper, D. Easterling, J. Lawrimore, T. Meyers, M. Helfert, G. Goodge, and P. Thorne. (2013) U.s. climate reference network after one decade of operations: status and assessment. NOAA.

[56] J. Romberger, *Chapter 18: Variable Frequency Drive Evaluation Protocol. The Uniform Methods Project. Methods for Determining energy efficiency savings for specific measures.* National Renewable Energy Laboratory, 2017.

[57] K. Brown. Psych: An open source plug-in for microsoft excel. University of California Davis, Western Cooling Efficiency Center.

[58] *ASHRAE Fundamentals Handbook.* American Society of Heating, Ventilation and Air-Conditioning Engineers, 2005.

[59] Series v cooling towers. Baltimore Aircoil Company. [Online]. Available: http://www.refrisistemas.com/docs/504edcf4Broshure.pdf (accessed: 03.08.2019)

[60] M. Frank and P. Wolfe. (1956) An algorithm for quadratic programming.

[61] *ASHRAE Fundamentals Handbook*. American Society of Heating, Ventilation and Air-Conditioning Engineers, 2017.

[62] T. Hartman, "Designing efficient systems with the equal marginal performance principle," *ASHRAE Journal*, vol. 47, p. 64, 2005.

[63] M. Hydeman and Z. Guo, "Optimizing chilled water plant control," *ASHRAE Journal 49*, 2007.

[64] Y. Ma, F. Borrelli, B. Hencey, B. Coffey, S. Bengea, and P. Haves, "Model predictive control for the operation of building cooling systems," *IEEE Transactions on control systems technologies 20*, pp. 796–803, 2011.

[65] J. Sun, X. Feng, Y. Wang, C. Deng, and C. K. Hoong, "Pump network optimization for a cooling water system," *Energy 67*, pp. 506–512, 2014.

[66] J. Sun, X. Feng, and Y. Wang, "Cooling water system optimization with a novel two-step sequential method," *Applied Thermal Engineering 89*, pp. 1006–1013, 2015.

[67] S. T. Taylor, "Optimizing design and control of chilled water plants: Part 3: Pipe sizing and optimizing δ t," *ASHRAE Journal 53*, pp. 22–34, 2011.

[68] S. Taylor, "Optimizing design and control of chilled water plants: Part 4: Chiller and cooling tower selection," *ASHRAE Journal 54*, pp. 60–70, 2012.

[69] S. T. Taylor, "Optimizing design and control of chilled water plants: Part 5: Optimized control sequences," *ASHRAE Journal 54*, pp. 56–74, 2012.

[70] X. Zhou, B. Wang, L. Liang, J. Yan, and D. Pan, "Optimization method for the chiller plant of central air-conditioning system parameters on association rules analysis for energy conservation," 2018.

[71] Y. Yao, L. Zhiwei, Z. Hou, and X. Zhou, "Optimal operation of a large cooling system based on empirical model," *Applied Thermal Engineering 24*, pp. 2303–2321, 2004.